THE UNIVERSITY OF ADELAIDE
Faculty of Engineering, Computer and Mathematical Sciences
School of Mechanical Engineering
MECH ENG 4135: Honours Project

MICYCLE

Preliminary Report

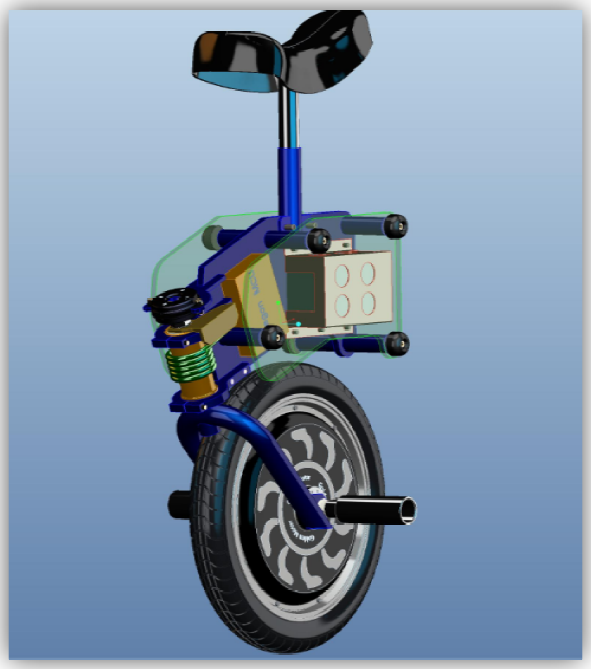

David CALDECOTT
Andrew EDWARDS
Matthew HAYNES
Miroslav JERBIC
Andrew KADIS
Rhys MADIGAN

Supervisor
Dr Ben CAZZOLATO

21 May 2010

Abstract

This preliminary report details the progress of a final year mechanical engineering project to design and build a self-balancing unicycle, known as the Micycle. The Micycle is intended to self-stabilise in the direction of travel, leaving the task of steering and providing lateral stability to the rider. The Micycle has significance for commuter transport, education in engineering, and in the future, could possibly be made completely autonomous (rider-less).

This report outlines the process and details involved in the design of the Micycle, including a literature review, formulation of specifications, component selection, design, analysis and testing.

The project goals aim to design and build a device which is practical, safe, marketable and educative. At the time of writing, no project goals have been completed, however, significant progress has been made towards the core goal of exhibiting the functional device at the University Open Day.

Acknowledgements

The authors would like to thank Associate Professor Dr Benjamin Cazzolato for his guidance and support during the project, as well as Michael Riese and Silvio De Ieso for their invaluable assistance.

We also thank the 2010 University of Adelaide Open Day Creativity and Innovation Fund for providing a critical source of funding towards this project.

Finally, we acknowledge the sponsorship and technical support provided by Maxon Motors Australia.

Disclaimer

The content of this report is entirely the work of the following students from the University of Adelaide. Any content obtained from other sources has been referenced accordingly.

David Caldecott
Date:

Andrew Edwards
Date:

Matthew Haynes
Date:

Miroslav Jerbic
Date:

Andrew Kadis
Date:

Rhys Madigan
Date:

Contents

1. Introduction **1**
- 1.1. Motivation . . . 1
- 1.2. Design objectives . . . 2
- 1.3. Project budget and timeline . . . 3
- 1.4. Progress . . . 4
- 1.5. Report outline and structure . . . 4

2. Literature review **6**
- 2.1. Review of existing self-balancing unicycle designs . . . 6
  - 2.1.1. Focus Designs SBU . . . 6
  - 2.1.2. Trevor Blackwell's Electric Unicycle . . . 8
  - 2.1.3. The Enicycle . . . 10
- 2.2. Enicycle steering analysis . . . 12
- 2.3. Safety review . . . 14
  - 2.3.1. Trevor Blackwell's Balancing Scooter . . . 14
  - 2.3.2. Focus Designs . . . 15
  - 2.3.3. Conventional unicycle safety . . . 16
- 2.4. Design recommendations . . . 16
  - 2.4.1. Safety recommendations . . . 16
  - 2.4.2. General recommendations . . . 17

3. Project goals and specifications **18**
- 3.1. Project goals . . . 18
  - 3.1.1. Primary goals . . . 18
  - 3.1.2. Secondary goals . . . 19
- 3.2. Specifications . . . 19

4. Preliminary concept design **24**
- 4.1. Steering mechanism . . . 24
  - 4.1.1. Concept designs . . . 24
  - 4.1.2. Concept evaluation . . . 25
- 4.2. Steering angle design . . . 28
- 4.3. Ergonomic considerations . . . 28
- 4.4. Preliminary CAD model . . . 30

5. Component selection **31**
5.1. Steering damper . . . 31
5.2. Motor . . . 33
5.3. Tyre and tube . . . 34
5.4. Seat and seat pole . . . 35
5.5. Motor controller . . . 35
5.6. Battery selection . . . 37
5.6.1. Lithium-ion batteries . . . 39
5.6.2. Alternative option: Sealed lead-acid . . . 39
5.7. Microcontroller . . . 39
5.8. Inertial measurement unit . . . 41
5.8.1. Microstrain 3DM-GX2 IMU . . . 41
5.8.2. SparkFun™ IMU Combo Board . . . 42

6. Mechanical design **43**
6.1. Chassis and enclosure design . . . 43
6.1.1. Chassis plate . . . 44
6.1.2. Seat pole connection and mass distribution . . . 44
6.1.3. Component enclosure . . . 45
6.1.4. Combined chassis design . . . 45
6.2. Fork assembly . . . 46
6.2.1. Spindle . . . 46
6.2.2. Fork . . . 47
6.2.3. Steering lever . . . 48
6.3. Spring design . . . 48
6.4. Static structural analysis . . . 50
6.4.1. Analysis goals . . . 50
6.4.2. Manual calculations . . . 51
6.4.3. ANSYS methodology . . . 52
6.4.4. Analysis results . . . 54
6.4.5. Conclusion . . . 58

7. Electrical design **59**
7.1. Component integration . . . 59
7.1.1. Motor to motor controller interface . . . 59
7.1.2. Microcontroller to motor controller interface . . . 60
7.1.3. Sensors to microcontroller interface . . . 60
7.2. Power distribution . . . 61
7.2.1. Power distribution board . . . 61
7.2.2. Initialisation . . . 61

8. Control design **64**
8.1. System dynamics . . . 64
8.1.1. Nomenclature . . . 65

8.1.2. Virtual work . . . 65
8.1.3. Lagrange equations . . . 65
8.1.4. Energy terms . . . 66
8.1.5. Lagrangian . . . 66
8.1.6. Equations of motion . . . 67
8.1.7. Non-linear state space form . . . 67
8.2. Simulink model . . . 67
8.3. VRML model . . . 69

9. Software design **71**
9.1. Software requirements . . . 71
9.1.1. Functional requirements . . . 71
9.1.2. Safety requirements . . . 72
9.2. Software architecture . . . 72
9.2.1. Higher level design - system finite state machine . . . 72
9.2.2. Lower level design - flowchart design . . . 73
9.2.3. Lower level design - programs, functions and interrupts . . . 74
9.3. Specific software functionality . . . 75
9.3.1. Error codes . . . 75
9.3.2. Software stops . . . 75
9.3.3. Polling for safety checks . . . 76

10. Manufacturing and testing **77**
10.1. Motor testing . . . 77
10.1.1. Test apparatus . . . 77
10.1.2. Method . . . 78
10.1.3. Results . . . 79
10.1.4. Errors . . . 80
10.1.5. Conclusion . . . 80

11. Future work **81**

References **83**

A. Gantt chart **85**

B. Budget **90**

C. Risk management and FMEA **92**
C.1. Risk management . . . 92
C.2. Failure modes and effects analysis (FMEA) . . . 94

D. Software flow charts **107**

E. Code **118**
E.1. Embedded M-file for Simulink block 118

F. Component datasheets **120**
F.1. ACE FDT70 rotary damper 120
F.2. MiniDRAGON+2 microcontroller 120
F.3. Golden Motor Magic Pie 120
F.4. Maxon motor controller 120
F.5. Microstrain 3DM-GX2 IMU 120
F.6. SparkFun IMU Combo Board 120

G. Mechanical drawings **131**

List of Figures

2.1. The Focus SBU (Focus Designs, 2009b) 7
2.2. The Electric Unicycle with safety lanyard visible (Blackwell, 2007a) . . . 9
2.3. The Enicycle Polutnik (2010) 10
2.4. Trail and rake as on a bicycle (Wikipedia, 2009) 12
2.5. Effects of negative and positive trail (Modified from Polutnik (2010)) . . 13
2.6. Trevor Blackwell on his Self-balancing Scooter (Blackwell, 2007b) 15

4.1. The Shock Absorber concept design 26
4.2. The Swivel Head Tube concept design 27
4.3. One of the Lego models used to develop the steering geometry 28
4.4. Steering geometry angles (shown on final CAD model) 29
4.5. The preliminary CAD model (with SLA batteries) 30

5.1. Two ACE FDT-70 steering dampers 32
5.2. Close up of tyre fitted to Magic Pie motor 35
5.3. Selected seat, seat pole and clamp 36
5.4. Maxon DEC 70/10 motor controller (selected) (Maxon Motors, 2010) . . 36
5.5. Roboteq BL1500 motor controller (considered suitable) (Roboteq, 2010) . 37
5.6. 'Pingu' battery (1 of 2) 38
5.7. 1 of 2 required SLA batteries (JayCar Electronics, 2010) 39
5.8. MiniDRAGON+2 development board (Wytec Company, 2010) 40
5.9. Microstrain IMU 42
5.10. SparkFun^{TM} IMU Combo Board (SparkFun, 2005) 42

6.1. Final chassis and enclosure design 43
6.2. The mannequin used to calculate the centre of mass 44
6.3. Spindle cross-section 46
6.4. Fork assembly model 48
6.5. Lever arm assembly 49
6.6. A rendered image of the final torsion spring design 49
6.7. Free body diagram 51
6.8. Fork assembly von Mises stresses when subjected to loads 55
6.9. Assembled fork assembly when subjected to loads 55
6.10. Stress on upper split ring collar when subjected to loads 56
6.11. Stress on lower split ring collar when subjected to loads 56
6.12. Maximum stress location on bearing sleeve 57
6.13. Chassis plate stress when subjected to loads 58

6.14. Chassis plate total deformation 58

7.1. The minimum setup required for the interface between the microcontroller and motor controller 59
7.2. Electrical functional diagram 63

8.1. The dynamic model of the Micycle 64
8.2. Block diagram of the Simulink model 68
8.3. Rotational response Simulink output 69
8.4. Linear response Simulink output 70
8.5. The preliminary VRML model 70

9.1. Finite state machine for the Micycle software architecture. Note that λ represents an automatic transition. 73

10.1. Experimental setup 78
10.2. Torque vs. current for 24 V and 36 V supply 80

C.1. Risk management level prioritisation level 92

List of Tables

4.1. Decision matrix for evaluating concept designs 27

5.1. Motor design requirements and specifications 34
5.2. Comparison of motor controller specifications 37
5.3. Comparison of LiFePO4 battery systems 38

7.1. Electrical component design specifications (*denotes extension goal) . . . 62

9.1. Summary of all programs, functions and interrupts in the software design. 74
9.2. Error codes for safety faults 75

10.1. Results with 24 V supply 79
10.2. Results with 36 V supply 79
10.3. Average rate of change of torque (A/Nm) with 24 V supply 79

C.1. Risks and mitigation measures 93

Nomenclature

ADCs Analogue to digital converter

ASBU An autonomous (rider-less) self-balancing unicycle.

AUD All dollar signs refer to Australian dollars (AUD) unless otherwise stated.

DAC Digital to analogue converter

FMEA Failure modes and effects analysis

FSM Finite state machine

IMU Inertial measurement unit

LED Light emitting diode

Li-ion Lithium-ion

LiFePO4 Lithium iron phosphate

MEMS Micro-electrical-mechanical systems

NiMH Nickel-metal hydride

ProE PTC ProEngineer Wildfire v5.0

SBU Self-balancing Unicycle

School The School of Mechanical Engineering, The University of Adelaide.

SLA Sealed lead-acid

University The University of Adelaide

VR Virtual reality

Chapter 1.

Introduction

This preliminary report details the progress of a project to design and build a self-balancing unicycle (SBU) known as the Micycle. A self-balancing unicycle (SBU) is similar to a regular unicycle, but rather than being controlled by the rider's feet on the pedals, sensors, a microcontroller and a motor are used maintain stability in the direction of travel. Lateral stability is controlled by the rider through steering or twisting one's body, in the same way as a regular unicycle. The rider can control the speed of travel by leaning forwards or back. In this sense, a SBU could also be described as a one-wheeled Segway™.

Several self-balancing designs have built in the past, and three of these designs are reviewed in Chapter 2 in order to provide design recommendations for the Micycle. Completely autonomous (rider-less) self-balancing unicycles (ASBU) also exist, in which lateral stability is typically controlled by use of an inertial force input (a rotating disk). However, the scope of this project is limited to the design of a rideable unicyle, primarily for its significance as a transport application. Therefore, the term 'self-balancing unicycle' is used to refer to a rideable unicycle in which lateral stability is not provided by a control system. This scope has led to a focus on four core values: practicality, user safety, marketability, and education (see Section 1.2).

1.1. Motivation

The idea of a practical unicycle, let alone a practical self-balancing unicycle, is often met with incredulity. In the public imagination, unicycles are comical devices employed by clowns with juggling balls, and unicyclists regularly endure such witty comments as, "lost a wheel, mate?" (Shuster, 2007). This may well be an example of 'tall poppy syndrome', as a unicycle is inherently difficult to learn and thus people find it easier to ridicule the idea. However, the best response to such comments is to pose another question: why use two wheels when one will do?

A unicycle, especially considered in light of today's commuter transport requirements, is in fact a practical device. Compared with a bicycle, it is lighter, more portable and considerably cheaper. Thus, a unicycle can easily be transported in car boots, trams,

trains, and even in lifts to office cubicles. Moreover, a 50% reduction in the occurrence of punctures and associated maintenance time could be reasonably expected. Still, a unicycle is much more difficult to ride than a bicycle.

However, with the difficulty of longitudinal balancing removed, a self-balancing unicycle is no more difficult to ride than a bicycle, yet maintains many of the benefits associated with a regular unicycle. The addition of electric power means that increased distances can be travelled with relative ease. Furthermore, a self-balancing unicycle also improves on other self-balancing scooters such as the Segway^{TM} by offering better portability, lower cost, and a heightened sense of freedom.

Therefore, a self-balancing unicycle has serious potential as a portable, sustainable transport solution. It also has a fun aspect and opens up a world of unicycling to many with balance and coordination difficulties. In addition, by solving a seemingly difficult self-balancing problem, it has strong educational possibilities. Finally, future work could include an add-on inertial module to make the Micycle completely autonomous.

1.2. Design objectives

The objectives of the Micycle have been developed by considering the potential of self-balancing unicycles in transport applications and the desire to use the device to further interest in control systems engineering. Therefore, where possible, it is desired that the design of the Micycle should be practical, safe, marketable and educative. The project goals and specifications which logically follow the recommendations from the literature review are presented in Chapter 3 and summarised here.

Practicality

- A stable, working prototype must be built which is suitable for users of different heights and weights.
- It should be easy to control and steer the device.
- The device should be portable and robust and have acceptable battery life.
- As an extension, the device should be able to ascend a three degree incline.

Safety

- A literature review of possible safety concerns should be performed prior to design.
- The risk of electric shock, danger from moving parts and from falling from the device should be minimised in design and further mitigated through safe operating procedures and equipment.
- The device must have the ability to manually and automatically shutdown.

- The device should have visual and auditory indicators warnings of any problem, including low battery levels.
- As an extension, the performance of the device should be adjustable for different users and operating conditions, and the performance data should be logged.

Marketability

- Within budget and manufacturing constraints, the device should look like a finished product.
- To the extent possible, the device should be affordable, use off-the-shelf components and the design should be easily reproducible.
- The device should be aesthetically pleasing.

Education

- Where possible, the design should be transparent; it should be easy to locate and explain the purpose of each component.
- A dynamic Simulink model and as an extension, a virtual-reality (VRML) model should be created for further use in University classes.

1.3. Project budget and timeline

The project budget is attached in Appendix B and the project Gantt chart is attached in Appendix A.

A grant of $1800 was provided by the University's Open Day Creativity and Innovation Fund. While this provided critical funding for the project, it also brought forward the due date for the completed device by ten weeks, adding substantial time pressure to the project.

Available resources

- $1200 funded by the School of Mechanical Engineering.
- $1800 supplementary funding from the University Open Day Creativity and Innovation Fund.
- 240 man hours of School Workshop manufacturing time.
- Inertial measurement unit ($3000) provided in kind by the University.

Summary of deliverables

- 10 May 2010: Final construction drawings issued.
- 22 May 2010: Preliminary report issued.
- 14 August 2010: University Open Day: complete functional device required.
- October 22: Final report due.
- October 27: Final year project exhibition.

1.4. Progress

At the time of writing, none of the project goals have been achieved. However, the project is on schedule and the following elements have been completed:

- Final mechanical drawings submitted to the School Workshop.
- All off-the-shelf components specified and ordered.
- Motor control with Maxon controller achieved.
- Preliminary electrical design completed.
- Preliminary control design, including Simulink model, completed.
- Software design approach and road map specified.

The future work to be completed is outlined in the final chapter, Chapter 11.

1.5. Report outline and structure

To the extent possible, this report attempts to represent the progress of the design and construction of the Micycle in a logical, linear fashion. Chapter 2 is a review of existing designs and the safety issues associated with these. The recommendations arising from this form the basis for the project goals and specifications in Chapter 3. Work began in parallel towards the concept design (Chapter 4) and the selection of off-the-shelf components (Chapter 5). Following this, the final mechanical design stages are documents in Chapter 6. Work then began on the electrical design (Chapter 7), control design (Chapter 8) and software design (Chapter 9). Finally the future work is outlined in Chapter 11.

As safety and the timely completion of the project were a priority, the team used risk management strategies to mitigate project risks. In addition, a thorough failure modes and effects analysis was performed to ensure safe operation of the Micycle. As this section is lengthy, it is attached in Appendix C.

However, it should be noted that as with many projects, work often took place in an iterative fashion and different sections of the design influenced others. For example,

the electrical and control requirements influenced the mechanical design choices, and the availability of off-the-shelf components and the necessary steering system severely limited the scope for extensive concept design.

Chapter 2.

Literature review

Over the past twenty years, the unicycle has been the subject of a diverse range of papers. Many of these studies have been on a theoretical or educational basis and have not involved building a test device. In addition, most tend to focus on emulating autonomous (unmanned) unicycles rather than producing a rideable device, which is the aim of the Micycle project.

This does not completely preclude the relevance of these papers; some findings and derivations are helpful for the control part of the Micycle design. For example, Schoonwinkel (1987) aims to emulate an actual unicycle, using an inertial disk to simulate the torque provided by the rider. Sheng (1997) further extends this approach further, using linkages to approximate the legs of the rider. In both studies, useful derivations of the system dynamics using Newton-Euler, Lagrangian and d'Alembert approaches are attached as appendices. Furthermore, undergraduate projects at other universities provide a insight into the necessary control design process. In particular, work by De Souza Matthew (2008) was used as a basis for the derivation of the Micycle system dynamics using the concepts of Virtual Work and the Lagrangian (see Chapter 8).

However, to maximise the relevance of this literature review to the rest of the design, it is necessary to focus on rideable self-balancing unicycles (SBUs). Due to the limited evaluative literature available on these designs, a critical design review is performed for the Focus Designs SBU, Trevor Blackwell's Electric Unicycle and the Enicycle. Design recommendations from this review are used to form the basis for the goals and specifications of the Micycle. As an extension of the Enicycle review, the steering linkage is reviewed in more detail in Section 2.2. Finally, in order to ensure safe design and operating of the Micycle, safety concerns are reviewed in Section 2.3.

2.1. Review of existing self-balancing unicycle designs

2.1.1. Focus Designs SBU

The Focus Self-Balancing Unicycle (Focus SBU) is an electrically controlled unicycle able to balance in a single axis, forward and reverse, using a control mechanism to

Figure 2.1.: The Focus SBU (Focus Designs, 2009b)

drive the electric motor. The aim of the design is to develop a means of cost effective commuter transportation that does not require rigorous human effort or the need to stop frequently and recharge. This discussion addresses the issues involved with the design of the chassis, electric motor, batteries and motor control of the Focus SBU.

The design of the Focus SBU is based around a commercially available unicycle chassis, with the crank replaced by foot pegs. This has allowed the Focus SBU to be the first self-balancing unicycle available to market. However, the chassis does not have a steering mechanism which reduces the maneuverability of the SBU and as the Focus SBU is faster than a generic unicycle, there is greater danger caused by this lack of agility. This is one of the reasons the design has incorporated an automatic fall detection shut-off and a safety switch that disables the motor.

The permanent magnet, direct current and variable drive motor coupled to a single speed system enables the Focus SBU to have good acceleration achieving, standing to 10 km/h in one second, and top speed of 16 km/h (Focus Designs, 2009b). However, the single speed system introduces extra moving parts, which require increased maintenance compared with a direct-drive brushless hub motor design. While the belt-drive design provides advantages such as absorbing shock loads and vibration isolation, there are negative issues inherent that affect this design, such as wear, aging and loss of elasticity (Budynas et al., 2008, p. 413). There are safety concerns due to the possibility that a rider's clothing could become caught in the setup, which are addressed through the use of a guard.

The performance of a SBU is greatly affected by the quality of the power source. The

Focus SBU uses a custom specified lithium-ion-iron-phosphate (LiFePO4) battery pack rated at 36 V. This provides the SBU with a 16 km range and a two hour recharge time (Focus Designs, 2009c), which is approximately three hours faster than that of the Enicycle (see Section 2.1.3). In addition, the custom made battery allows for regenerative recharging. While braking and operating down an incline, the SBU can recharge the battery pack, which enables an extended operation time.

According to Focus Designs (2009b), the underlying control system uses input from the rider's lean angle, using gyroscopes and accelerometers, and passes this through a feedback controller to drive the motor stabilising the rider. The exact details of how this feature is implemented and the stability margins are unavailable.

To conclude, the Focus SBU is easily and cheaply produced by adaptation of a standard unicycle chassis. Also, the drive train configuration contributes to good range and acceleration characteristics. However, increased maintenance and safety concerns due to the single speed belt drive setup and the lack of a steering mechanism detract from the overall system. Hence, the design would benefit from improved steering mechanics to address these concerns.

2.1.2. Trevor Blackwell's Electric Unicycle

The Electric Unicycle is an attempt made by Trevor Blackwell to produce a single wheeled vehicle as a logical progression from his self balancing scooter. Blackwell (2007a) felt that two wheels were redundant and that only one was necessary to make an effective transportation device. The Blackwell design was not intended to be a commercial product, but rather as a one-off product. To this extent, the design was most focused on ease of design, construction and low cost. Other considerations, such as performance, reliability and ergonomics were not explicitly addressed as they would have been in a commercial product. This discussion examines the different subsystems and components used in the Electric Unicycle.

The mechanical design is driven by cost and ease of design. The frame is made from common 1" diameter tubing TIG welded together at right angles. However, the rigid frame is difficult to balance on and control. Blackwell (2007a) recommends that the rider is able to ride a unicycle before attempting to ride the device. Moreover, the vehicle's turning is cumbersome. The rider's arms need to be swung to generate angular momentum to turn the vehicle. This needs to be done at reduced speed due to the difficulty of balancing the vehicle.

Control is achieved by a closed loop feedback loop from a solid state gyroscope for forwards and backwards tilt control of the motor. Although detailed performance specifications are not available, the control of the system is described as smooth and produces an effect similar to balancing oneself on a unicycle (Blackwell, 2007a).

The drive system for the Blackwell design is a permanent magnet DC motor and uses a gearbox and belt to drive the wheel. This is a common, cheap drive configuration.

Figure 2.2.: The Electric Unicycle with safety lanyard visible (Blackwell, 2007a)

There are some drawbacks in the control of the system however. The use of a belt drive and a gearbox to transfer the power increases the time delay of controlling the system and leads to backlash in the control. This reduces the ability of the motor to control the tilt angle and leads to a less stable, less smooth control system (Taj, 2000). Moreover, the gearbox is described as extremely noisy; this is detrimental enough for the designer to describe it as the component which he most would like to replace (Blackwell, 2007a).

The remainder of the components are off-the-shelf parts. The selection of these was dictated by cost and availability. The nickel metal-hydride (NiMH) batteries are used due to their low cost and reliability. The design also incorporates a dead man's switch which terminates power to the motor if the rider falls off. This adds an extra degree of safety to the design.

Trade-offs have been made in the design. A robust, simple design has been produced by sacrificing the ease of riding and turning the vehicle. However, this results in a design which is not suitable for a commercial product. It is not practical to expect the rider to already be able to ride a unicycle, and there is no explicit mechanism for turning; the rider needs to swing their arms. This is not user friendly. In practice, turning the vehicle is very jittery and often borders upon instability (Taj, 2000). The design is too unstable and lacks the control that would be expected of a commercial product.

A number of key improvements need to be made to improve the ride quality of the device. For smoother turning, there needs to be an explicit turning mechanism within the vehicle itself. For smoother pitch acceleration, the controller needs the quickest possible response; to this extent, the less gearing between the motor and the rim of the

Figure 2.3.: The Enicycle Polutnik (2010)

wheel, the better. A final note is that the use of the dead man's switch is an excellent design decision. This makes the vehicle much safer to operate.

To conclude, the Blackwell design functions effectively, however, steering and backlash issues detract from the usability of the design. The Micycle design should aim to improve on these issues, possibly by avoiding use of a gear drive.

2.1.3. The Enicycle

The Enicycle is an electric self balancing unicycle. It has been designed to provide a competitive environmentally friendly alternative to any low speed intermediate distance vehicle. The Enicycle incorporates a steering linkage, which makes steering and lateral balancing considerably easier than in other designs. Due to the complexity of this linkage, it is discussed separately in Section 2.2. The following discussion is an analysis of the Enicycle's major systems, including the drive, control, power supply and outer frame.

The drive system of the Enicycle consists of 1000 W electric, brushless hub motor controlled by a microcontroller (Polutnik, 2010). Brushless motors have a longer life, are lighter and smaller, virtually maintenance free and create lower acoustic noise than their brushed counter parts (Robinson, 2006). In addition, the direct drive system also reduces the mechanical complexity, acoustic noise and maintenance requirements associated with a geared model, such as the Focus SBU. However, without a gearing system, the motor must be sufficiently powerful to able to provide sufficient low-end torque. This in turn

necessitates a more powerful motor and hence higher costs than for a motor suitable for use in a geared drive system. Thus, there is a trade-off between the lower costs associated with a geared drive system and the aesthetic and mechanical advantages of a direct drive system. In the case of the Enicycle, however, it would be extremely difficult to make a geared drive system work with the steering geometry of the Enicycle, therefore, the extra expense of the hub motor is well justified.

The Enicycle's control system uses feedback from electrical sensors input into a dynamic model to drive the electric motor. Micro-electrical-mechanical systems (MEMS) gyroscopes and accelerometers are used to detect the angular rate and position of the Enicycle. MEMS are cheap, small sensors which use relatively less power than many other competitive options. The main disadvantage of these sensors is that their performance is unacceptable for many applications due to inherent inaccuracies that result from deterministic errors such as bias drift and non-linear scaling effects. However, these errors can be compensated with fuzzy logic methods (Hong, 2008). The available videos of the Enicycle (Polutnik, 2010) indicate that it moves in a responsive and controlled manner. It appears, therefore, that the MEMS sensors have been integrated into the Enicycle with some success.

The Enicycle is powered by standard, rechargeable nickel-metal hydride (NiMH) D cells connected together in a larger battery pack (Polutnik, 2010). These have a supply voltage of 44 V and an average current rate of 10 A h, which is enough power for a maximum speed of 15 km/h and an approximate range of 30 km (Polutnik, 2010). The use of separate D cells allows for easy manipulation and maintenance of the power supply. If more current or voltage is needed more batteries can be added, and if a fault occurs, only the damaged batteries need to be replaced. However, the main disadvantages encountered with the use of these batteries is the large amount of charge time required, estimated at around 5 hours, and the added weight component of all the batteries. Both of these factors can be reduced with the use of lighter faster charging batteries such as lithium-ion polymer batteries. Such a change, however, would increase cost and add more complexities to the charging and the discharging system.

The frame is a compact, functional design in which the majority of components are not covered or sealed in. This leaves all the mechanical components open to the elements; the Enicycle has not been designed for all weather conditions. It lacks simple components like mud or wheel guards. The frame also lacks any lighting or indicator systems and the light emitting diode readout is in a position that requires the rider to dismount to read it. These are all small features that do not take much effort to add but do add to the overall finish of the design. The Enicycle aspires to be a commercially competitive product and appears to have been designed without aesthetics in mind. This may have been a mistake, as how good a product looks will always determine how well it sells.

To summarise, the Enicycle has a unique design however it is not a perfect design. It is compact, functional and contains many innovative features such as the control system and steering mechanism but it can still be improved. There is still room for technological development in the steering and battery systems and there are small additions that could

make the overall appearance of the Enicycle more aesthetically pleasing.

2.2. Enicycle steering analysis

The steering system of the Enicycle can be analysed by breaking it down into three main components, the angle of the primary axis, the angle of the forks and the main stabilising mechanism. To understand the reasons for the Enicycle design, it needs to be understood how each of these separate components affects the overall system.

The angle of the primary axis about which the wheel rotates defines the responsiveness of the Enicycle's steering system. In bicycling terminology it is referred to as the head tube angle or head angle, as this is normally the main tube through which all steering occurs. The head angle determines the plane in which the front wheel rotates and leans when an input force is applied to the steering system. Vertical lean and horizontal rotation are the two components that determine the turning action of the wheel. A smaller head angle that is closer to horizontal will cause the wheel to lean more, while a larger head angle closer to vertical will cause the wheel to rotate more. The head angle also determines the trail, displayed in Figure 2.4. This is the horizontal distance between the projection of the steering axis and the surface contact point of the tyre.

Figure 2.4.: Trail and rake as on a bicycle (Wikipedia, 2009)

Through experimentation, Jones (2006) determined that positive trail (forward of the tyre/surface contact point) makes for a more stable steering system, while negative trail (back from the tyre/surface contact point) creates a more unstable steering system. This occurs as a result of the torque created around the steering axis by the friction force that acts perpendicular to the wheels steering direction. Figure 2.5 demonstrates this with positive trail and the relating steering axis in green and negative trail and the relating steering axis in red. It can be seen that as each axis rotates in the direction of the white arrow, the friction force represented by **F** has different effects.

Figure 2.5.: Effects of negative and positive trail (Modified from Polutnik (2010))

With negative trail, the friction force creates a torque in the same direction as the applied turning force. This amplifies the effect of the input force, increasing responsiveness and instability. With positive trail, the torque created by the friction force opposes the applied turning force reducing the effect of the input force, creating a more stable and less responsive system.

While a stable system is generally desirable, designing the steering system of the Enicycle as unstable is to some extent beneficial. Lateral stability is important when riding the Enicycle, as small movements and shifts of weight can unbalance a rider. A more responsive system will allow any rider to compensate and correct these movements more quickly. The negative trail of the Enicycle allows for this as well as more lateral movement of the wheel. More lateral movement of the wheel means that the wheel can move further to counterbalance body movements. Combined with the greater responsiveness of the steering system, this makes lateral balance recovery more effective.

The Enicycle has a head angle of approximately 67.5 degrees. By itself, the Enicycle's head angle creates positive trail, making the steering system a stable system, similar to the positive trail axis in Figure 2.5. The steering would be responsive and light enough to control with the rider's feet, while still stable enough to not overreact to inputs. This

stability has been affected by changing the fork angle.

The addition of a bend, which alters the fork angle from that of the head angle, makes the Enicycle more compact and comfortable to ride. This change in geometry has also moved the wheel axle forward of the steering axis. As a result, the trail of the Enicycle has changed from positive to negative, increasing responsiveness and making the Enicycle easier to turn but more unstable to steer. A shallower fork angle also means that the wheel axle undergoes more vertical rotation for each degree of steering axis rotation. So while horizontal rotation stays the same, the lean experienced by the wheel increases. This increases the response and reaction characteristics of a system that is already unstable.

The unstable nature of the Enicycle's steering geometry has meant that a torsion spring is necessary to provide a restoring force. The torsion spring added to the top of the Enicycle's head tube adds a restorative force that counteracts the input force applied by the rider. It reduces the responsiveness and instability of the steering system by reducing the input force. As a result, the steering system is stable, but still allows for a responsive, compact design.

2.3. Safety review

User safety is an important requirement for the design of the Micycle. In order to develop an understanding of the specific design and operating requirements, three similar devices are reviewed below. Trevor Blackwell's Self-Balancing Scooter, the Focus Designs SBU and a standard unicycle are similar, unstable devices which provide a comprehensive basis for safe design and operating recommendations for the Micycle.

2.3.1. Trevor Blackwell's Balancing Scooter

Trevor Blackwell (2007b) has designed and built a self-balancing scooter, similar to a Segway™. Blackwell lists a number of safety recommendations on his website, summarised below:

Equipment and space requirements:

- Falling is very likely during testing of the device.
- Personal protective equipment is recommended, including a helmet, sturdy shoes, pants, wrist guards, shin guards, elbow guards.
- A wide open flat space is required.
- Wet weather and slippery surfaces should be avoided.

Figure 2.6.: Trevor Blackwell on his Self-balancing Scooter (Blackwell, 2007b)

Design requirements:

- A combination of a dead man's switch and a kill switch, so that power is cut if the rider becomes separated from the device.
- The maximum motor speed should be limited so that the motor has sufficient reserve power to maintain stability.
- The design should be easy to jump off in case of an impending fall.
- Use a dependable motor controller, as any spike or malfunction in the motor controller has potential to cause injury.
- Consider testing requirements. Since testing requires constant adjustment of control gains, it is best to design to make this process easy (Blackwell, 2007b).

2.3.2. Focus Designs

Focus Designs (2009a) have produced an operating manual for their commercial SBU, which makes a number of recommendations for the safe use of the device. This manual is aimed at the end user, rather than the builder and tester, so personal protective equipment is not required to the same degree as recommended by Blackwell. Focus Designs recommend bright, visible clothing, that is not loose and cannot be caught in any moving parts. They also recommend protective eye-wear to protect from insects, which seems a little unlikely, but it is a scenario worth considering.

Focus Designs have incorporated several safety features into their design. The SBU requires a key switch to turn on and has a safety kill switch in the form of a 50" lanyard

clip which attaches to clothing. The SBU automatically detects falls and shuts off; presumably this is triggered by detection of excessive angular position or rate. A status LED indicates power status and shifts to red when battery is low. A status tone is sounded when the rider is close to exceeding the capabilities of the device, or when the battery is low and the device is about to shut down (Focus Designs, 2009a).

Interestingly, the Focus Designs user manual states that the device should only be switched on when on the ground in a level, ready to ride position (Focus Designs, 2009a). Otherwise the wheel will spin in an attempt to self-balance. This would be easy to avoid by programming the SBU to check its initial vertical position (from the accelerometer input) as part of a self-check at start up. It is not known why Focus Designs have not addressed this issue directly.

2.3.3. Conventional unicycle safety

The safety equipment requirements for learning to ride a conventional unicycle are similar to those above. A helmet and protective padding are generally recommended. In addition, the seat height should be adjusted so that the rider's feet comfortably reach the ground when seated, and when the rider is more comfortable with the device, adjusted so that the rider's toes just reach the ground (Carlson, 2009a). A shopping trolley is also recommended as a useful supporting device for the rider when learning (Carlson, 2009b). This, or something similar, could be extended to the testing of the Micycle.

2.4. Design recommendations

These recommendations build on the knowledge gained from similar devices and form the basis for the goals and specifications in Chapter 3. These recommendations are separated into the safety recommendations arising from the safety review and the more general recommendations arising from the review of the subsystems of the three existing SBU designs.

2.4.1. Safety recommendations

From the above discussion, a summary of the equipment and design safety requirements for the Micycle can be made. The following equipment is required:

- During normal riding, a helmet is required for head protection in case of falls.
- In addition, during testing, protective padding of limbs is required and could be accomplished by knee pads, elbow pads, etc.
- A wide open space is required for riding.
- The device should not be used in wet weather or at night.

- A user manual, or safe operating procedure and user training should be provided.

The key design recommendations for safety are:

- The device should be sufficiently robust to withstand dropping during testing and regular use. The rider should therefore be focused on their own safety and not preventing damage to the device.
- Power to the motor should be cut if the device falls or becomes separated from the rider.
- The device status, including remaining battery power should be indicated with clear visual and auditory warnings.
- Speed limiting is necessary to prevent unsafe speeds and to maintain stability margins.
- The potential for uncontrolled motion due to start up in an inclined position should be avoided.
- The seat height should be adjustable.

2.4.2. General recommendations

The following design recommendations can be made in regards to the component selection and overall design.

- A direct drive motor should be used if possible to reduce backlash, simplify the drive system, reduce noise and improve safety.
- A steering mechanism should be incorporated into the device to improve ease of use.
- Lithium-ion iron-phosphate (LiFePO4) battery chemistry is preferable to other types.
- Control should be achievable with relatively cheap MEMS sensors.
- Consideration should be given to aesthetic issues, particularly when designing the outer protective covering.

The above recommendations are thus integrated into the goals and specifications in the following chapter.

Chapter 3.

Project goals and specifications

The following goals and specifications have been developed from the project aims and the recommendations arising from the literature review. The goals are the broad requirements that must be fulfilled by the project. The specifications outline in detail how these goals will be measured.

3.1. Project goals

The goals are divided into two categories. The primary goals are the core deliverables of the Micycle project. The secondary goals are extension items, to be completed if time permits, or may form the basis for future work.

3.1.1. Primary goals

1. A working prototype will be built.
2. The prototype can stably support a user while stationary.
3. The prototype must be able to sustain stable forward motion while being ridden on flat terrain over a distance of 50 m, at a speed greater than 2 km/h and less than 15 km/h
4. The prototype must be able to turn around a radius of 50 m.
5. The prototype must incorporate a kill-switch to enable it to be deactivated quickly in case of emergency.
6. The prototype must be capable of sustaining continuous operation at one third power for 15 minutes.
7. The prototype must include functionality to alert the user with an audible warning when battery charge level is low. This is tied to a visual indicator of battery charge level.
8. The prototype must utilise automatic gain adjustment to compensate for battery charge depletion.

9. The prototype must incorporate a speed limit functionality that caps its translational speed.
10. A dynamic model of the plant will be created using Simulink.
11. The prototype must include a manual gain adjustment toggle to control ride quality.

3.1.2. Secondary goals

1. A virtual reality (VR) model of the device may be built by exporting the CAD model as VRML into Simulink.
2. The inertial measurement unit (IMU) on loan from the School may be replaced by a custom-built gyro and accelerometer board.
3. The prototype may include functionality that allows the user to adjust the level of ride quality by toggling gains.
4. The prototype may incorporate a data-logging mechanism in order to collect performance data.
5. The prototype may include brake lights for pedestrian safety.
6. The prototype is able to ascend or descend a 3 degree incline while maintaining stability.
7. The prototype may incorporate automatic an automatic weight sensor, to enable adjustment of gain based on user weight.

3.2. Specifications

The schedule of specifications begins on the following page.

Micycle Specifications Schedule

1. Safety

1.1 Compliance with OH&S requirements

The prototype must comply with OH&S requirements to the satisfaction of the School OH&S Officer. Failure to adhere to these requirements may render it impossible to continue testing the prototype.

1.2 User safety

1.2.1 Stability

Supports one person without spontaneously pitching over forwards or backwards.

1.2.2 Strength/sturdiness

zStructure able to support one person weighing up to 100 kg.

1.2.3 Visibility

Reflectors ensure visibility at night from all angles under headlights.

1.2.4 Collision

1.2.4.1 Maximum speed

Upper bound of speed: 15 km/h.

1.2.4.2 Braking distance

The device can decelerate from maximum speed to stand-still within 5m.

1.2.5 Electric shock

- *Electrical insulation/isolation prevents exterior metal components from becoming live.*
- *Battery power can be easily disconnected to reduce risk of electric shock while performing maintenance and repairs.*

1.2.6 Moving parts

External moving parts have acceptable risk of pinching/crushing of extremities – to be judged by OH&S officer.

1.2.7 Surface traction

Wheel achieves traction on a variety of surfaces found outdoors and indoors in an urban setting, including:

- carpet
- pavement
- asphalt
- polished linoleum flooring

1.2.8 Emergency shut-off

The device incorporates an emergency shut-off switch.

1.2.9 Perceived safety – subjective criterion

The device must feel stable and safe to the user.

- *Foot-rests broad enough to ensure a subjective feeling of lateral control and stability.*

1.2.10 Robustness

The device is able to withstand tipping onto a hard surface from the upright position without sustaining damage to its structural integrity or functionality.

1.3 Pedestrian safety

1.3.1 Pedestrian collisions

- *Braking distance minimised to reduce risk of collision. (See 1.2.4.2)*
- *Maximum speed limited to prevent serious injury to pedestrians in the event of a collision. (See 1.2.4.1)*

1.4 Traffic safety

Brake-lights activate when the device decelerates.

2. Budget

2.1 School allowance

The School will provide reimbursement for capital expenditure up to a maximum of $2000.

2.2 Provision in kind

The School will supply an inertial measurement unit (IMU) for use on the prototype.

3. Time constraints

3.1 Work-order submission

Work orders for the Mech. Eng. workshop will be completed on a "first-in, first-out" basis. Thus, the sooner drawings are submitted to the workshop, the less lead-time until the prototype is constructed.

3.2 Workshop time

Workshop labour to build the prototype is limited to 200 hours for the project. Any additional labour required must be outsourced at additional expense and time.

3.3 Final report

The final project report is to be submitted by October 22.

3.4 Project exhibition

The prototype will be exhibited at the project exhibition on October 27.

4. Functionality and performance

4.1 Ergonomics

4.1.1 Saddle

Off-the-shelf unicycle saddle used.

4.1.2 Posture

Seat height adjustable.

4.2 Durability

Device built to remain intact and useable when subjected to rigorous testing for the duration of the project (see 1.2.10).

4.3 Ease of maintenance

4.3.1 Component access

- *Ability of a familiar user to access and replace batteries in under two minutes.*
- *Ability of a familiar user to access controller board in under two minutes*

4.3.2 Replacement parts

Selected components readily available for purchase in the event of failure during testing.

4.4 Functionality in varied environments

4.4.1 Surface traction

Device maintains adequate traction on a variety of surfaces. (See 1.2.7)

4.4.2 All-weather capability

- *Device maintains adequate traction in both wet and dry weather.*
- *No exterior components or fittings prone to damage due to wet weather.*

4.4.3 Surface gradient

Device is guaranteed to traverse flat terrain. Effectiveness on a 3 degree incline is optional to the implementation, as per the extension goals of the project contract.

4.5 Portability

4.5.1 Weight

Unloaded weight does not exceed 25 kg.

4.5.2 Size

Storage possible in a rectangular prism of dimensions 1.2m x 0.6m x 0.6m

4.6 Self-balancing criterion

The prototype is able to right itself from a deviation of +/- 2.5 degrees from vertical.

4.7 Turning circle

The prototype achieves a minimum turning radius of 4 m while stable.

5. Marketability

5.1 Aesthetics

The device shall be designed to be aesthetically pleasing where possible, with exposed internal components kept to a minimum.

6. Sustainability

6.1 Energy efficiency

Energy consumption of less than 0.2 kWh per km travelled.

6.2 Disassembly

Device is designed for ease of disassembly, so that parts can be reused or recycled.

7. Security

7.1 Immobilisation

- *A key is required to enable the device to be started.*
- *Provision is made to ensure that the device can easily be secured with a conventional bicycle lock.*

Chapter 4.

Preliminary concept design

The preliminary concept was developed through a iterative process in parallel with the selection of components for the design. However, it is helpful to describe the initial concept development prior to concept selection so that the placement and use of each component is more obvious.

There was not a great opportunity for extensive concept brainstorming over the entire Micycle design as the broad shape of the design is driven by the necessary steering geometry. Instead, the different steering concepts discussed are presented and evaluated here. This allows formalisation of the steering design angles are formalised. The ergonomic considerations that influenced the concept design are also discussed. Finally, the preliminary CAD model is presented.

4.1. Steering mechanism

In designing the Micycle, the most difficult design choices to make were those involving the steering mechanism. Due to the fact that there is only one wheel, the turning mechanism is not straightforward as it would be in a design with multiple wheels. Here, three distinct conceptual designs for the steering are considered and evaluated. The Enicycle steering mechanism was the concept chosen.

4.1.1. Concept designs

Modified Enicycle design

The Enicycle steering mechanism uses a combination of spring and damper, as described in Section 2.2. The spring adds a restoring force to increase the stability during a turn and the dampener reduces small perturbations from the road when turning. Turning is achieved through pressing down on the pedals to pivot the wheel.

The Enicycle steering geometry design is modified by replacing the linear damper with a rotary damper. This results in a more compact design. This design is shown in the preliminary model, Figure 4.5.

Shock Absorber design

The Shock Absorber Design (Figure 4.1) is functionally very similar to the Enicycle Design. Turning is achieved in the same manner. However, it differs in that it uses shocker absorbers, which provide both the stability of spring as well as the dampening from the dampener in a single unit. The design makes use of two shock absorbers. When a force is applied to the foot supports, the central spindle pivots, extending one absorber and compressing the other. This provides the necessary restoring force.

Swivel Head Tube design

This design has no spring or dampener to restore the wheel. Rather it makes use of a larger head angle, almost 90 degrees, to ensure that the system is much less sensitive in turning and does not go unstable without a restoring force on the wheel. The advantage of this is that it uses a more natural turning mechanism, but this comes at the price of stability.

4.1.2. Concept evaluation

Deciding upon a steering mechanism concept was aided by constructing a decision matrix to evaluate the three options. The matrix uses several criteria, which were given point weightings (given in brackets):

Controllability (4) This is the primary goal of each of the above design concepts.

Cost (3) The cost of the system is crucial as the project has a limited budget.

Stability (2) Inherent stability in the mechanical design ensures that the vehicle is much easier to learn to ride, increasing the accessibility of the design.

Structural integrity (1) It is important that the system does not failure structurally, especially for user safety.

Durability (1) It is preferred that the system has a long operational lifetime.

Ease of manufacture (1) The design should aim to be easy to manufacture to make the most of the limited manufacturing workshop time available. Although important, this criterion should not be achieved at the expense of design integrity.

Aesthetics (1) Looks are also desirable.

The decision matrix dictates that the most suitable steering mechanism concept for the Micycle is the Enicycle Design. The design team felt that the Swivel Head Tube Design is too unstable and lacks the robustness for the design. The Shock Absorber Design has potential, but it is anticipated that it will be difficult to tune the system for the required response when turning. In addition, the appropriate shock absorbers are expensive and difficult to replace with different stiffness models.

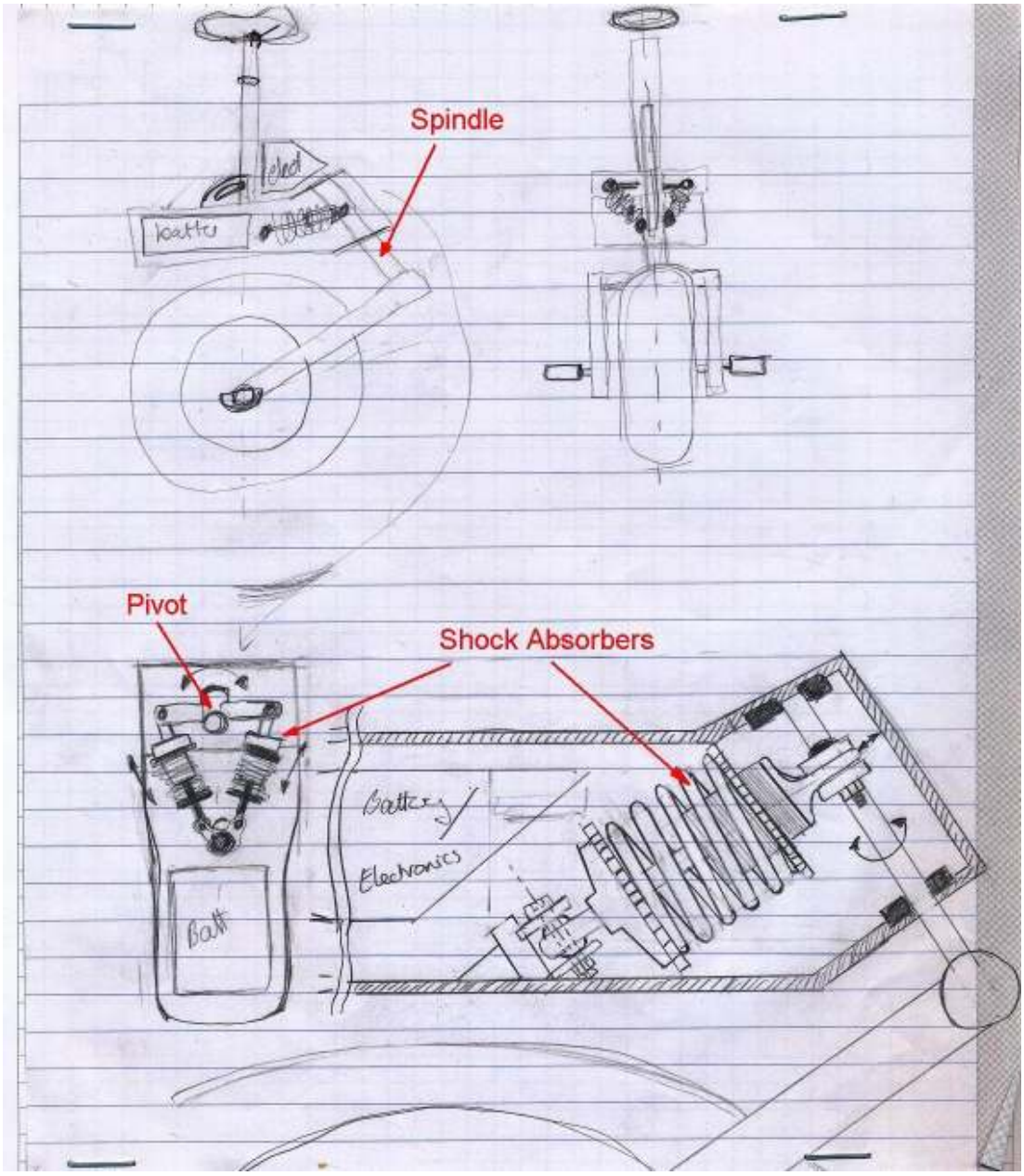

Figure 4.1.: The Shock Absorber concept design

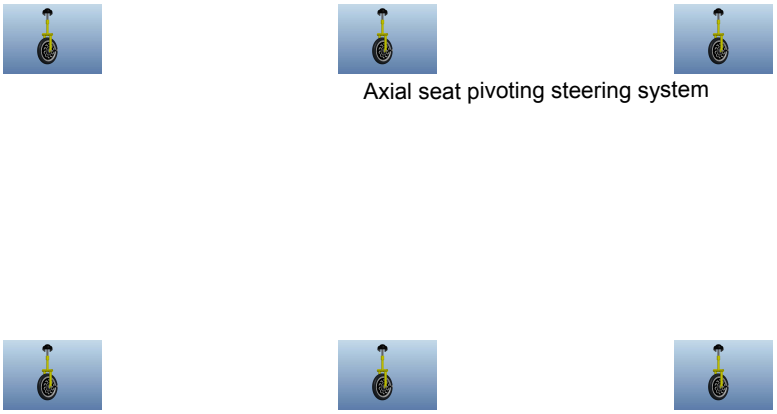

Figure 4.2.: The Swivel Head Tube concept design

Table 4.1.: Decision matrix for evaluating concept designs

Criteria	Weight	Enicycle	Shock Absorber	Swivel Head Tube
Controllability	4	5	4	2
Cost	3	3	3	5
Stability	2	5	4	2
Structural integrity	1	3	3	4
Durability	1	5	4	4
Ease of manufacture	1	3	4	4
Aesthetics	1	3	5	3
Total		53	49	42

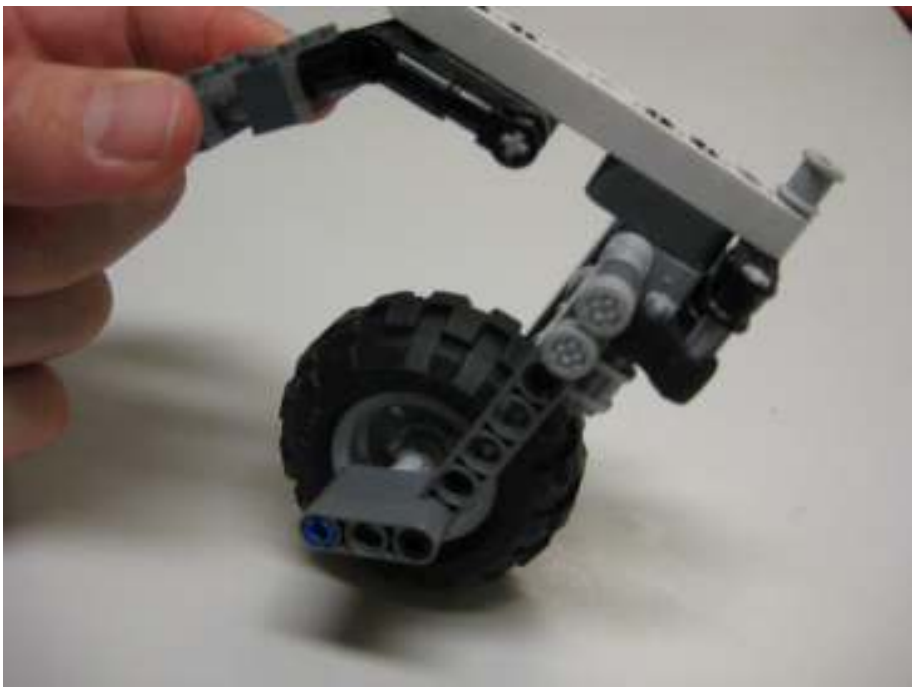

Figure 4.3.: One of the Lego models used to develop the steering geometry

Hence, the Enicycle Design was selected as the steering mechanism concept for the Micycle. The above design was modified in the final Micycle design, but the fundamental concept remains the same.

4.2. Steering angle design

The final angles for the steering geometry were developed through experimentation with Lego models (see Figure 4.3). Various configurations were attempted, but it turns out that the optimum geometry agrees with that used by the Enicycle. The final design angles were thus based on the Enicycle geometry, but with a slight modification.

From examining videos of the Enicycle in motion, it was observed that the full range of turning is rarely used. Therefore, the Micycle was designed with a shallower head tube angle (22.5 degrees) and fork angle (45 degrees). These angles are described in Figure 4.4

4.3. Ergonomic considerations

The Micycle is designed with the comfort of the rider in mind. As a proof-of-concept prototype for a marketable product, ergonomics are a significant consideration. This

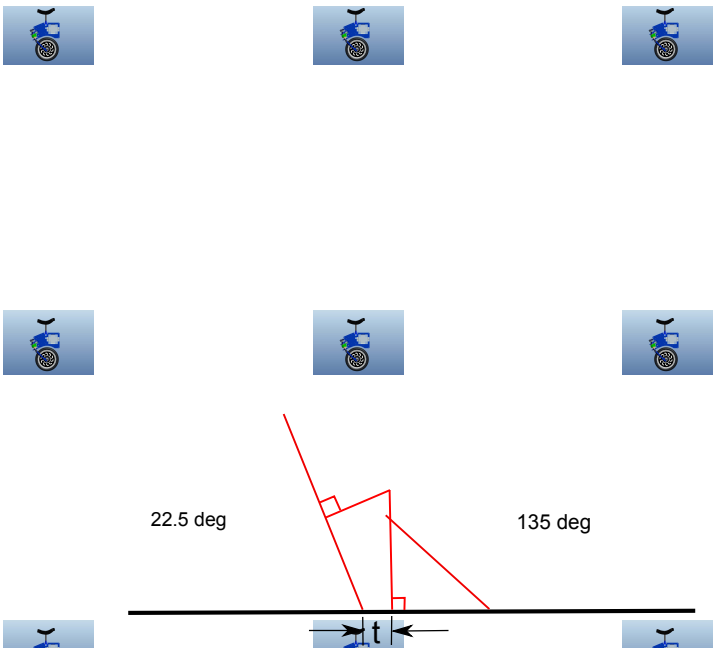

Figure 4.4.: Steering geometry angles (shown on final CAD model)

consideration is addressed in a number of aspects of the design, including the overall geometry, saddle selection and foot-peg positioning.

A rider cannot feel comfortable if they does not perceive the Micycle to be stable, and so the geometry is designed to ensure that the combined system of rider and Micycle is balanced while the rider is seated in a relaxed position. The saddle is upright, and the foot pegs are located on a vertical line through the rider's centre of gravity, so that the rider is leaning neither forward nor back when the Micycle is stationary. Hence, when traveling forward, the rider is inclined slightly forward, which is intuitive and natural.

The Micycle does not possess shock-absorbers to mitigate forces transmitted from bumps in the ground, but the rider is partly isolated by the geometry of the design. The inclined fork acts like a lever-arm that will flex slightly under shock loading, and absorb some of the energy of the impulse before it can reach the rider.

A cushioned unicycle saddle is provided, with a seat collar that allows height to be adjusted according to suit the preferences of the individual rider. This allows the Micycle to be ridden in a comfortable posture for extended periods.

The foot pegs protrude far from the hub-motor to aid with the rider's roll stability. Additionally, this spacing serves to prevent the rider's knees from knocking on any of the hardware.

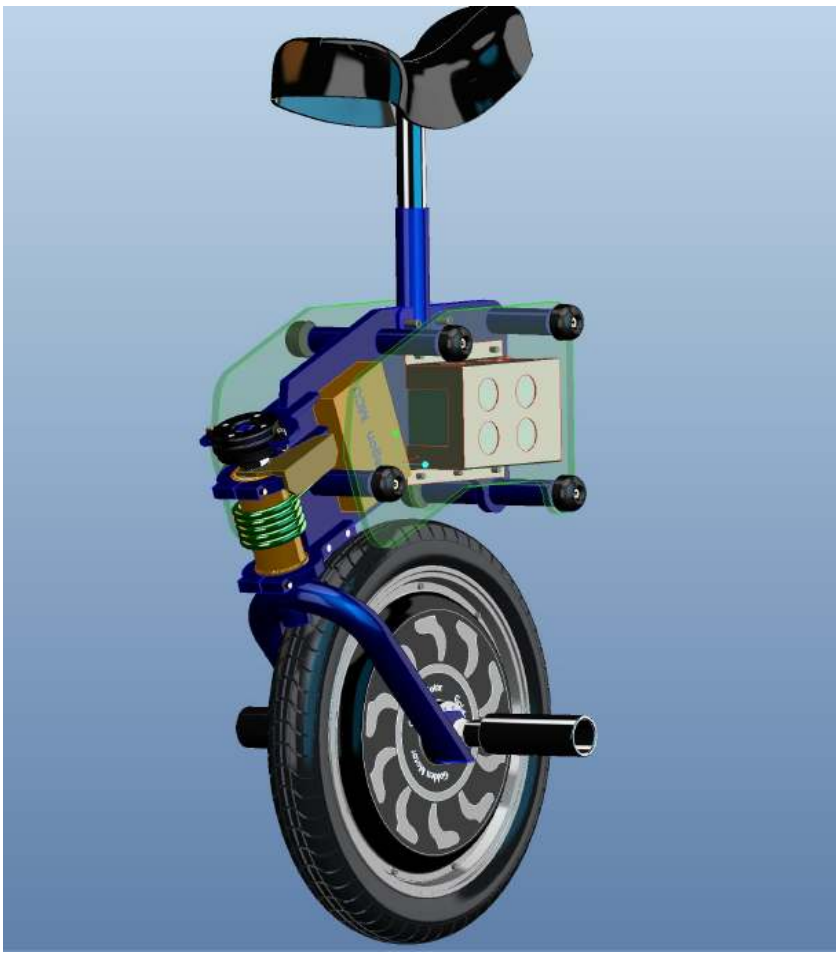

Figure 4.5.: The preliminary CAD model (with SLA batteries)

4.4. Preliminary CAD model

The above considerations led to the development of the preliminary CAD model (Figure 4.5). This model uses sealed lead-acid (SLA) batteries, as at that stage the budget did not have provision for the purchase of lithium-ion batteries. Also, as exact components were not known, the other component boxes are effectively placeholders.

Several changes were made to the preliminary model as exact components became known (see Chapter 5). Further changes became necessary when the mechanical design calculations, including ANSYS simulation, determined the final structural requirements (see Chapter 6).

Chapter 5.

Component selection

This chapter describes and justifies the selection the off-the-shelf components for the Micycle, while the integration of these components into the final design is described in the following chapter. These components include the rotary steering damper, the brushless hub motor, tyre and tube, seat and seat pole, motor controller, batteries, microcontroller and inertial measurement units. The selection of these components was largely driven by the desire to find the best suitable components and remain within budget. Some uncertainty about the final budget due to a pending grant application made it necessary to develop a contingency plan for the battery selection. Fortunately, the grant approval allowed purchase of adequate components for the project.

5.1. Steering damper

An ACE rotary damper was selected to provide steering damping for Micycle in order to improve the steering performance and subjective stability of the Micycle. This section explains the reasons for the use of the rotary damper and the sizing and selection procedure. In particular, it is noted that it is difficult to estimate the required damping torque with certainty.

The steering damper is required to reduce vibrations and oscillations in the steering arm of the Micycle. These disturbances may be caused by rough surfaces or through rider torque input on the foot supports. The damper improves the subjective stability of the Micycle by minimising the steering response to small disturbances, preventing vibration and accidental over steer.

It is difficult to accurately estimate the required resistive torque necessary to adequately damp steering vibrations. Too much torque results in a steering system which is too stiff and unresponsive, while too little torque means that the damper is ineffective. It is difficult to estimate the size of the input disturbances provided by the rider. In addition, the damping force provided by viscous dampers is proportional to the speed of the damper motion, so the required resistive torque at a given speed must be estimated.

The process used to calculate the required damping torque is based on estimating the appropriate resistive force in steering by the rider's feet. Some experimenting with

Figure 5.1.: Two ACE FDT-70 steering dampers

bathroom scales indicated that the steering force from the rider should be approximately a 20 kg force acting vertically down on the foot supports. This force should be sufficient to induce a rotation of 20 rpm (1 revolution per 3 seconds), and this turning speed should be appropriate for a translational speed of 10 km/h, based on observations of bicyclists and the motion of the Enicycle. Calculations based on the Micycle steering geometry show that this is roughly equivalent to an input torque of 15 Nm about the steering axis. Therefore, the required damping torque is 15 Nm at 20 rpm.

The two main types of dampers available are linear and rotary dampers. Linear dampers are more widely available and suitable for a greater range of damping force. However, when used in a rotary damping application, a linkage is required to connect the linear damper to the axis of rotation. This mechanism is less compact than for a rotary damper, which may be simply attached to the rotating shaft. However, rotary dampers are more difficult to obtain commercially and have a smaller torque range as the damping medium is located at a small radius from the rotating shaft. For larger required torques, the volume and weight of rotary dampers increases substantially. In addition, many rotary dampers have a limited action, or only rotate in one direction. While a rotary damper is desirable for its compactness in this application, it must provide the required damping torque, have sufficient angular range and bi-directionality.

The ACE FDT-70 is the largest, compact, bi-directional rotary damper that was found to be feasible for this project. The damper specifications are attached in Appendix F. The damper provides a nominal torque of 8.7 Nm at 20 rpm. This is less than the design torque, so two dampers were ordered, and the Micycle is designed to be used

with either one or two rotary dampers. This should provide some allowance for errors in estimating the design damping torque, and also allow for the steering stiffness to be coarsely adjusted for different riders. The delivered cost of two rotary dampers was $100.

In testing, it will be necessary to determine whether one or two rotary dampers are used.

5.2. Motor

The motor is a key component of the design. It drives the device and is the actuator of the control system. It is fundamental to the mechanical design; the motor specifications dictate the rest of the mechanical design. The hub motor chosen for the Micycle is the Golden Motor 'Magic Pie'. This motor is available in a number of configurations and the model selected is the MP-16F, which is a 16" cast iron, solid, front wheel motor. The motor was chosen based on three main criteria: cost, performance and compatibility of the motor with the rest of the design.

From prior research and the literature reviews, it was decided that a hub motor should be used. A hub motor is a motor integrated into a wheel, where the motor itself does not rotate, but rather the wheel rotates about the motor. A hub motor is particularly suited to the design as it prevents imbalances and eliminates backlash in the control system. A hub motor is a more elegant solution than a motor with a drive train.

The cost, performance and the integration of the motor with the rest of the design are the three main criteria used in choosing a suitable motor for the project. While not as crucial as these three key criteria, aesthetics are also important.

The motor needs to provide sufficient torque to actuate the system. The system is inherently unstable and thus adequate actuation is a safety critical requirement of the system to ensure that the motor does not saturate and potentially injure the rider. The motor also needs to have sufficient torque so that a speed of 15 kph can be achieved. Calculations found that the worst case scenario of required torque to be 11 Nm when the pitch angle of the vehicle was 2.5 degrees. This worst case situation at operating conditions was then multiplied by 2, due to it being a safety critical system, to give a required minimum torque of 22 Nm.

Cost is approximately $300 to $600 as this is what is permitted by the budget. The ability to integrate the motor with the rest of the design is a non-functional requirement and thus needs to be reviewed on a per motor basis. The specifications required for the design are given in Table 5.1.

This motor is within the allocated budget. The specific configuration retails at under $400 including shipping. This offers much better value than alternative motors. In general, 1 kW motors generally cost about $1000 whilst other similarly priced motors were much less powerful, ranging from roughly 200 W to 300 W.

Table 5.1.: Motor design requirements and specifications

	Design requirements	Golden Motor 'Magic Pie' MP-16F
Motor type	Hub motor	Hub motor, cast aluminium rim
Max. torque	$22\,\mathrm{N}\cdot\mathrm{m}$	$30\,\mathrm{N}\cdot\mathrm{m}$(see Section 10.1)
Supply voltage	24-48 V	24-60 V
Cost (delivered)	$300-$600	$400
Motor design	n/a	56 magnets, 56 poles, 63 slots

The Golden Motor Magic Pie produces sufficient torque for the design. Additionally, the motor has 56 magnets and 56 poles, allowing a smooth acceleration of the motor to be produced. It is also a brushless system, meaning that the motor produces less wear, less noise and higher efficiencies than brushed motors.

The motor is also compatible with the rest of the design. The compatibility with standard front bicycle forks ensures that matching components can be easily designed. This ensures a sound mechanical design that is easier to control and maneuver.

Therefore, the motor chosen is an acceptable trade off between the three key criteria of cost, performance and design compatibility. Additionally, it is aesthetically pleasing with its 'jet engine' hub design.

5.3. Tyre and tube

The tyre and tube requirements are dictated by the Magic Pie motor choice. A Schwalbe City Jet HS 257 16" Tyre is used in the project with a 16" Presta valve inner tube.

Although the motor has an inner diameter of approximately twelve inches, this corresponds to a 16" bicycle tyre (specified by outer diameter). Scooter and motorbike tyres are too thick for the motor and a bicycle tyre had to be used. Even then, the motor corresponds to a 16" bicycle tyre diameter and this is a relatively uncommon size for bicycle tyres with large tread width.

Tyre selection is governed by availability of tyres in this size. Tubed bicycle tyres are used as they are readily available. Both slick and treaded tyres are available, however, and slick tyres were chosen as it is not a requirement that the vehicle need to traverse off road. Slick tyres reduce the rolling resistance of the Micycle in operation. This decreases the drain on the batteries when the vehicle is in operation.

The inner tube used in the tyre is a standard Presta valve bicycle tube for a 16" tyre. This is commonly available, cheap to repair and easy to fix in the case of a puncture.

Figure 5.2.: Close up of tyre fitted to Magic Pie motor

5.4. Seat and seat pole

The selection of the seat, seat post and seat clamp was driven by cost, availability and compatibility. At the time of purchase, the seat was found on sale on Unicycle.com for $50. The seat pole and clamp were purchased to match the seat.

The seat is comfortable and has hard plastic sections on the front and back. These absorb impact and prevent damage to the seat fabric. The section on the front also acts as a hand grip. In addition, the quick release clamp and seat pole allows for easy adjustment of the seat height.

5.5. Motor controller

The Roboteq BL1500 controller and the Maxon DEC 70/10 are both suitable for the requirements of the project. However, the Maxon was used in the project due to sponsorship from Maxon Motors Australia.

For this project, the motor controller must be able to accurately scale the current output and rapidly switch between forward and reverse. The controller also must supply sufficient current and voltage requirements so that the motor outputs sufficient torque for balancing stability control. While the Magic Pie was supplied with an inbuilt controller, this is designed for an electric bike and only works in the forward direction. As a result, it had to be removed. However, the parameters of this controller are a guide to the

(a) Micycle seat (bottom)(Unicycle.com, 2010)

(b) Seat post (Unicycle.com, 2010)

(c) Seat tube clamp (Unicycle.com, 2010)

Figure 5.3.: Selected seat, seat pole and clamp

Figure 5.4.: Maxon DEC 70/10 motor controller (selected) (Maxon Motors, 2010)

Figure 5.5.: Roboteq BL1500 motor controller (considered suitable) (Roboteq, 2010)

Table 5.2.: Comparison of motor controller specifications

Manufacturer:	Maxon	Roboteq
Supply voltage	10-70 V	12-40 V
Maximum output current	20 A	70 A
Continuous output current	10 A	40 A
Switching time	50 Hz	62.5 Hz
Current controller bandwidth	300 Hz	n/a
Budget cost	$370	$420

requirements for a replacement controller. The inbuilt controller accepts a maximum of 60 V supply voltage and 20 A supply current. However, testing of the motor indicated that satisfactory performance can be obtained with 36 V, 10 A supply (see Section 10.1).

The final decision for the motor selection was between the Maxon DEC 70/10 and the Roboteq BL1500. The design team is of the opinion that the Maxon has better precision and is of higher quality, however, it is more expensive and has a lower current limit. The Roboteq controller appears to be more flexible in terms of upper current limits, however, the expected performance was unknown. Eventually, sponsorship from Maxon Motors Australia led to the purchase of the Maxon controller.

5.6. Battery selection

The two types of rechargeable batteries considered for use in the Micycle were sealed lead-acid (SLA) and lithium-ion (li-ion). The Li-ion batteries were considered as a preferred option due to their high energy density. However, they are expensive and require extra cell balancing hardware. SLA batteries were specified as second options as they are inexpensive. However, additional funding eventually allowed for the purchase of two lithium-ion batteries from Ping Battery.

The battery design requirements are based upon the goals and specifications (Section 3), wherein the Micycle is required to operate at one third of peak power for fifteen minutes. Assuming continuous operation at 10 A (the maximum continuous output

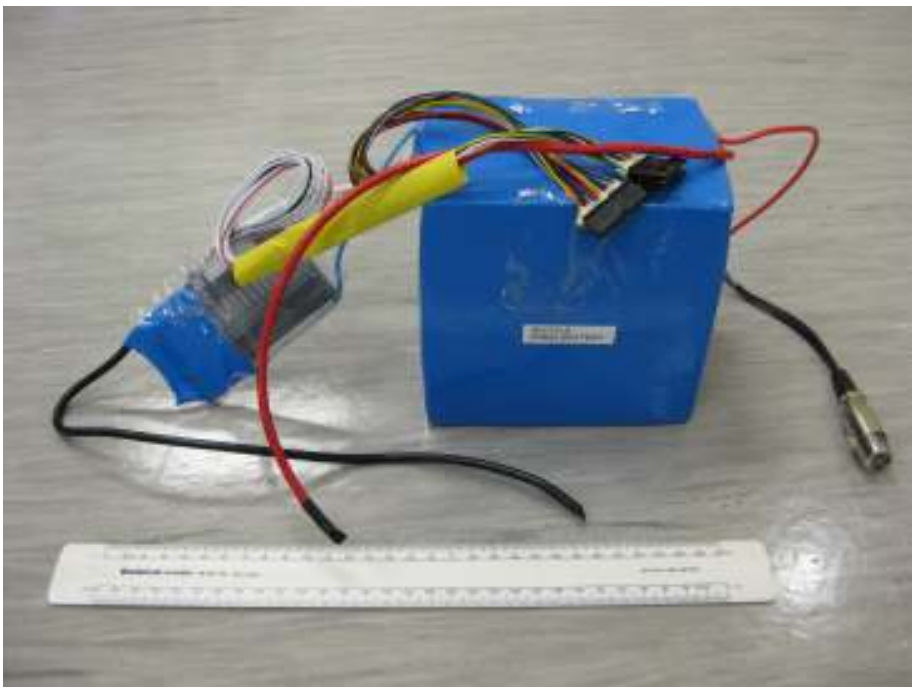

Figure 5.6.: 'Pingu' battery (1 of 2)

current permitted by the Maxon motor controller), the required battery capacity is 1 Ah, with a maximum continuous drain rate of 10 A.

However, while the above requirements adequately meet the project goals, a higher battery capacity was sought in order to allow for a safety factor, and for the purpose of exhibiting the Micycle at the University Open Day. The two options below both aim for 10 Ah capacity, which should provide one hour of operation at maximum continuous current load.

Table 5.3.: Comparison of LiFePO4 battery systems

Battery system type:	LiFePO4	SLA
Retailer	Ping Battery	JayCar
Dimensions (mm)	150x105x150	150x65x95
Voltage (V)	36	24
Capacity (Ah)	10	9
Max current (A)	40	135
Weight (kg)	3.5	5.1
Charge time (h)	2.5	n/a
System cost	$420	$100

Figure 5.7.: 1 of 2 required SLA batteries (JayCar Electronics, 2010)

5.6.1. Lithium-ion batteries

Li-ion batteries have the greatest energy density of rechargeable batteries, so they are suited to this weight restricted application. However, one concern is the volatility and cell balancing problems associated with Li-ion batteries. Cell balancing problems in Li-ion can be overcome with a charge balancing circuit (usually integrated into retail packs), however, this increases the relative cost of Li-ion batteries. Lithium-ion iron phosphate (LiFePO4) cells are a particularly stable type of chemistry and were selected due to the shipping difficulties (risk of explosion) associated with other chemical types of Li-ion cell.

Two LiFePO4 battery packs were selected for the Micycle. The LiFePO4 packs were sourced from Ping Batteries as the low cost allowed for purchase of two batteries. This permits continuous use of the Micycle while the other battery is being charged, which is expected to be useful for the University Open Day and the Project Exhibition.

The LiFePO4 battery specifications are given in Table 5.3.

5.6.2. Alternative option: Sealed lead-acid

SLA batteries are inexpensive. However, the low energy density and subsequent weight of the batteries means that they are less desirable than lithium-ion batteries for this application. Therefore, it was decided that this option would only be pursued if budget constraints did not permit the use of other expensive batteries. The SLA battery specifications are provided in Table 5.3.

5.7. Microcontroller

The project requires an embedded system which can provide all the functionality that the design requires. This is best accomplished using a compact microcontroller. The

Figure 5.8.: MiniDRAGON+2 development board (Wytec Company, 2010)

microcontroller which has been selected for this project is the HCS12 MiniDRAGON+2 Development Board with the MCP4725 I2C DAC daughter board.

There are a number of functional requirements dictated by the project's goals and specifications:

- Analogue and digital inputs and outputs.
- Multiple input/output lines.
- Pulse width modulation capabilities.
- Speaker or ability to output to audio.
- Compatibility with available integrated development environments.
- Easily accessible hardware connections to ensure rapid development of the system.
- Sufficient processing power to control the system.
- Sufficient voltage to interface with peripheral devices.
- Small physical footprint.

The HCS12 MiniDRAGON+2 Development Board address these requirements. The full specifications are extensive and can be found in Appendix F, but the relevant specifications are:

- Small PC board size: 3.25" X 4.75" or 3.25" X 3.35".
- 16 MHz crystal, 8 MHz default bus speed and up to 25MHz bus speed via PLL.
- Like Freescale EVB, supports C and Assembly language source level debugging using Code Warrior.

- On-board speaker driven by timer or PWM.
- Solderless breadboard.
- 8 16-bit timers
- 8 PWMs
- 16-channel 10-bit A/D converter
- 112 Pins, up to 89 I/O-Pins

The board meets all of the functional requirements but does not have the ability to output an analogue signal. This ability is met by using the MCP4725 I2C DAC daughter board. This provides the ability to output an analogue signal to the motor controller controller.

There are additional benefits to using the MiniDRAGON. Several group members have already used the Dragon family and this familiarity will ensure a faster development of software using the board. Additionally, the School has a large number of resources and has experience with using this family of microcontrollers.

5.8. Inertial measurement unit

Two different sensor options are available for control of the Micycle. A Microstrain inertial measurement unit (IMU) has been provided on loan by the University. This is an expensive component (~$3000), therefore, as an extension goal, sensing will also be attempted using a cheaper inertial measurement board. The required specifications and the specifications of both sensing devices are discussed below.

For the device to be reliably controlled, both angular position and angular rate must be measured directly. The angular position can be measured by an accelerometer, which as it rotates detects the change in the component of gravity vector perpendicular to the sensing axis. The angular rate can be measured using a single axis gyroscope to measure the angular rotation about the plane of the wheel. Of course, it is also possible to measure just one state with one of these sensors and derive the other state with the control logic. However, this is unreliable, as the accelerometer is prone to noise and vibration which severely limits the quality of the differentiated angular rate. Secondly, the gyroscope is subject to 'drift', meaning that the accuracy of the integrated angular position measurement decreases over time. Therefore a combination of both sensors is required.

5.8.1. Microstrain 3DM-GX2 IMU

The Microstrain 3DM-GX2™ is a high-performance inertial measurement unit which uses MEMS technology. It includes a triaxial accelerometer, triaxial gyro, triaxial mag-

Figure 5.9.: Microstrain IMU

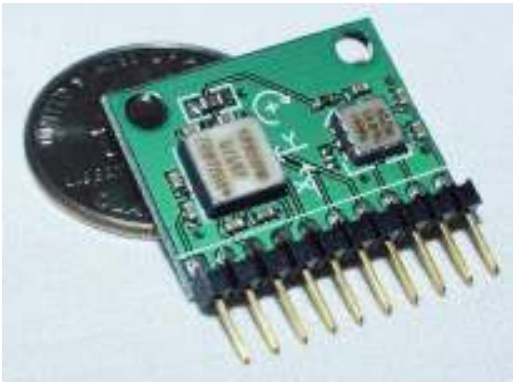

Figure 5.10.: SparkFun™ IMU Combo Board (SparkFun, 2005)

netometer and temperature sensors. The 3DM-GX2™ is able to output inertial measurements (acceleration, angular rate and magnetic field) which are temperature compensated and corrected for sensor misalignment. Angular rate quantities are further corrected for G-sensitivity and scale factor non-linearity to third order.

5.8.2. SparkFun™ IMU Combo Board

An 'IMU combo board' (ADXL203/ADXRS61x) from SparkFun™ (2005) is suitable for fulfilling the extension goal of replacing the Microstrain IMU with a cheaper model. This board is available with three different angular rate resolutions, with respective angular rate maximums of $300^\circ\,s^{-1}$, $150^\circ\,s^{-1}$, and $50^\circ\,s^{-1}$. It is difficult to estimate what the maximum angular rate of the Micycle will be during typical use. To determine this, the output from the Microstrain IMU will be measured during the initial testing of the Micycle so that the appropriate board variant can be ordered.

Chapter 6.

Mechanical design

This section details the design of custom components for the Micycle. These include the fork and spindle assembly, the chassis and enclosure, the spring design and the seat pole connection. Finally, a static structural analysis is performed on the critical components to determine both the minimum material strengths and design thickness. The design process focused on achieving five key goals: ease of manufacture, weight balance, durability, design flexibility and aesthetics.

6.1. Chassis and enclosure design

The chassis and enclosure design takes into account structural force requirements as well as the need to both protect and display electrical components. The chassis and enclosure consists of a central plate surrounded on both sides by parallel perspex sheets, attached with cylindrical spars with bump stop ends. This design is durable, readily replaceable and allows for flexibility of components and weight balancing. Finally, it allows for a more streamlined and self-contained design than that of the Enicycle or the Focus Designs SBU.

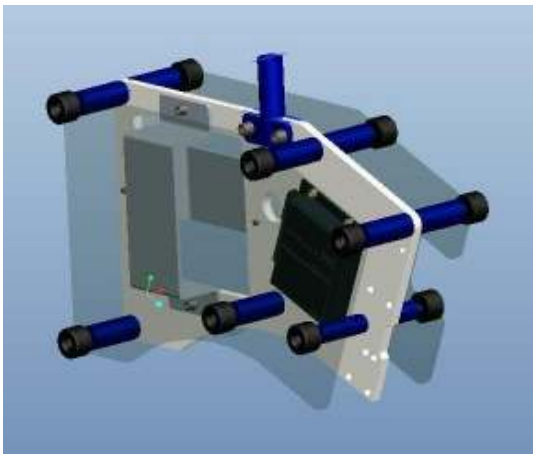

Figure 6.1.: Final chassis and enclosure design

Figure 6.2.: The mannequin used to calculate the centre of mass

6.1.1. Chassis plate

The chassis plate functions as a structural member, distributing the force from the seat to the spindle and fork assembly. Secondly, it acts as an anchoring and support point for the electrical components. This plate design has several advantage for the Micycle. First, it allows flexibility in that the locations of certain components can be modified by drilling new holes, without needing to modify the entire design component. Secondly, through its dual function, it is more aesthetically pleasing than using a beam for a structural member with several protruding component boxes. Finally, it allows for the different components to be laid out in clear view for educational purposes.

The material specified for the base plate is 5005 aluminium with a tested yield strength of 180 MPa. This was formulated from the ANSYS simulation, outlined in Section 6.4. The use of aluminium minimises the weight while providing adequate strength, and good machinability and resistance to corrosion.

6.1.2. Seat pole connection and mass distribution

The connection between the seat, seat post and the plate design is required to be adjustable. This was permitted through the use of a unicycle specific seat and seat post clamp an aluminium tubing connector, as shown in Figure 5.3, as generally used on bicycle and unicycle seat post clamps. The connector is welded to the plate, permitting the seat to be adjustable.

Furthermore, the weight bias of the Micycle is a critical requirement of the design to allow the Micycle to balance in an upright position. ProE was used in calculating the centre of gravity of the Micycle, both on its own when combined with a mannequin

placed on the model. As the rider's legs have the effect of moving the combined centre of gravity forwards, the seat position must be placed slightly to the rear of the Micycle.

6.1.3. Component enclosure

The enclosure of the electrical components is an integral part of the design. The enclosure consists of two cover plates which protect the microcontroller, extension boards, motor controller, power circuitry and batteries. Perspex sheeting was selected, but sheet metal and perforated sheet metal were also considered.

The enclosure is required to address several design criteria related to functionality, safety and durability. The design allows the user easy access to the batteries and electrical components by removal of cover plates. The strength of the enclosure is integral as it is required to provide resistance to collisions and wear and isolates the user from electrical shock.

Sheet metal option was considered less preferable as it does not provide the strength required, lacks electrical insulation and has sharp edges that could perforate the user in the event of a collision. Due to this, the option was not developed during the design process.

Perforated metal would provide the design with the strength required to support the rider and house the components. However, it was feared that the material would become easily scratched and lose its aesthetic appeal. In addition, water can permeate through the structure.

The perspex option is not as effective as a support structure and may become scratched through use. However, it is aesthetically pleasing, provides insulation from the electrical components and allows the user to visually observe the system without having to dismantle the housing. Furthermore, indicator lights for braking or turning may easily be added as a feature later. Finally, as the project acquired funding to exhibit the project at the University Open Day, the increased transparency of the design was a desired attribute.

6.1.4. Combined chassis design

The final design is a hybrid of an aluminium plate to attach the electrical components, including a clamp setup to attach the batteries, with a perspex window fitted with rubber grommets to reduce wear and cracking of the perspex. This aesthetically pleasing design addressed the design criteria, while allowing the electrical components to be visible.

The decision was made to leave the top and sides of the enclosure open, as the risk of dirt or water entering with the intended use is low. This allows for simple construction and easy access during the testing and educational phases of the build process. In the future, additional perspex plates could be added to fully enclose the electrical components.

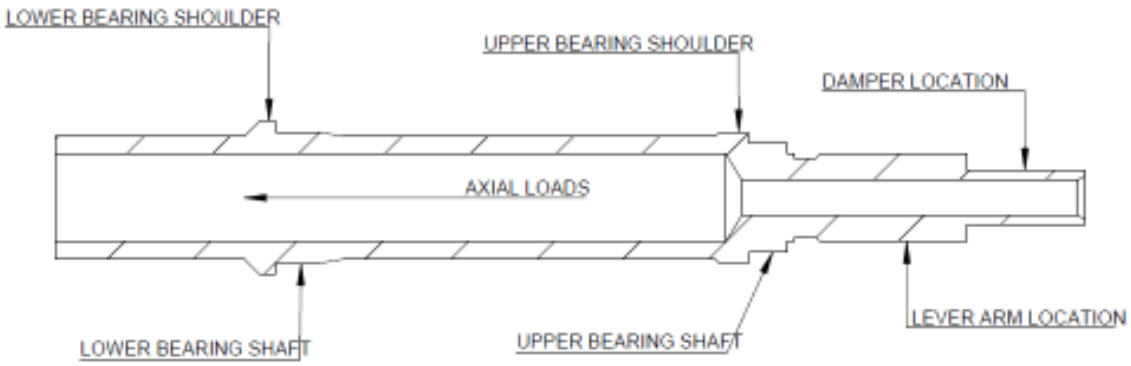

Figure 6.3.: Spindle cross-section

The final design, as shown in Figure 6.1, incorporates aluminium spacers, rubber grommets and bash plates as this is the area of the Micycle that absorbs the majority of collisions. These extra features are necessary to increase the rigidity of the design and provide the spacing required for the electrical components. While this is only a prototype design, these measures are necessary to increase the lifetime and functionality of the device.

6.2. Fork assembly

The fork assembly incorporates the spindle, fork and steering lever. The spindle attaches the chassis to the fork while the fork provides the geometry required to attach the asymmetric motor such that its rim is centrally located. The lever arm allows connection of the torsion spring to the fork and acts as a steering stop in combination with the chassis plate.

6.2.1. Spindle

The spindle of the fork assembly is the central component that is used to attach the chassis to the motor and fork assembly. As this component is subjected to the greatest loads, it has been analysed with manual calculations and ANSYS simulations to determine an appropriate combination of material and part thickness (see Section 6.4).

The static structural analysis results indicate that the fork assembly, inclusive of the spindle, should be manufactured from a material with yields strengths in excess of 310 MPa. In light of these results 4130N “chromoly” alloy steel, with minimum yield strength of 480 MPa was selected.

The spindle was designed as the shaft for the slim series SKF 619052RS1 and 619062RS1 bearings, FDT-70 rotary dampers and the lever arm. The vital dimensions are constrained by the bearing and damper choice for shaft diameters and profiles at differing

locations. The two bearings chosen are of differing sizes to allow the slightly larger lower bearing to slide over the shoulder of the upper bearing's location.

The chosen bearings have an radial static load rating of:

$619062RS1 \;\; C_O = 4.55\,\text{kN}$

$619052RS1 \;\; C_O = 4.3\,\text{kN}$

The bearings have a load rating of up to $0.5C_O$ kN axially (Axial Load Factor) .

The total load rating of the bearings is defined by Equation 6.1.

$$P_n = X_o F_r + Y_o F_a \tag{6.1}$$

$X_o = Radial\,Load\,Factor$

$Y_o = Axial\,Load\,Factor$

$F_r = Actual\,Radial\,Load\,\text{kiloN}$

$F_a = Actual\,Axial\,Bearing\,Load\,\text{kilo}$

This allows the axial loads through the spindle to be distributed on two shoulders as compared to one, as would be the case of two bearings separated by a spacer bush. This also has the benefit of distributing the axial loads between the two bearings. The distribution of these axial loads is of importance since the bearings chosen are a single row deep grove ball bearing design. This design type has limited thrust load capability.

6.2.2. Fork

The fork design addresses two major issues. These are the asymmetrical motor rim combination, and fork geometry requirements for the steering system. The Magic Pie motor has an offset centre plane which is required to be aligned with the centre plane of the spindle. Failure to realign these planes would result in the tyre being in a plane that is not central to the rider. As such, the fork legs are offset.

The forks also incorporate rubber bump stops attached to the ends on the horizontal section to reduce damage to the Micycle in case of collision. The bump stops should also reduce the shock to electronic components with in the Micycle. The simple design permits ease of manufacture using the TIG welding process and 4130N alloy steel still has sufficient machinability to allow the spindle to manufactured on a lathe.

Figure 6.4.: Fork assembly model

6.2.3. Steering lever

The steering lever assembly acts as a mechanism to attach the restoring force torsion spring to the fork assembly and to limit the ultimate steering travel. The lever assembly is shown in Figure 6.5.

The lever is attached to the fork spindle by means of a slotted hole at the location described in Figure 6.3. Thus, the lever's angle is locked to that of the fork and changes in relation to the chassis assembly under steering action.

The torsion spring is attached to the lever by means of a block machined into a complex shape to allow clearance of the upper split ring collar. The spring is mounted in a through hole of this block and positively locked with a set screw.

The maximum steering lock has been fixed at $\pm 15^o$ from the straight ahead position. This is achieved by the lever being symmetric to both sides of the chassis back, with the ends of the lever cut at the appropriate angle so as to meet the cover plate at $\pm 15^o$to provide a lock stop.

6.3. Spring design

The torsion spring mounted on the rear of the Micycle acts to centre the steering so that the wheel re-aligns to its nominal position after the rider equalises pressure on the foot pegs upon completion of a turn. The dimensions of the spring were constrained by the frame design, and the spring rate was determined by the geometry of the frame and angle of tilt at full lock, which is 15 degrees. The final spring design is shown in Figure 6.6.

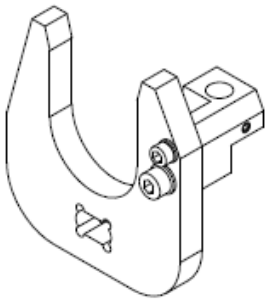

Figure 6.5.: Lever arm assembly

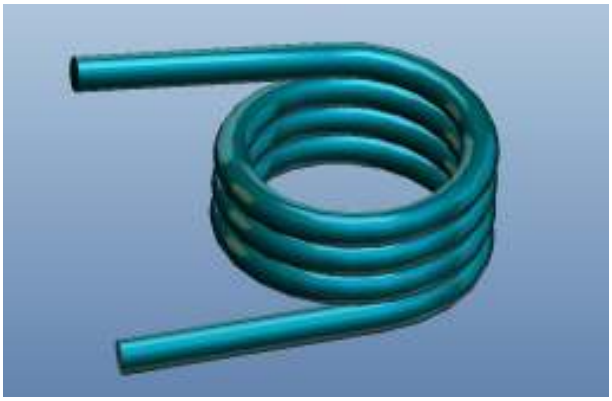

Figure 6.6.: A rendered image of the final torsion spring design

The spring was custom-made by Industrial Engineers and Springmakers according to the following specifications:

- Inner diameter = 65 mm
- Wire thickness = 11.1 mm
- Number of active coils = 3.6
- Arm length = 80 mm
- Tangential arms - parallel and unidirectional

The torsion spring was designed from first principles using the third-party spring calculation software, MITCalc (MITCalc, 2010). The restoring torque needed to right a load of 100 kg from a 15 degree angle of tilt, given the geometry of the Micycle chassis, was calculated to be approximately 3 Nm/deg, and this value was used as the design spring rate.

The inner diameter of the spring was required to be greater than 55 mm to fit over the bearing sleeve of the fork assembly. The inner diameter of a torsion spring expands and contracts as the arms are deflected under loading. The resultant inner diameter, D_Θ, of a

torsion spring under deflection is given by Equation (6.2). (Spring-Makers-Resource.net, 2010):

$$D_\Theta = \frac{DN}{N + \Theta} \tag{6.2}$$

Where:

D = Nominal inner diameter

Θ = Number of revolutions of deflection

N = Number of turns

The final diameter after contraction at full lock is 64.25 mm, which is ample clearance for the bearing sleeve.

The length of the spring is constrained by the spacing between the split ring collars on the steering assembly, and was required to be no greater than 100 mm. The theoretical length of the final design iteration was 51 mm. The spring arms were required to be 80 mm in length and tangential in order to interface properly with the steering assembly and chassis plate.

The design process assumed that the material properties were as specified in the Australian Standards for cold-worked carbon steel spring wire (Standards Association of Australia, 2003).

The torsion spring was designed with fatigue loading in mind, and is able to withstand shock loading should the rider shift weight suddenly. It can be expected to endure 500,000 loading cycles, which is sufficient for the life cycle of the Micycle.

The spring is powder-coated in blue to match the overall visual theme of the Micycle.

6.4. Static structural analysis

A static structural analysis was perform on the Micycle model to ensure the structural integrity of the Micycle chassis. This analysis combined manual hand calculations with ANSYS modeling utilising the Workbench 11 environment for the analysis of the Micycle fork, steering and chassis plate assembly.

6.4.1. Analysis goals

It was decided that a margin of safety of 1 based on a 100 kg rider should be the goal for the Micycle design. The analysis was performed by simulating the full weight of the rider acting through the seat in order to produce a conservative analysis.

6.4.2. Manual calculations

Manual calculations involved constructing a free body diagram used for calculating moments and reaction forces described in Figure 6.7. Forces perpendicular to the bearing shaft could then be calculated. These forces were then applied in the following ANSYS simulations.

Initially the design failure load was calculated using Equation (6.3)

$$Margin\,of\,Safety = \frac{Failure\,Load}{Design\,Load} - 1 \tag{6.3}$$

Hence,

$$Failure\,Load = Margin\,of\,Safety \times Design\,Load + Design\,Load \times 1 \tag{6.4}$$

Then the minimum design Failure Load $= 2000\,\mathrm{N}$.

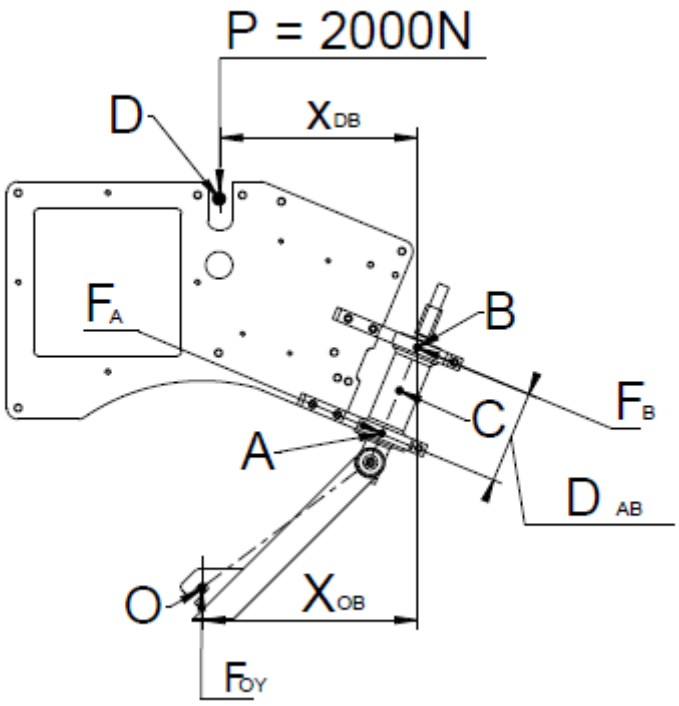

Figure 6.7.: Free body diagram

The manual calculations involved calculating moments about **B** due to load **P** described in Equation (6.5).

$$M_B = P \times X_{DB} \tag{6.5}$$

This moment is equivalent to the couple produced from F_B and F_A acting on points **A** and **B** either side of **C** as described in Equation (6.6),

$$M_{Couple} = (F_B \times d_{CB}) + (F_A \times d_{CA}) = M_B \tag{6.6}$$

Using these conditions F_A & F_B could be calculated. Since F_A & F_B are both equal in magnitude and parallel with opposing directions they act as a couple on the bearing sleeve, therefore,

$d_{CA} = d_{CB}$

$F_A = F_B$

To balance the static model the reaction force at **O,** $F_{oy}$is required to be 2000 N upwards and vertical to prevent the model being statically indeterminate.

Therefore,

$P = -F_{OY}$ and $\sum F_Y = 0$.

$X_{OB} = X_{DB}$

This allows $\sum Moment = 0$ as described in Equation (6.7)

$$F_{O_Y} \times X_{OB} = P \times X_{DB} \tag{6.7}$$

This assumption was made as it is reasonably close to the physical model, though not strictly correct as the self weight of the Micycle has been omitted from the analysis and the position of load P is not directly aligned with point **O**. The variation at the current time is approximately 20 mm. This approximation allows for a simplified manual calculation as the model would otherwise be statically indeterminate, as it is only simply supported at **O**.

Other dimensional variations from the model include small changes in component geometry made subsequently during the ANSYS analysis iteratively to ensure that the Micycle met the analysis design goals.

6.4.3. ANSYS methodology

The ANSYS simulation used attached ProE parts in the simulation environment all

This section details the design of custom components for the Micycle. These include the fork and spindle assembly, the chassiowing for model changes to be performed in ProE. This allowed for easier model manipulation than in the 'Workbench Design Modeler' environment.

Initially it was attempted to simulate the chassis back, steering linkage and forks as one assembly. This proved to be problematic with multiple contact regions. It was found

that with contact regions set to "bonded" ANSYS would converge on a solution for the simulation. This was deemed to be insufficient as the joint between the chassis plate and the split ring collars involved bolted connections and the bonded connections bonded all faces in contact and did not realistically represent the model.

To remedy the situation 'Pinned connections' were attempted in the model for the split ring collar parts and bolts. This also proved problematic to solution times and convergence due to node limitations and difficulty constraining parts from free body motion warnings in ANSYS.

To reduce processing time for the model the 'direct solver' was activated as per the suggestion of ANSYS. The simulation was run multiple times with differing mesh sizes for the overall mesh sizing, contact sizing and face sizing in critical areas. The results from these simulations showed a lack of convergence with stresses not converging to within 2%.

Following these simulation runs the solver was set to 'program controlled iterative solver'. The model proved to be too large and resulted in memory shortages and resulted in system aborted the simulations.

To rectifying these difficulties small chamfers, rounds and threads were removed from the assembly components to simplify the mesh and reduce the risk of poor mesh warnings and errors. The bearings were replaced with plain cylindrical thick wall tubes, the chassis plate removed and the split ring collars omitted from the simulation. Loads were then applied to the locations of the split ring collars with the 'bearing load' conditions set. This allowed only compression loads to be transmitted to the bearing sleeve. The contact conditions between remaining contacting surfaces was set to the "no separation" condition and contact sizing was applied to the faces in question. The solver chosen was the 'iterative solver' with the magnitude of the loads set to the values calculated in the manual hand calculations.

The split ring collars and chassis plate were then simulated as individual components with the mesh density was increased at critical locations using loads calculated from the free body diagram. These simulations were then run multiple times with increasing mesh densities till the von Mises stresses converged to 2%.

The chassis back had a further buckling analysis performed using the results of the static analysis of the chassis back.

The results from the simulations allowed refinements to be made to the model. Where stresses were found to be excess of the specified material's yield strength, the components were altered in the ProE environment and updated to the simulation model to be re-run. This iterative process was used until the model was consistent with the design goal of a margin of safety of 1.

6.4.4. Analysis results

Manual calculations

The results from the manual calculations using the methodology described in Section 6.4.2 are:

- $P \,\&\, F_{OY} = 2000\,\mathrm{N}$
- $F_A \,\&\, F_B = 4159\,\mathrm{N}$
- $M_A = M_B = Couple_{AB} = 416\,\mathrm{N\,m}$

The manual calculation results were used for two purposes, firstly the $F_A \,\&\, F_B$ results were used in the selection of the bearings specified in Section 6.2.1. Secondly all the results were then used in the ANSYS simulation as loads with the moment used to used to verify the ANSYS model by checking ANSYS' moment reaction. These manual calculation however do contain some assumptions that need to be addressed with further work.

ANSYS

Results for stresses in the fork assembly

$\sigma_{max} = 311\,\mathrm{MPa}$

Represents the maximum von Mises stress in the fork located near the base of the bearing spindle shown in Figures 6.8 and 6.9. The material used for the fork is "chromoly" alloy steel of grade 4130 in normalised condition with yield strength well in excess of $480\,\mathrm{MPa} - 590\,\mathrm{MPa}$ dependent on the normalising performed (Fischer, 2006, p. 133). With welding and air quenching the yield strength may be reduced in the order of 15% in the weld zone (Swaim, 2001).

$M_{Reaction} = 434\,\mathrm{N\,m}$

The moment reaction was calculated in the horizontal component of the fork. This value matches the manual calculations to an accuracy of 4%. Variation can be attributed to the manual calculation model having slightly differing geometry to the final ANSYS simulation model.

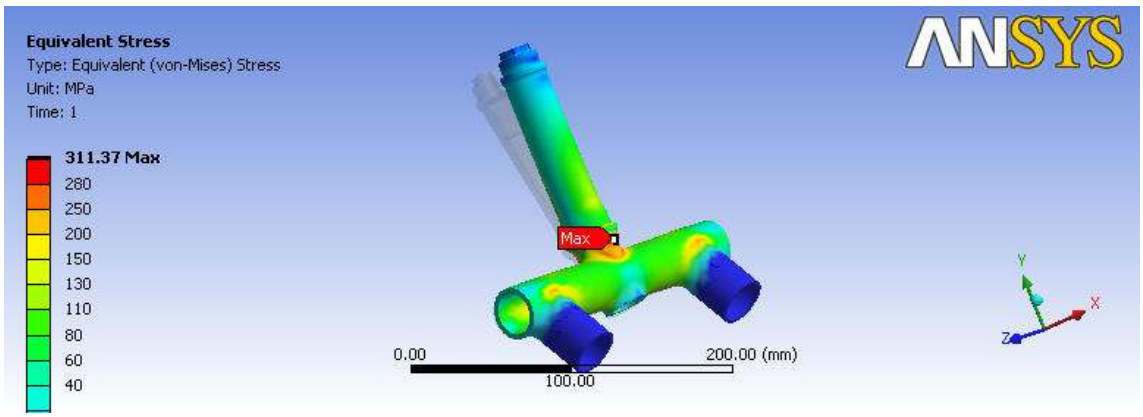

Figure 6.8.: Fork assembly von Mises stresses when subjected to loads

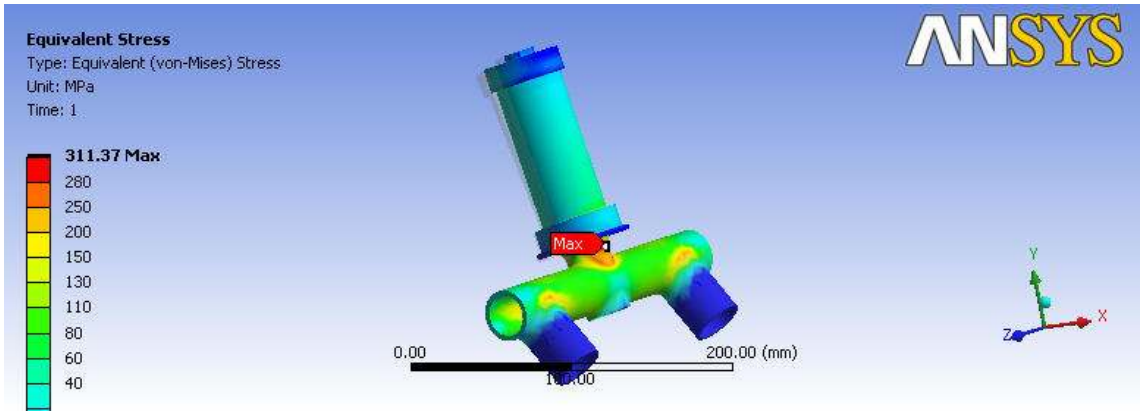

Figure 6.9.: Assembled fork assembly when subjected to loads

Results for the upper split ring collar

$\sigma_{max.probe} = 64.0\,\text{MPa}$

$\sigma_{max} = 129\,\text{MPa}$

The two solutions represent different areas on the collar, Figure 6.10. The "probe" value is represents the maximum stress on the inner surface of the split ring. The second value shows the maximum stress located near the bolted connection used to clamp the split ring.

The 128 MPa result is not of any real value itself as it is situated on a sharp square edge with no rounding. These situations cause FEA programs to inflate the stress, as the edge is modeled as a sharp edge of infinitesimal sharpness. The stress calculated becomes depended on mesh density and its proximity to an impossibly small edge which is a stress raiser. The values in the near vicinity of this maximum are important, however, and clearly there are no problems with stresses approaching the yield strength of the component's material.

The material specified for this part and subsequently all aluminium components on the Micycle is 5005 grade aluminium with a yield strength of 180 MPa.

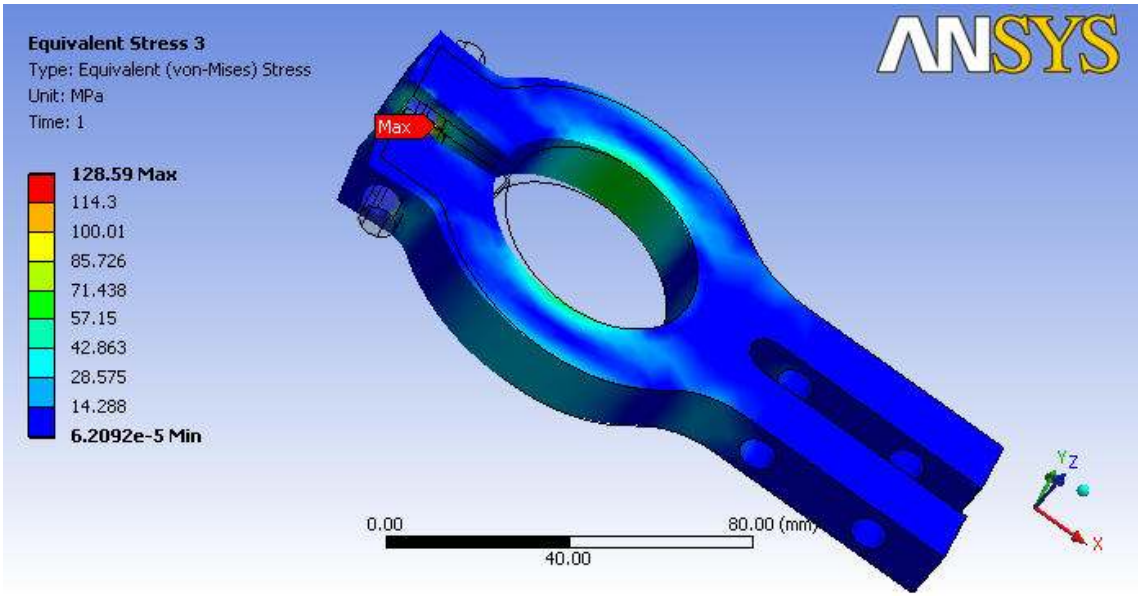

Figure 6.10.: Stress on upper split ring collar when subjected to loads

Results for the lower split ring collar

$\sigma_{max} = 14.7\,\text{MPa}$

The location of the probe in this simulation is the small curved other surface behind the maximum tag on Figure 6.11. All locations on the component are the yield strength of the component's material.

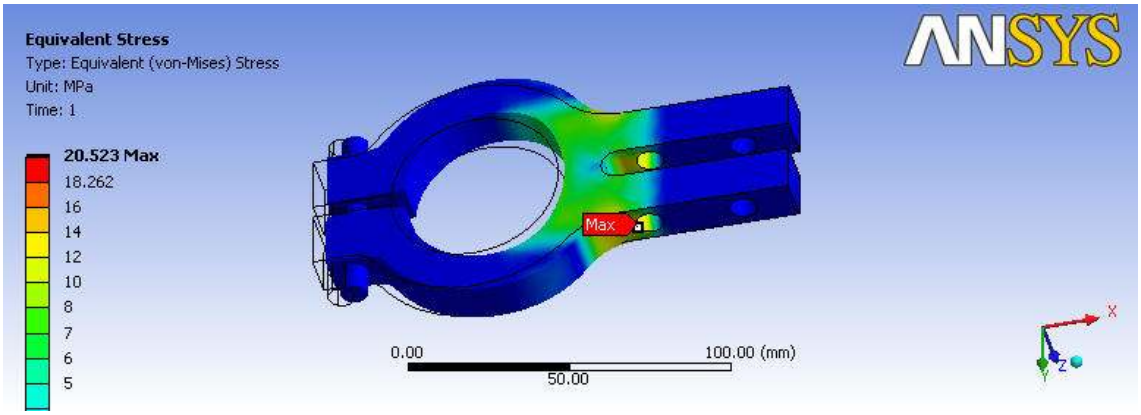

Figure 6.11.: Stress on lower split ring collar when subjected to loads

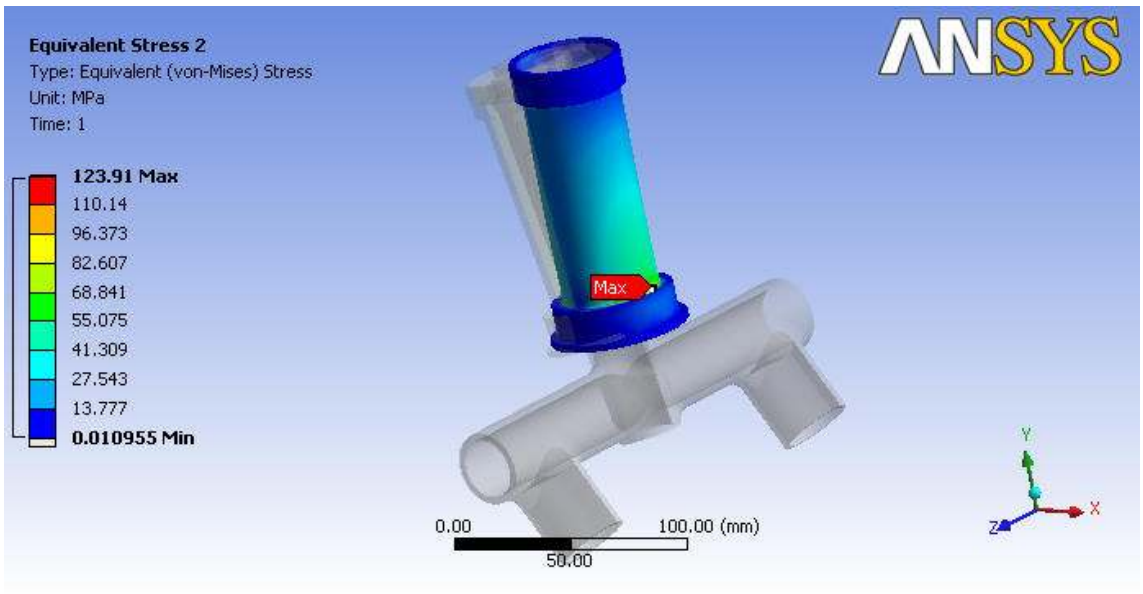

Figure 6.12.: Maximum stress location on bearing sleeve

Results for the bearing sleeve

$\sigma_{max} = 124\,\text{MPa}$

Figure 6.12 shows the maximum stress located at the corner of the base. The model has since changed to include a large round between the two cylindrical faces to reduce any stress raiser effects from the geometry.

Results from the pre-stressed buckling analysis of the chassis plate

$Load\,Multiplier_{Buckling} = 38.8$

The "Load Multiplier" in ANSYS refers to a factor that is applied to the load to determine the critical buckling load. When the load multiplier is above unity, the load applied is lower than the critical buckling load, hence a value lower than unity implies that the critical buckling load has been exceeded.

The value of 38.8 shows a large safety factor in buckling. This result alone can be deceiving as this simulation represents the ideal loading condition which is not likely to occur at significant loads. The Micycle during operation is likely to experience loads which are not in the same plane as that of the plate. This can be caused by differential pressure on the foot supports and the rider's bodily movements.

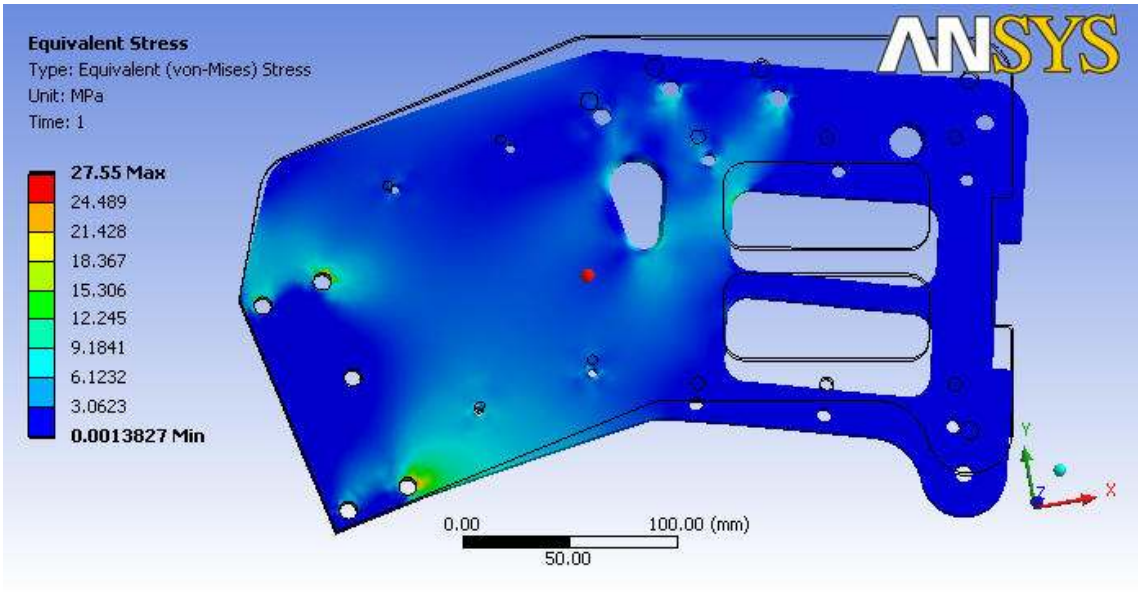

Figure 6.13.: Chassis plate stress when subjected to loads

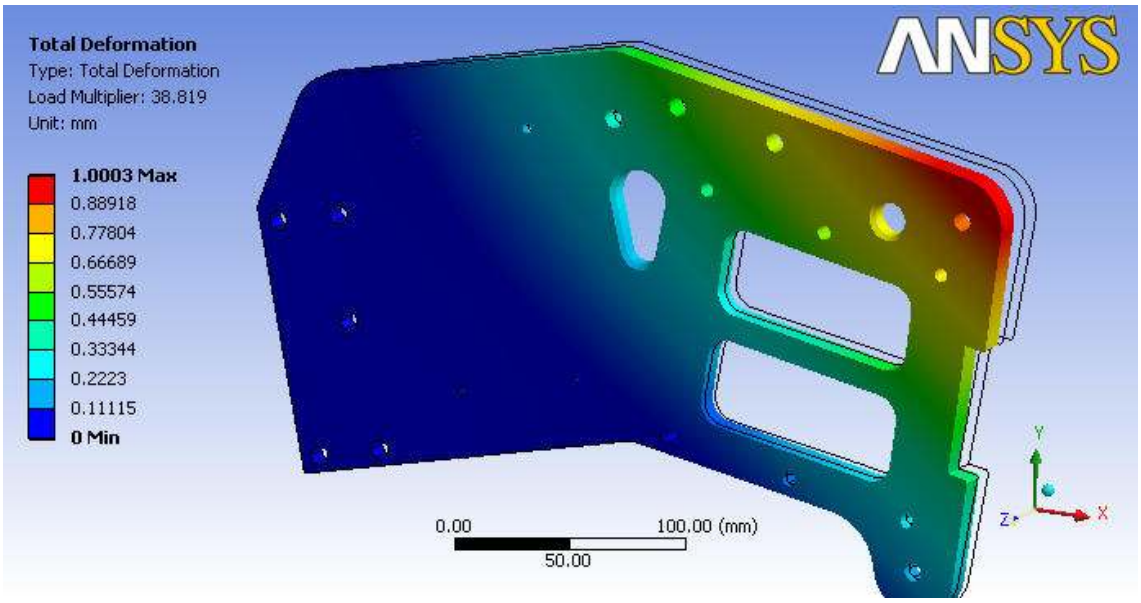

Figure 6.14.: Chassis plate total deformation

6.4.5. Conclusion

Analysis of the Micycle chassis utilising the manual and ANSYS techniques has shown the chassis meets the design goal of supporting a 100 kg rider with a margin of safety of 1. Further refinements to this analysis are currently being made to improve the manual calculations and subsequent ANSYS simulations.

Chapter 7.

Electrical design

This chapter documents the electrical design of the Micycle. This involves the design of the interfacing between components and circuits required to supply power to the sensors, motor controller and MiniDRAGON+2. The electrical functional diagram is presented at the end of this chapter, in Figure 7.2.

7.1. Component integration

The component integration outlines the interfacing required between the motor, motor controller and microcontroller. The interfacing between the various sensors and the microcontroller is also discussed.

7.1.1. Motor to motor controller interface

The motor to motor controller interface requires the correct orientation of 3 hall sensors and 3 motor phase windings, permitting a total of 36 different combinations. The correct wiring configurations for the motor and motor controller was visually verified by the increase in performance of the motor while in this configuration. The addition of motor chokes, which are currently being designed, will further increase the performance of the motor.

Figure 7.1.: The minimum setup required for the interface between the microcontroller and motor controller

There are three connections for phase windings and three connections for hall sensors on the motor controller. This means that there are 3x2x1 = 6 possible combinations that the phase windings can be connected and the equivalent number of combinations for the hall sensors. This leads to 36 combinations in which the hall sensors and motor phase windings can be connected. As the hall sensors and phase windings are related, only 6 of these combinations will result in correct functionality of the motor, even then three of these will be in reverse. Thus, to determine which combination should be used, the hall sensors were held fixed whilst each combination was tried for the motor phase windings. The correct orientation of the motor windings and hall sensors increases the controllability and performance of the motor.

The performance of the motor was being reduced by the motor controller restricting the output current to the motor because of low motor impedance. This issue is alleviated though the use of motor chokes. The chokes are currently being designed by the School Workshop and use ferrite cores to increase the impedance of the motor, hence permitting increased output current from the motor controller.

7.1.2. Microcontroller to motor controller interface

The interface between the microcontroller and motor controller is determined by the current control mode used by the motor controller. This requires a 0 to 10 V output from the microcontroller, for set point adjustment, and an external switching circuit, to switch between forward and reverse operation.

The microcontroller requires a digital-analogue converter (DAC) daughter board to convert the digital microcontroller output signal. Furthermore, the analogue signal is required to output a voltage between 0 and 10 V; this is permitted through the use of an operational amplifier. The motor controller also provides the microcontroller with the ability to track the speed and torque output of the motor.

The microcontroller provides the motor controller with the external set value. The set value ranges from 0 to 10 V with 0 corresponding to off and +10 corresponding to full. The forward and reverse function is determined by the external switching circuit connected to port 17 and 20. This switches the commutation of the motor between forward and reverse. These functions are shown in Figure 7.1.

7.1.3. Sensors to microcontroller interface

The MiniDRAGON+2 requires input from the Microstrain IMU, battery level display and manual gain adjuster to address the primary goals. Additional inputs from strain gauges and SparkFun IMU are used to address the extension goals. Furthermore, a data logging output is required to address another extension goal. The specifications of these components, connections and form factor are shown in Table 7.1. The interface required between components is shown in Figure 7.2.

The Microstrain IMU is interfaced with the microcontroller through a serial connection. The battery level display is implemented using a voltage divider, to restrict the voltage to between 0 to 5 V, from the battery to allow the microcontroller to determine the current voltage level. This will be interfaced with an light emitting diode (LED) array to allow the user to visually determine the current voltage level. The data that this provides will allow the software to regularly adjust the gain of the control system to levels dependent on the voltage being applied to the motor.

The manual gain adjuster is designed to allow the user to manually adjust the performance of the Micycle through a simple digital interface. The digital interface is a simple four button pad that has levels from 0 to 3 corresponding to the rider's required level of performance.

The Spark Fun IMU is interfaced with the microcontroller through an analogue circuit. The strain gauges are designed to provide the software with input proportional to the riders weight and therefore provide the controller with the ability to automatically adjust the controller gain to suit the user.

The data logging output provides the ability to diagnose errors and track changes to the microcontroller. This is currently being specified and requires an additional daughter board to be purchased.

7.2. Power distribution

The power distribution chapter outlines the component specifications and connections required for the design of a circuit board to distribute the required power to the various components. The initialisation procedure is also discussed and it is integral to the functionality of the electrical design.

7.2.1. Power distribution board

The electrical functional diagram, shown in Figure 7.2, provides an overview of the circuit design required to implement the electrical design required for the project. The design of the power distribution board will be undertaken with the guidance of the SchoolWorkshop based on the component specifications listed in Table 7.1.

The construction of the electrical circuit board will be undertaken by the School Workshop. Further design, to allow the extended goals to be completed, will be undertaken through direct consultation with the Workshop and adhere to the general constraints discussed above.

7.2.2. Initialisation

The initialisation procedure of the electrical components allows the various sensors to be initialised before the microcontroller. The sensors are required to be initialised before

the microcontroller as this allows the sensors to be active during the microcontroller boot procedure. This alleviates potential faults created by the microcontroller not interfacing with the sensors. Capacitors will be used to initialise these components in the correct order and will be determined by the start-up times of the components, with the IMU intended to be the first component.

The IMU initialisation will precede the other components, therefore, the initialisation procedure will be designed around the start up time of the IMU. This design will be undertaken in consultation with the School Workshop and in conjunction with the design of the power distribution board.

Component	Part No.	Form Factor (mm)	Output (V)	Supply (V)
Microstrain IMU	3DM-GX2	41x63x32	n/a	5.2-9
SparkFun IMU*	ADXL	18x18	0-2.5	5
Motor controller	DEC 70/10	103x120x27	9-63	10-70
Data logger*	n/a	n/a	n/a	n/a
MiniDRAGON+2	HCS	83x85	Multiple	9
Strain gauge*	n/a	n/a	n/a	n/a
Manual gain adjuster	n/a	n/a	n/a	n/a
Power distribution board	n/a	max. 100x80	Multiple	36

Table 7.1.: Electrical component design specifications (*denotes extension goal)

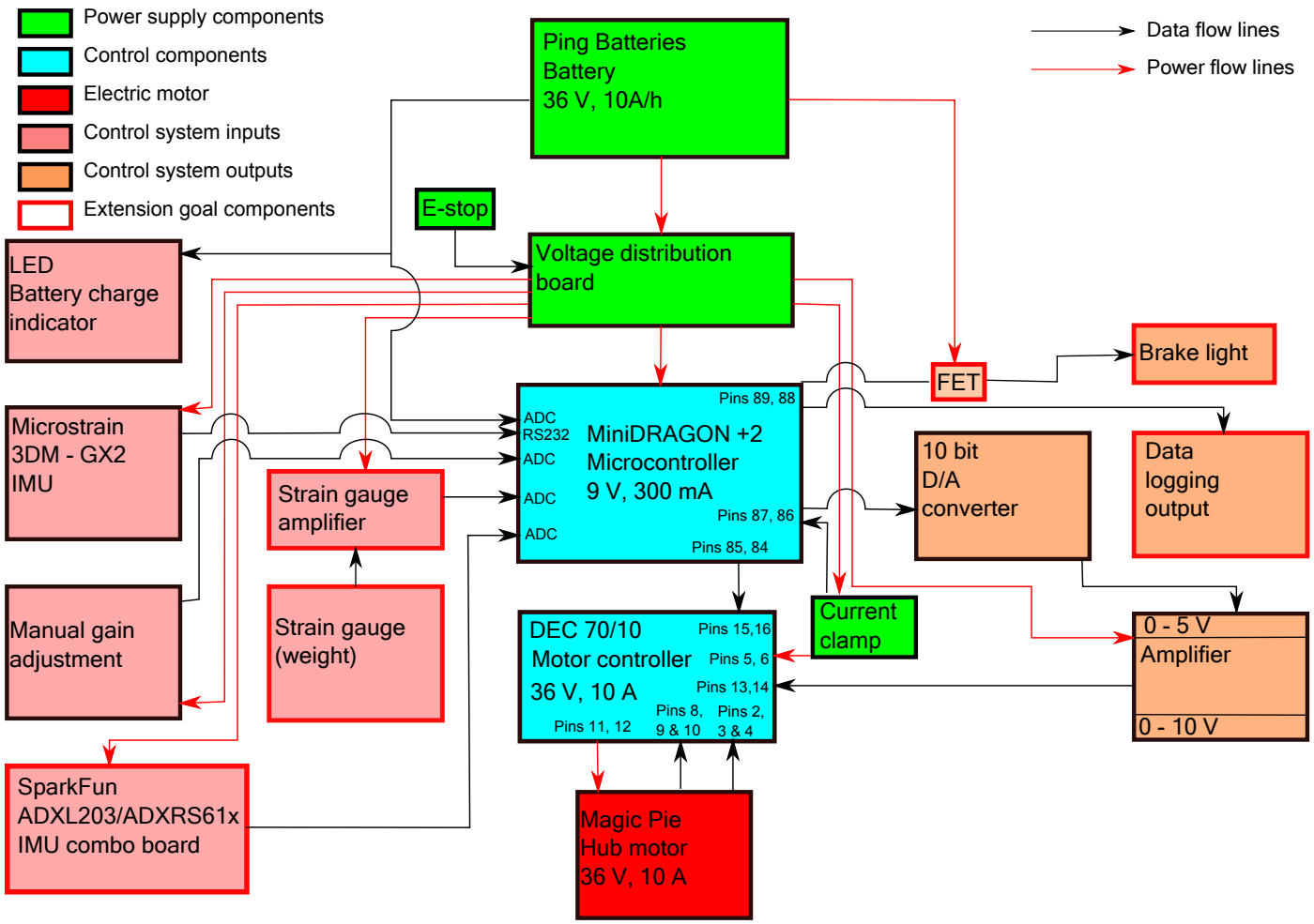

Figure 7.2.: Electrical functional diagram

Chapter 8.

Control design

In this chapter, the equations of motion are derived using the Lagrangian approach and written in non-linear state space form. The dynamics are verified using a Simulink model, which is then visualised with a VRML model.

8.1. System dynamics

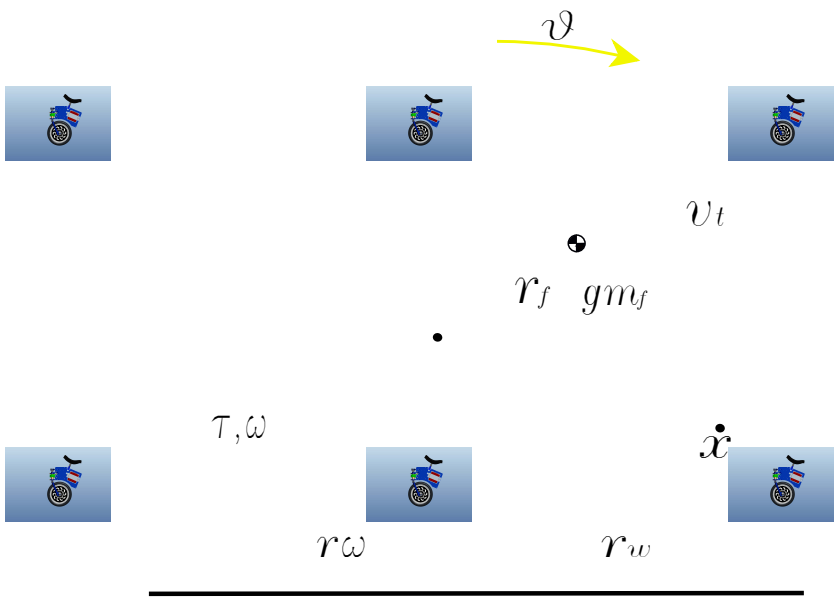

Figure 8.1.: The dynamic model of the Micycle

8.1.1. Nomenclature

First, it is necessary to define some terms.

τ =applied torque.

θ =angle of tilt of frame w.r.t. vertical.

$\dot{x}$ =translational velocity of centre of wheel.

v_f =velocity of the centre of mass of the frame.

r_w =radius of wheel.

ω =angular velocity of wheel.

r_f =distance from centre of wheel to centre of mass of frame and rider.

β =coefficient of translational viscous friction (rolling resistance).

γ =coefficient of rotational viscous friction (bearing friction and motor losses).

I_{fg} =moment of inertia of frame w.r.t. its own centre of mass.

I_{wg} =moment of inertia of wheel w.r.t. its own centre of mass.

8.1.2. Virtual work

The inputs into the system can be obtained by from the virtual work equation.

First consider the case where x is held fixed and θ is varied infinitesimally due to the input force (the pure rotation case):

$\delta w = (\tau - \gamma\dot{\theta}) \times \delta\theta$

Conversely, consider θ held fixed and x varied infinitesimally due to the input force (the pure translation case).

$\delta w = (\frac{\tau}{r_w} - \beta\dot{x}) \times \delta x$

Superpose the above to form the virtual work equation:

$$\delta W = \frac{\tau}{r_w}.\delta x + \tau.\delta\theta \tag{8.1}$$

8.1.3. Lagrange equations

From the Lagrangian, the Lagrange equations are thus:

$$\frac{\partial}{\partial t}\left(\frac{\partial \mathcal{L}}{\partial \dot{x}}\right) - \left(\frac{\partial \mathcal{L}}{\partial x}\right) = \frac{\tau}{r_w} - \beta\dot{x} \tag{8.2}$$

$$\frac{\partial}{\partial t}\left(\frac{\partial \mathcal{L}}{\partial \dot{\theta}}\right) - \left(\frac{\partial \mathcal{L}}{\partial \theta}\right) = \tau - \gamma\dot{\theta} \tag{8.3}$$

Where $\mathcal{L} = T - V$ is the Lagrangian, where T is the total kinetic energy of the system and V is the total potential energy of the system.

8.1.4. Energy terms

Translational kinetic energy (TKE)

TKE of wheel: $^1/_2 m_w \dot{x}^2$

TKE of frame: $^1/_2 m_f v_f^2$

where $\vec{v}_f = \vec{\dot{x}} + r_f\vec{\dot{\theta}}$

Using dot product to square vectors: $\left(\vec{\dot{x}} + r_f\vec{\dot{\theta}}\right)^2 = \dot{x}^2 + 2r_f\dot{x}\dot{\theta}\cos\theta + r_f^2\theta^2$

TKE of frame: $^1/_2 m_f\left(\dot{x}^2 + 2r_f\dot{x}\dot{\theta}\cos\theta + r_f^2\theta^2\right)$

Rotational kinetic energy (RKE)

RKE frame = $^1/_2(I_{fg}\dot{\theta}^2)$

Angular velocity of wheel: $\omega = \dfrac{\dot{x}}{r_w}$

RKE wheel = $^1/_2\left(\dfrac{I_{wg}\dot{x}^2}{r_w^2}\right)$

Potential energy

$V = mgh = m_f g r_f \cos\theta$

8.1.5. Lagrangian

$\mathcal{L} = T - V$

$$\mathcal{L} = {}^1/_2 m_w\dot{x}^2 + {}^1/_2 m_f\left(\dot{x}^2 + 2r_f\dot{x}\dot{\theta}\cos\theta + r_f^2\theta^2\right) + {}^1/_2(I_{fg}\dot{\theta}^2) + {}^1/_2\left(\frac{I_{wg}\dot{x}^2}{r_w^2}\right) - m_f g r_f cos\theta \tag{8.4}$$

8.1.6. Equations of motion

Taking the derivatives of (8.4) per (8.2) and (8.3) results in the following equations of motion:

$$a\ddot{x} + b\cos\theta.\ddot{\theta} = b\dot{\theta}^2\sin\theta + \frac{\tau}{r_w} - \beta\dot{x} \tag{8.5}$$

$$b\cos\theta.\ddot{x} + c\ddot{\theta} = \tau + bg\sin\theta - \gamma\dot{\theta} \tag{8.6}$$

where the constants are collected such that:

$a = m_f + m_w + \frac{I_{wg}}{r_w^2}$

$b = m_f r_f$

$c = m_f r_f^2 + I_{fg}$

8.1.7. Non-linear state space form

The equations need to be written in terms of the highest order derivatives. They can be written in matrix form:

$$\begin{bmatrix} a & b\cos\theta \\ b\cos\theta & c \end{bmatrix} \begin{bmatrix} \ddot{x} \\ \ddot{\theta} \end{bmatrix} = \begin{bmatrix} b\dot{\theta}^2\sin\theta + \frac{\tau}{r_w} - \beta\dot{x} \\ \tau + bg\sin\theta - \gamma\dot{\theta} \end{bmatrix} \tag{8.7}$$

Solving through inversion and premultiplication gives the results:

$$\begin{bmatrix} \ddot{x} \\ \ddot{\theta} \end{bmatrix} = \left(\frac{1}{ac - b^2\cos^2\theta}\right) \begin{bmatrix} bc\dot{\theta}^2\sin\theta - b^2 g\sin\theta\cos\theta + \tau\left(\frac{c - br_w\cos\theta}{r_W}\right) - \beta c\dot{x} + \gamma b\cos\theta.\dot{\theta} \\ bga\sin\theta - b^2\dot{\theta}^2\sin\theta\cos\theta + \tau\left(\frac{ar_w - b\cos\theta}{r_W}\right) - \gamma a\dot{\theta} + \beta b\cos\theta.\dot{x} \end{bmatrix} \tag{8.8}$$

8.2. Simulink model

In order to verify that the system dynamics had been correctly modelled, a Simulink Model of the system dynamics was constructed using the non-linear, state space dynamics derived for the system. The dynamics are expressed within the embedded Matlab function block (see Appendix E.1).

This system verified that the modelled dynamics were indeed correct. The theta outputs (see Figure 8.3) show the system falling over, passing through the floor and oscillating about a position until the response has been decayed away by damping forces. The

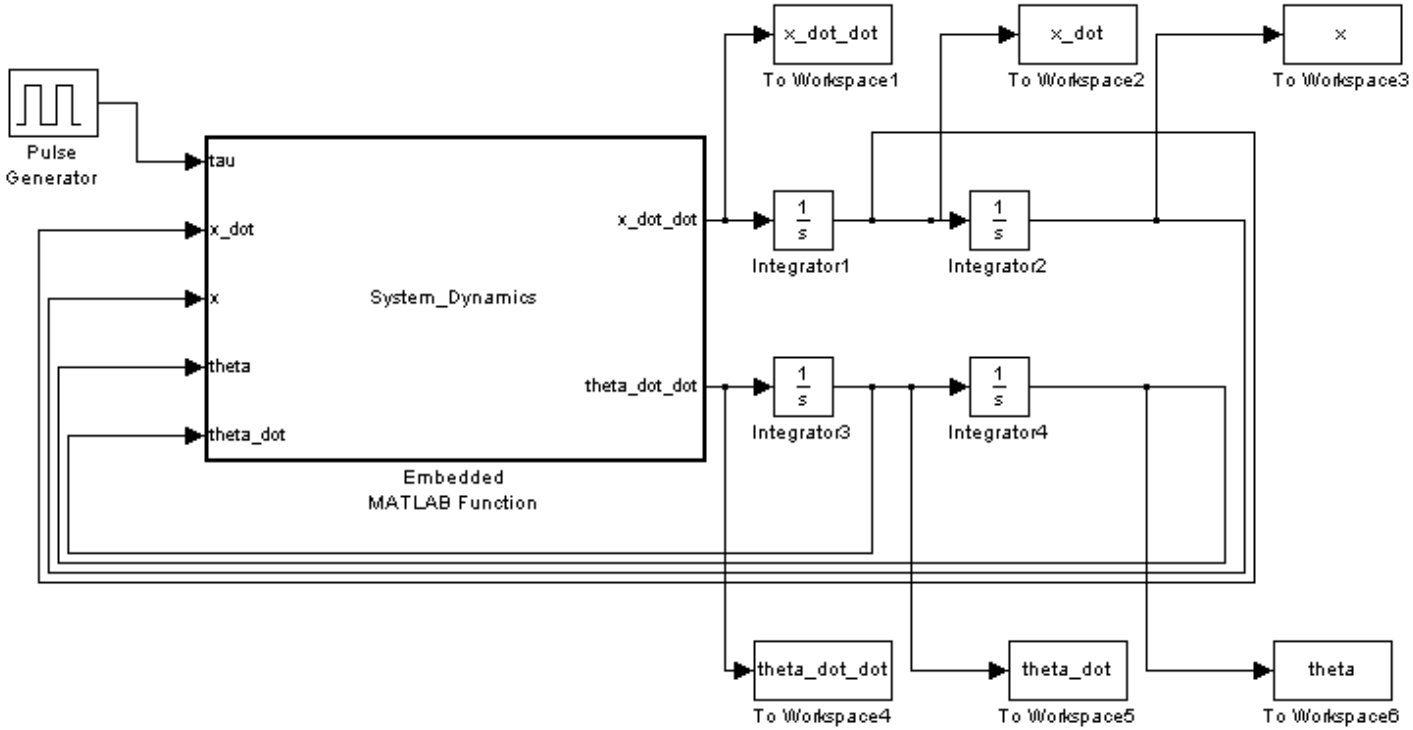

Figure 8.2.: Block diagram of the Simulink model

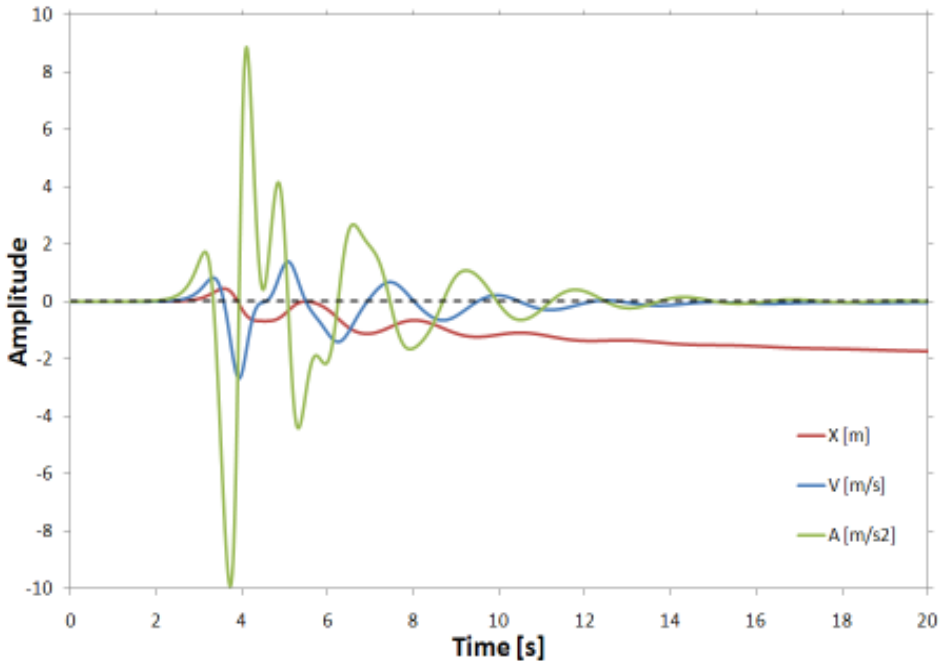

Figure 8.3.: Rotational response Simulink output

steady state angular position is minus π radians. This is what is expected as it means that the damping has eventually lead to the system settling upside down. The above response in angular acceleration and velocity is also what is expected.

The linear response graph (Figure 8.4) is also what is expected. It shows the system gradually settling out at a final position of minus 2 metres as it turns and it then eventually ends up upside down.

8.3. VRML model

A preliminary VRML model has been created to help visualise the output from the system as characterised in the figures above. The VRML model shows the system falling over, through the floor, and oscillating for some time when the damping coefficient are low. In addition, the wheel tends to drift in the translational x-direction. This preliminary model is shown in Figure 8.5.

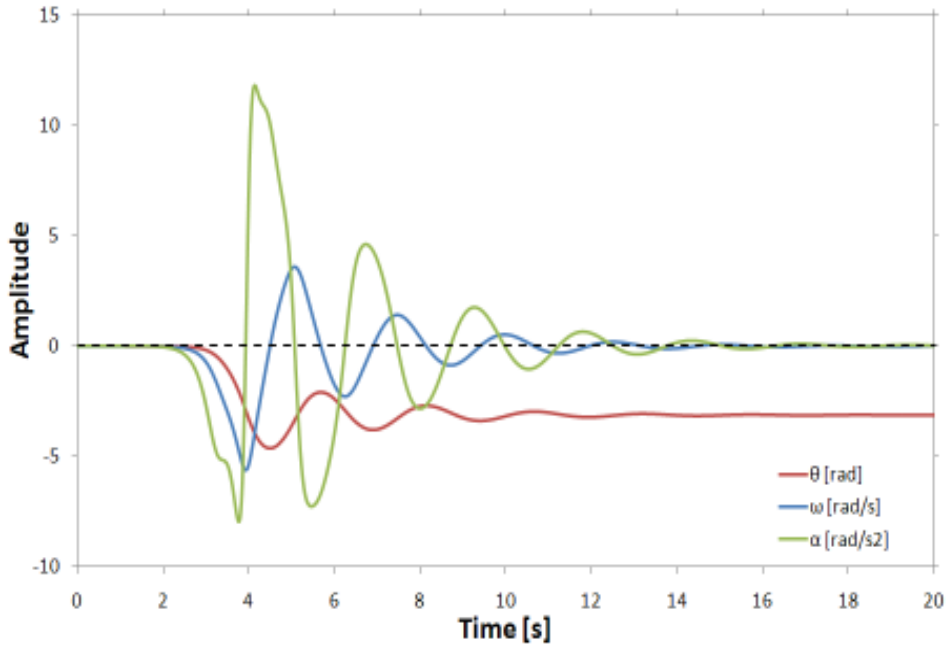

Figure 8.4.: Linear response Simulink output

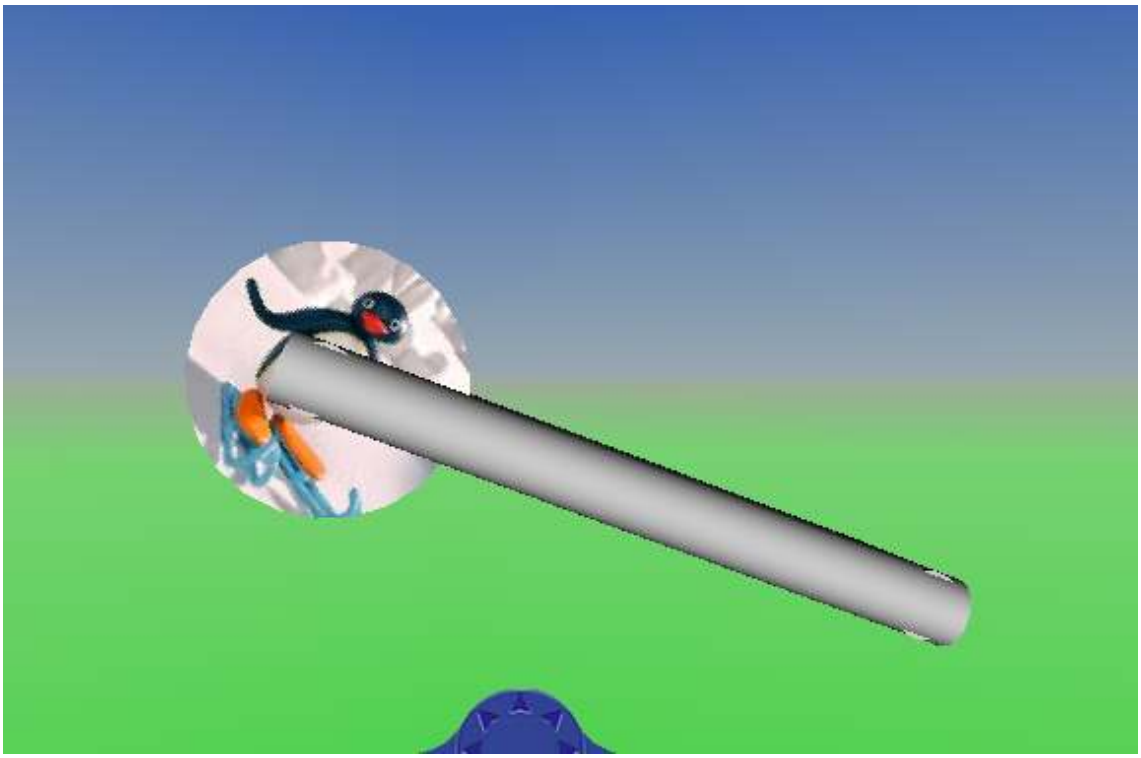

Figure 8.5.: The preliminary VRML model

Chapter 9.

Software design

This section outlines the software design of the Micycle. First, the software requirements and their formulation are discussed. The software architecture and implementation are both then described, and finally, the specific functionality is detailed. The software functional flowcharts can be found in Appendix D.

9.1. Software requirements

This section details the formulation of software requirements. This includes both functional and safety requirements.

9.1.1. Functional requirements

Functional software requirements were driven by the project specifications and goals (Chapter 3). These goals are translated into specific software requirements:

- An initialisation of the MiniDRAGON+2 microcontroller. All pins, memory and buses have to be mapped appropriately and communications with external devices need to be established.
- An ability to modify control gain values.
- Reading in of system parameters from the IMU.
- Apply an appropriate transfer function to generate a control signal of the motor and control the system..
- Sending a control signal to the motor controller through a DAC.
- Brake light when system is decelerating.
- Low battery warnings; a LED shall demonstrate that the battery is low and a buzzer to sound intermittently.

9.1.2. Safety requirements

The Micycle software is a safety critical system. The Micycle project presents both significant business and personal risks. There is the potential of serious injury to the user to the project. To this extent, the safety requirements of the software were developed in conjunction with a failure modes and effects analysis (FMEA) performed on the Micycle. These requirements are:

- The IMU, Maxon motor controller and all ADCs require correct initialisation so that the communications interface is fully functional before the device is used.
- Angular pitch position of the system needs to remain within a specified range at all times.
- Angular velocity in the pitch direction must not exceed a specified value.
- Current drawn through the motor needs to be limited in software.
- Speed of the Micycle is required to be limited in software.
- Need to ensure that the Maxon motor controller and communications with the microcontroller are functioning correctly at all times.
- Need to ensure that the IMU and communications with the microcontroller are functioning correctly at all times. The system needs to be able to discern the fault in the case of an IMU failure being detected.
- A low pass filter on all IMU measurements needs to be implemented to minimise the risk of noise spikes.
- The system is not allowed to enter operation unless it is in a fully upright position.
- The system requires both a hard stop and a soft stop to stop the system appropriately if a fault is detected.
- The system requires an error code system to provide diagnostic feedback.

9.2. Software architecture

The software architecture for the Micycle has been fully developed. This section details a higher level view of the design as well as the lower level, specific design of the system.

9.2.1. Higher level design - system finite state machine

The basic flow of control for the system on the highest level is illustrated in the finite state machine (FSM) in Figure 9.1.

Two key states are at the core of the software design are two key states. These are q2, the Control state and q3, the Safety Check state. The software architecture is constantly

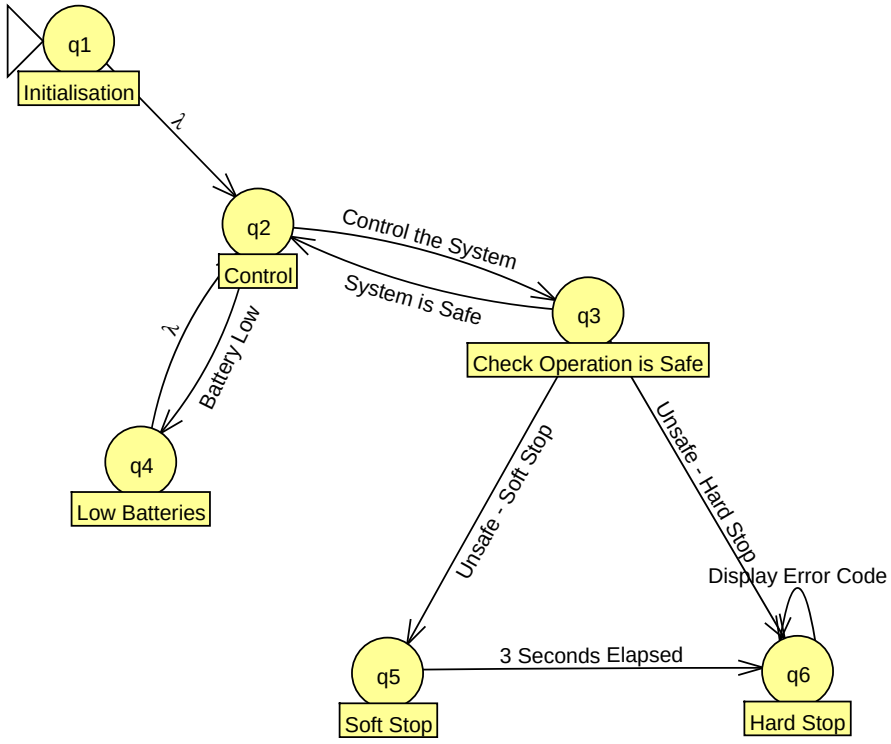

Figure 9.1.: Finite state machine for the Micycle software architecture. Note that λ represents an automatic transition.

switching between the two. This is what is to be expected, the software controls the system, checks that everything is still safe, then continues to control the system, then continues to switch between these two as long as the vehicle is in operation. This design highlights the emphasis on safety found in the Micycle, the software is constantly polling the system to ensure that everything is still functioning as it should.

In addition to the two main states are a number of other states of operation. There is an Initialisation state, q1, which correctly initialises the system. Note that there are safety checks within this state before operation of the Micycle has begun. There is also a Low Battery state, q4. This turns on the warnings to the users when the Micycle's batteries are low on charge. Finally, there are the stops for the system if a safety fault has been detected. These are q5, the Soft Stop and q6, the Hard Stop. Specific safety faults require one or the other, depending on the fault itself. A Soft Stop also becomes a Hard Stop after three seconds.

9.2.2. Lower level design - flowchart design

The lower level details of the Software Architecture has also been fully designed. All programs, function calls and interrupts have been specified. Along with all logic and

flow of control, they are detailed in Appendix D, which contains the complete set of flowcharts for the software system. These flowcharts should be referred to for all specific details on the software design.

9.2.3. Lower level design - programs, functions and interrupts

Table 9.1 is a brief summary of all programs, functions and interrupts in the system and their design function.

	Thread Name	Functionality
Programs	Main.c	Main execution thread for the system, constantly calling the Control() function.
Functions	Initialisation()	Fully initialises the system; will not start system if there are any initial safety faults.
	Control()	Checks that there are no safety faults before generating a control signal to actuate the motor.
	Check_Dynamics()	Checks that the motor current, angular position, angular velocity and vehicle speed are within safe bounds.
	Check_IMU()	Checks that IMU is fully functional.
	Check_Maxon()	Checks that motor controller is fully functional.
	Low_Battery()	Activates the low battery buzzer and low battery LED if the battery is low on charge.
	Update_Gains()	A one off update of the control gains during system initialisation.
Interrupts	Hard_Stop(error code)	A hard stop to the vehicle with appropriate error code output to the 7 segment display.
	Soft_Stop(error code)	A soft stop to the vehicle. Will generate a hard stop after 3 seconds.
	Stop_Timer()	Timer to elapse when a soft stop should generate a hard stop.
	Buzzer_Timer()	Period of time between low battery beeps when battery is low.
	Battery_Timer()	Period of low battery beeps when battery is low.

Table 9.1.: Summary of all programs, functions and interrupts in the software design.

9.3. Specific software functionality

This section details certain specific functionality in the software. There are several areas where it is necessary to elaborate and justify the design decisions made in the software.

9.3.1. Error codes

A consequence of the extensive safety features implemented in the software design means that there are over a dozen safety faults which will trigger a soft or hard stop. From the user's perspective, it is very difficult to determine exactly what it was that went wrong, the user will simply experience the system triggering a stop. To this extent, it was decided that an error code system would be developed for each safety fault. This is particularly important during the testing and debugging phase where the safety fault cut off values will be undergoing tweaking to appropriate values. The seven segment display on the MiniDRAGON+2 was used with each safety fault trip mapping to a hex value displayed on the seven segment display. This is shown in Table 9.2.

Safety Trip	7 Segment Error Code
Battery drained	0
Vehicle speed too fast	1
Excessive current through motor	2
Pitch position outside safe range	3
Angular velocity too fast	4
General operational failure in the Maxon	5
ADC outside expected bounds	6
IMU did not initialise correctly	7
Maxon did not initialise correctly	8
IMU - abnormal power rating	9
IMU - RS232 pin disconnected	A
IMU - parity check failed	b
IMU - indeterminate communication error	C

Table 9.2.: Error codes for safety faults

9.3.2. Software stops

The nature of the design means that stopping it is not trivial. Due to the fact that the system is inherently unstable, it is not simply a case of cutting the power to the motor. In certain situations, such as when the system trips from travelling too fast, this could be more dangerous than leaving the system to run. To this end, there are two types of software stops which have been implemented in the software. These are a hard stop and a soft stop.

A hard stop is akin to cutting the power to the motor. It uses the enable pin on the Maxon motor controller to stop the motor controller from actuating the motor. It will also beep twice when this happens. Finally, the system will output the appropriate error code and the mushroom button needs to be pressed to reboot the system to resume operation. A hard stop is not to be used when the vehicle is travelling at speed. It is used for hardware and communication errors during initialisation, ensuring that the vehicle does not enter operation with a sporadic connection to the motor controller or IMU. It is also used when there is a hardware fault in either the IMU or motor controller during operation. If either of these is not working then it is not possible to perform a gentle stop and it is best to turn the system off as soon as possible, rather than potentially exacerbating the situation.

A soft stop is performed when the system trips and is travelling at speed. In this situation it is dangerous to simply turn the motor off. Rather, a new control algorithm is applied to gently decelerate the system. This will reduce the vehicles velocity to near zero, allowing the vehicle to be stopped safely. A three beep warning will be sounded when the new algorithm is enacted. Note that the soft stop also starts a timer, three seconds after the soft stop has triggered a hard stop will be triggered to stop the vehicle.

9.3.3. Polling for safety checks

The software system makes use of polling to check if a safety parameter has not been met. That is, the system checks all the safety parameters just before it controls the system, it controls the system slightly and then it continues to check again. Strictly speaking, this is bad practice in a safety critical system. Safety checks should be typically driven by interrupts rather than polling. This is to ensure fast response to deviations in safety parameters and that the program does not enter an infinite loop whereby the safety values are no longer being checked.

Nevertheless, the use of polling rather than interrupts for safety checks was a design decision. With the number of values to be checked and the amount of processing required on each value before it can be checked (the sensor values require filtering and some of the communications require parity checking), it is simply not feasible to use the additional hardware required for this processing in the design.

Accordingly, allowances have been made in the software design to minimise the risk from this bad practice. The main execution thread where the polling occurs has been deliberately left short and simple. There are no loops, so that the thread cannot get caught in an infinite loop where it is not polling. Time out checks have been implemented to ensure that the system does not hang waiting for an input. The simple structure of the main thread also means that the latency between a safety parameter being exceeded and the detection by software is also minimal. Finally, the safety checks themselves generate interrupts if a fault is detected to stop the system as quick as possible. These design choices create a situation where the safety system is still robust and fast to respond.

Chapter 10.

Manufacturing and testing

This chapter outlines the process of manufacturing and testing different components and assemblies of the Micycle. At this point, only the Golden Motor Magic Pie motor has been tested with the inbuilt controller.

10.1. Motor testing

The Magic Pie motor was subjected to testing on arrival. This aimed to determine whether the motor was functioning correctly, if the stall torque is sufficient for stable riding, and in order to calculate the torque constant of the motor for the controller design.

The Magic Pie motor is supplied with an inbuilt motor controller. As this is not a bidirectional controller, it is not adequate for the Micycle. However, the motor was tested as supplied with the Magic Pie motor controller to ascertain the torque constant of the motor constant and the maximum stall torque. This also aids in benchmarking the performance of the Maxon motor controller.

The torque constant is expressed in the following equation:

$$T = k_\tau I \tag{10.1}$$

where:

T =Torque ($\mathrm{N} \cdot \mathrm{m}$)

k_τ =Torque constant ($\mathrm{N} \cdot \mathrm{m/A}$)

I =Current (A)

Therefore, the torque constant can be found by testing the motor at stall conditions and recording the torque and current values produced.

10.1.1. Test apparatus

- Test supports (inverted bicycle)

- Magic Pie motor and accessories
- Load cell
- Fastening straps
- Lambda power supply
- Electrical connections
- Multimeter

Figure 10.1.: Experimental setup

10.1.2. Method

1. The motor was secured in the test rig.
2. A load cell was then attached to the test rig and motor with the use of a strap. The strap was then wrapped around the motor wheel and over itself, so that as the motor wound up, friction would force it to stall as the strap pulled tight. This allowed the motor to run before it reached stall conditions generating more accurate results.
3. The motor was connected to the Lambda power supply and the load cell was connected to the voltmeter.
4. The initial offset of the load cell and the output for a 62 kg load was then recorded using the voltmeter. This was done to determine the scale of the load cell output.
5. The voltage of the power supply was then set to 24 V and stall conditions were tested and recorded for varying current values.
6. This process was then repeated for a voltage value of 36 V.

10.1.3. Results

The results of the test are listed below in Tables 10.1 and 10.2. It should be noted that there was a high level of noticeable noise observed throughout the testing procedure. The noise was most prevalent in the 15 A readings.

Table 10.1.: Results with 24 V supply

Current (A)	Strain Gauge Voltage (mV)	Force (N)	Torque (Nm)
5	730	147	21.3
7.5	920	185	26.9
10	1080	217	31.6
12.5	1200	242	35.0
15	1380	278	40.4

Table 10.2.: Results with 36 V supply

Current Limit [A]	Strain Gauge Voltage [mV]	Force [N]	Torque [Nm]
5	780	157	22.8
7.5	920	185	26.9
10	1060	214	31.0
12.5	1200	242	35.0
15	1300	262	38.0

The results from Tables 10.1 and 10.2 are plotted in Figure 10.2.

The torque constant of the motor was then determined by averaging the rate of change of torque for each current change of the 36 V test results. This set of values was chosen as it is the expected operating voltage of the Micycle. It should be noted that the values recorded for the current input of 15 A have been ignored due to the high prevalence of noise. The results of these calculations and the resulting torque constant value are listed in Table 10.3 below.

Table 10.3.: Average rate of change of torque (A/Nm) with 24 V supply

Current range (A)	Rate of change of torque [A/Nm]
5 => 7.5	1.64
7.5 => 10	1.64
10 => 12.5	1.64
Average slope [A/Nm]:	1.64
Torque constant [A/Nm]:	1.64

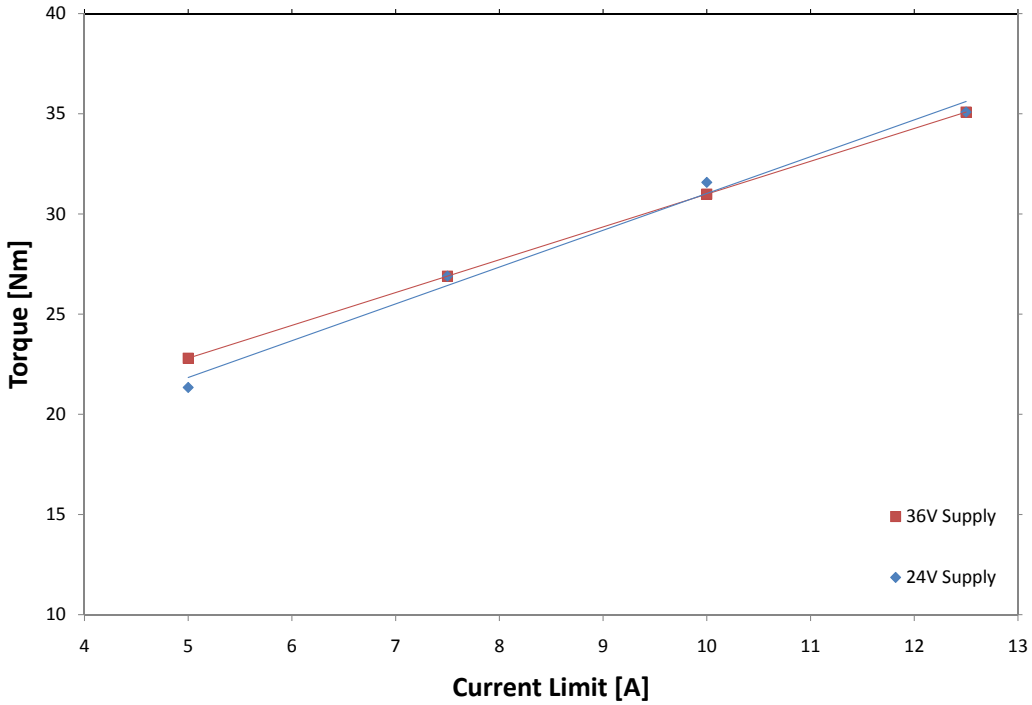

Figure 10.2.: Torque vs. current for 24 V and 36 V supply

10.1.4. Errors

The results from the motor test have shown that the Magic Pie motor has a torque constant of 1.64 A/Nm. The main factor affecting the accuracy of this result was the amount of noise encountered when recording results. If the method of testing could be refined further to include a filtering system then a more accurate value might be determined. Due to the fact that this is a preliminary testing process in which only an estimate of the torque constant was required the method used was appropriate. A more accurate testing procedure may be required when testing with the Maxon motor controller.

10.1.5. Conclusion

First, the stall torque of 30 Nm exceeds the 22 Nm torque required for stabilisation of the Micycle and rider (see Section 5.2). Secondly, the results have allowed for reasonable estimation of the torque constant of the Magic Pie motor. Finally, these results will serve as a benchmark for the future testing of the motor with the Maxon motor controller and help to indicate any possible problems.

Chapter 11.

Future work

Future work is required to complete the design and build of the Micycle for the University Open Day on August 15, 2010. The complete work schedule is shown in the project Gantt chart (Appendix A). The remaining work sections are described below. At the time of writing, the project is on track to meet the key deliverable dates.

Mechanical build: The final constructions were submitted to the School Mechanical Workshop on May 10. The Workshop is currently manufacturing the design.

Mechanical assembly and test: The assembly will need to be checked for full functionality. The steering response will need to be checked. The frame needs to be tested under a 200 kg load to ensure user safety.

Electrical build: The electrical design has yet to be submitted to the School Electrical Workshop. This is an immediate priority.

Electrical test: constructed design will need to be tested under simulated loads and checked as per the failure modes and effects analysis (FMEA) (see Appendix **??**).

Software work: The software code needs to be written and tested in response to simulated inputs, taking into account the FMEA.

Controller design: This includes the build of a full VRML model and a controller design based on the Simulink block. The Micycle will then be tested with the aid of a dSPACE tether. When suitable performance is obtained, testing will be attempted with a live user.

Documentation: Supporting documentation, including the final report, safe operating procedures and an exhibition poster are yet to be created.

Extension goals: Finally, when the above work is completed, work on the extension goals may begin. These include the development of brake lights and indicators, data logging, testing on an incline, integration of the SparkFun IMU and and an automatic weight sensor (see Chapter3).

References

Blackwell, T. (2007a), 'The electric unicycle', http://tlb.org/eunicycle.html (accessed 14/04/2010).

Blackwell, T. (2007b), 'Notes on safety', http://www.tlb.org/scootersafety.html (accessed 11/01/2010).

Budynas, R., Nisbett, K. and Shigley, J. (2008), *Shigley's mechanical engineering design*, Sydney: McGraw-Hill, 1 edn.

Carlson, E. (2009a), 'Tips on unicycle safety', http://learntorideaunicycle.blogspot.com/2009/10/tips-on-unicycle-safety.html (accessed 23/04/2010).

Carlson, E. (2009b), 'Unicycle training wheels and aids', http://learntorideaunicycle.blogspot.com/2009/10/unicycle-training-wheels-and-aids.html (accessed 23/04/2010).

D'Souza-Mathew, N. (2008), 'Balancing of a robotic unicycle', Tech. rep., Cambridge University.
URL http://www.roboticunicycle.info/documents/MyFinalReport.pdf

Fischer, U. (ed.) (2006), *Mechanical and Metal Trades Handbook*, Germany: Leinfelden-Echterdingen: Verlag Europa-Lehrmittel, 1 edn.

Focus Designs (2009a), 'SBU-owners-manual', http://focusdesigns.com/sbu-owners-manual/ (accessed 08/03/2010).

Focus Designs (2009b), 'SBU performance', http://focusdesigns.com/design/performance/ (accessed 24/04/2010).

Focus Designs (2009c), 'SBU specifications', http://focusdesigns.com/wp-content/uploads/2009/09/SBUSpecSheet.pdf (accessed 04/04/2010).

Hong, S.K. (2008), 'A fuzzy logic based performance augmentation of mems gyroscope', *Journal of Intelligent & Fuzzy Systems*, vol. 19, no. 6, pp. 393–398.

JayCar Electronics (2010), 'JayCar electronics catalogue', http://www.jaycar.com.au/productResults.asp?whichpage=2&pagesize=10&keywords=&CATID=18&SUBCATID=250&form=CAT (accessed 12/05/2010).

Jones, D. (2006), 'The stability of the bicycle', *Physics Today*, vol. 59, no. 9, pp. 51–56.

Maxon Motors (2010), 'DEC 70/10 product', http://shop.maxonmotor.com/ishop/article/article/228597.xml (accessed 12/05/2010).

MITCalc (2010), 'Spiral cylindrical torsion springs', `http://www.mitcalc.com/doc/sprtorsion/help/en/sprtorsion.html` (accessed 11/01/2010).

Polutnik, A. (2010), 'Enicycle prototype', `http://enicycle.com/prototype.html` (accessed 11/03/2010).

Robinson, S. (2006), 'Drive and control electronics enhance the brushless motor's advantages', *Electronic Design*, vol. 54, no. 18, pp. 54–60.

Roboteq (2010), 'Brushless dc motor controllers', `http://www.roboteq.com/brushed-dc-motor-controllers/bl1500-50a-brushless-dc-motor-controller-with-hall-sensor-inputs.html` (accessed 12/05/2010).

Schoonwinkel, A. (1987), 'Design and test of a computer stabilized unicycle', Ph.d. dissertation, Stanford University, CA.

Sheng, Z. and Yamafuji, K. (1997), 'Postural stability of a human riding a unicycle and its emulation by a robot', *IEEE Transactions on Robotics and Automation*, vol. 13, no. 5, pp. 709–720.

Shuster, S. (2007), 'Sex, aggression, and humour: responses to unicycling', *British Medical Journal*, vol. 335, pp. 1320–1322.

SparkFun (2005), 'IMU combo board datasheet', `http://www.sparkfun.com/datasheets/Accelerometers/IMU_Combo_Board-v2.pdf` (accessed 7/05/2010).

Spring-Makers-Resource.net (2010), 'How torsion springs are different and similar to compression springs', `http://www.spring-makers-resource.net/torsion-springs.html` (accessed 11/01/2010).

Standards Association of Australia (2003), *Carbon Steel Spring Wire for Mechanical Springs*, North Sydney: Standards Australia.

Swaim, W. (2001), 'FAQs on welding 4130', `http://archive.metalformingmagazine.com/2001/01/Lincoln.pdl` (accessed 10/05/2010).

Taj, J. (2000), 'Motion control made easy', `http://www.galilmc.com/learning/articles/motioncontrolmad.pdf` (accessed 04/05/2010).

Unicycle.com (2010), 'Unicycle parts', `http://www.municycle.com.au/View.php?action=Page&Name=UnicycleParts` (accessed 12/05/2010).

Wikipedia (2009), 'Bicycle dimensions.svg', `http://en.wikipedia.org/wiki/File:Bicycle_dimensions.svg` (accessed 19/05/2010).

Wytec Company (2010), 'HCS12: MiniDRAGON-Plus2 development board', `http://www.evbplus.com/minidragonplus2_hc12_68hc12_9s12_hcs12.html` (accessed 12/05/2010).

Appendix A.

Gantt chart

The project Gantt chart is attached overleaf.

ID	Task Name
1	**Problem Clarification**
2	Project Specifications
3	**Conceptual Design**
4	Concept Generation
5	Concept Sketches
6	Concept Selection
7	Final Concept Sketch
8	**Risk Assessment**
9	**Component Selection**
10	Hub Motor Research
11	Hub Motor Ordered
12	Motor Torque Testing
13	Motor Controller Research
14	Motor Controller Ordered
15	Battery Research
16	Battery Ordered
17	Spring Research
18	Spring Ordered
19	Dampener Research
20	Dampener Ordered
21	Saddle Research
22	Saddle Ordered
23	Tyre Research
24	Tyre Ordered
25	**Contract Writing**
26	Draft Contract Writing
27	Contract Draft
28	Final Contract Writing
29	Contract Lock-in
30	**Innovation Fund**
31	Application Writing
32	Application Due
33	**Gantt Chart Creation**
34	Draft Writing
35	Draft Submission
36	Final Writing
37	Final Submission

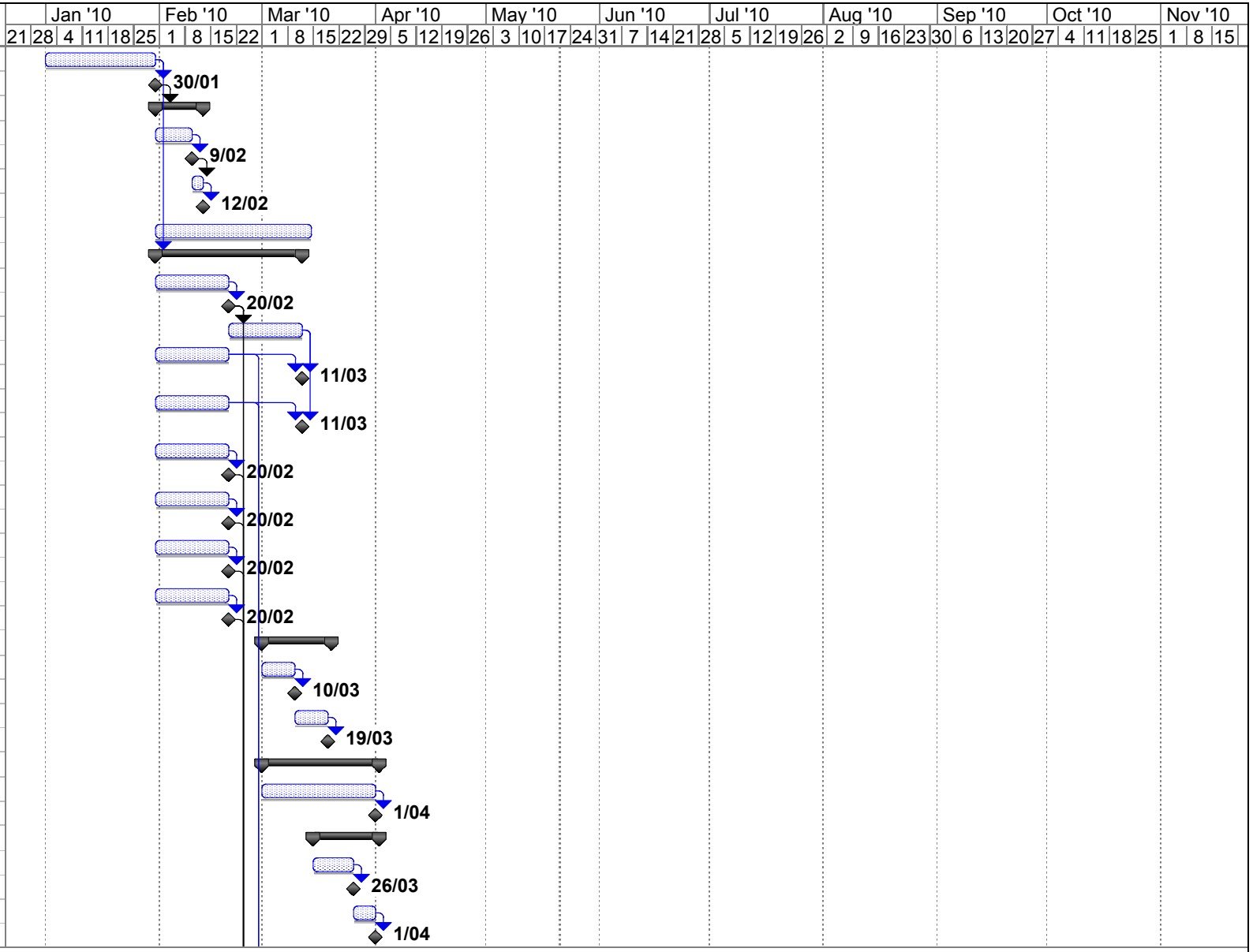

Project: gantt
Date: Fri 21/05/10

Task		Milestone		External Tasks	
Split		Summary		External MileTask	
Progress		Project Summary		Split	

ID	Task Name
38	**Literature Review**
39	Enicycle Research
40	Eunicycle Research
41	Focus Designs Research
42	EDGAR Research
43	SON of EDGAR Research
44	Ball-bot Research
45	Lit Review Report
46	**Detail Mechanical Design**
47	Hub Motor Modelling
48	Dampener Modelling
49	Spring Modelling
50	Saddle Modelling
51	Tyre Modelling
52	**Frame Design**
53	Material Selection
54	Frame Modelling
55	Technical Drawing Submission
56	Component Manufacture
57	**Mechanical Assembly**
58	Mechanism Built
59	**Electrical Design**
60	Adapter Board Design/Build
61	Power Regulation
62	**Motor Controller Implementation**
63	Vendor Software Research
64	Vendor Hardware Research
65	System Parameter Spec
66	**Initial Implementation**
67	Write Drivers
68	**Final Implementation**
69	Driver Debugging
70	**Hardware Testing (Rig)**
71	Spec Tests
72	Torque Tests
73	**Final Systems Integration**
74	Electronics Fittings

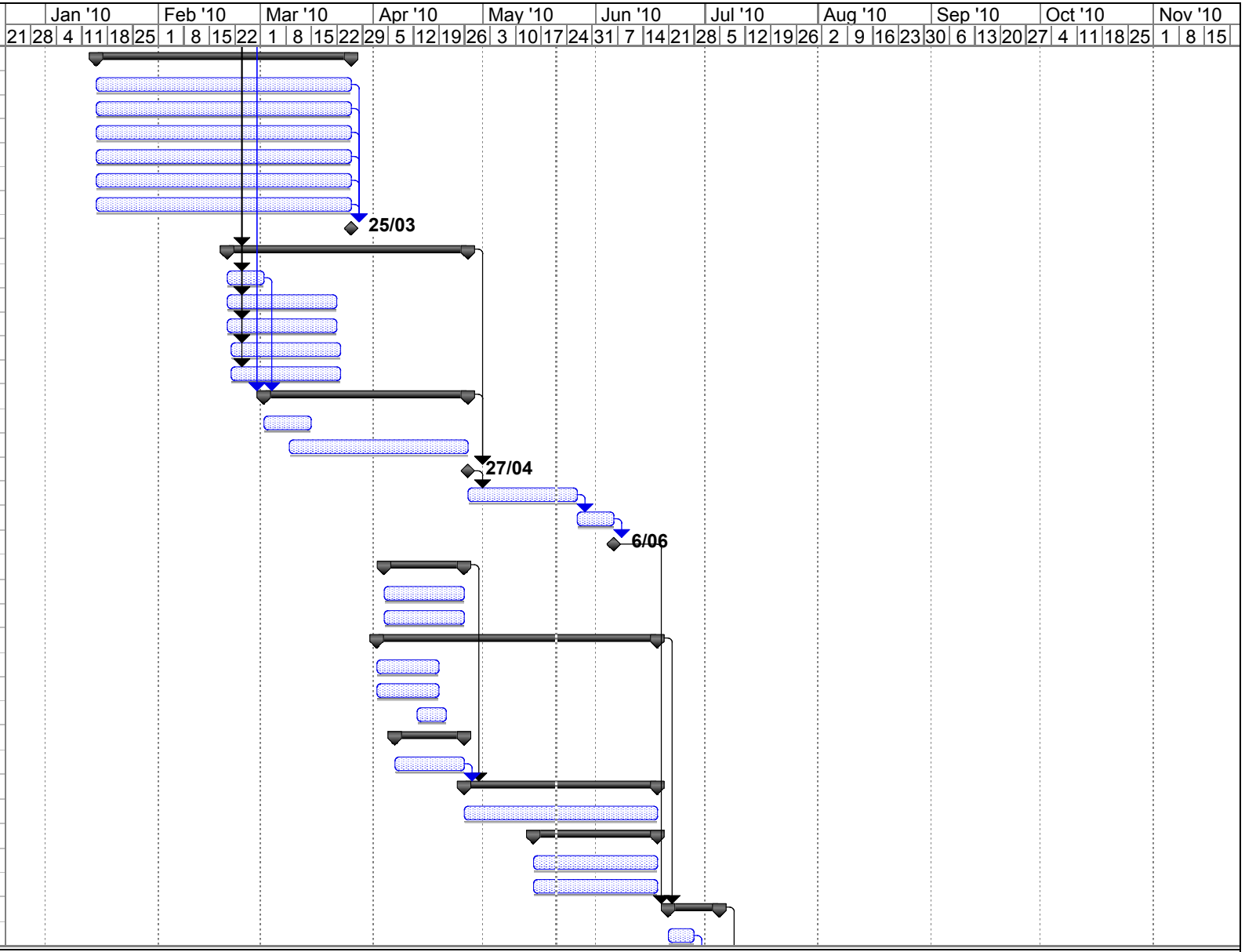

Project: gantt
Date: Fri 21/05/10

Task
Split
Progress
Milestone
Summary
Project Summary
External Tasks
External MileTask
Split

ID	Task Name
75	Wiring
76	Prototype Complete
77	**Prelim Report Compliation**
78	Draft Compilation
79	Draft Submission
80	Final Compilation
81	Final Submission
82	**Controller Design/Testing**
83	Background Research
84	OL Plant Modelling
85	Initial Design
86	CL Plant Modelling
87	CL Tuning (Simulink)
88	**Tethered Implementation**
89	Testing/Tuning
90	**Untethered Implementation**
91	Testing/Tuning
92	Additional Testing/Tuning
93	**Open Day**
94	**FMEA**
95	**Safe Operating Procedure**
96	**Microcontroller Programming**
97	Software Research
98	Architecture Design
99	Modular Breakdown
100	Implement Modules
101	Module Testing
102	Integration
103	Integration Testing
104	**Project Seminar**
105	Seminar Abstract
106	Abstract due
107	Preparation
108	Seminars
109	**Final Report**
110	Drafting
111	Draft Submission

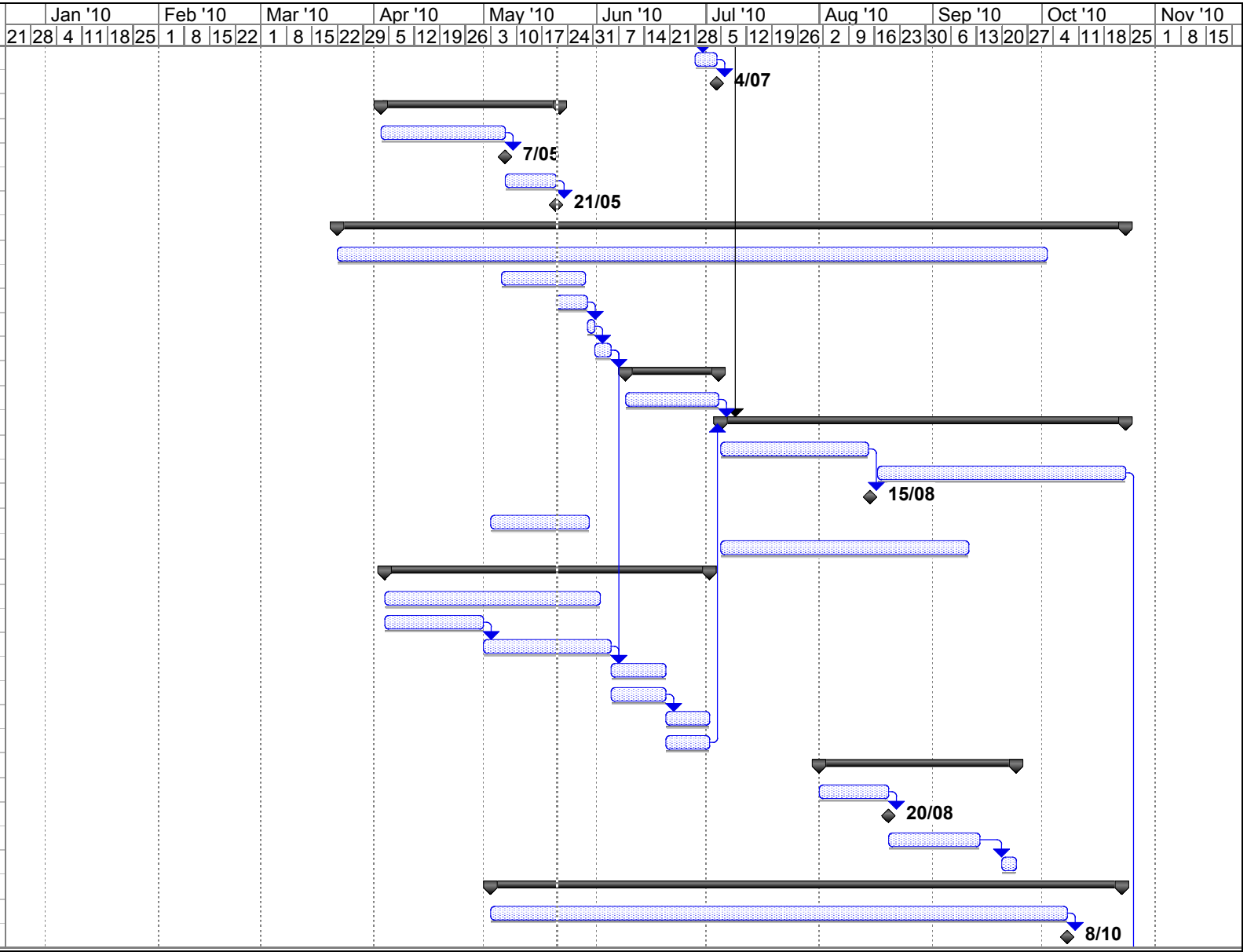

Project: gantt
Date: Fri 21/05/10

Task	Milestone	External Tasks	
Split	Summary	External MileTask	
Progress	Project Summary	Split	

ID	Task Name
112	Finishing
113	Final Submission
114	**Project Exhibition**
115	Exhib Abstract
116	Abstract Due
117	Poster Write-up
118	Procurement/Setup
119	Exhibition
120	Cleanup
121	Equipment Return
122	Workbook Cleanup
123	Workbook Due
124	Proj. Outcomes Writing
125	Proj. Outcomes Due

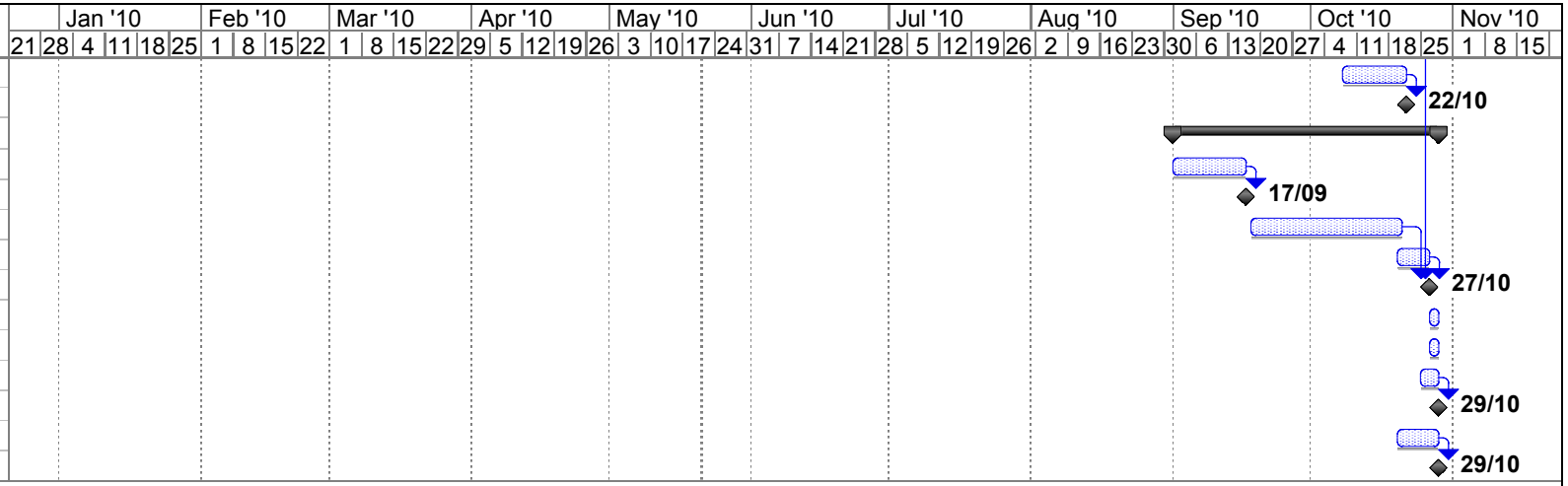

Project: gantt
Date: Fri 21/05/10

Task	Milestone	External Tasks	
Split	Summary	External MileTask	
Progress	Project Summary	Split	

Appendix B.

Budget

The project budget spreadsheet is attached overleaf.

Micycle Budget

Item	Supplier	Description	#	P&H USD	Price USD	P&H AUD	Price AUD	Price AUD	Status
Motor	Golden Motor.com	Magic Pie front kit	1	$115.00	$282.00	$127.78	$313.33	$441.11	Arrived
MCU	TBA	Dragon	1			$0.00	$130.00	$130.00	Arrived
	Sparkfun.com	IMU ADXL203/ADXRS61x	1			$0.00	$150.00	$150.00	To Order
	Sparkfun.com	MCP4725 I2C DAC	1					$25.00	To order
Motor Control	Maxon Motor(Sydney distributor)	DEC/70/10	1			$25.00	$396.00	$421.00	Arrived
				$15.00	$36.00	$13.50	$32.40	$45.90	On Order
Batteries/Charger	Pingo	Lithium	1		$761.00		$0.00	$840.00	Arrived
							Sub Total	$2,053.01	

Chassis

Tyre + Tube	Chain Reaction Cycles	16in tube and tyre	1			$0.00	$0.00	$53.45	Arrived
Seat+pole	Unicycle.com	Unicycle saddle seat	1			$11.00	$50.00	$83.50	Arrived
Forks	Work Shop	workshop	1			$0.00	$0.00	$25.00	On Order
Pegs	Peter Stevens	Folding Pegs	1			$0.00	$13.95	$13.95	Arrived
Seat clamp	Unicycle.com	Seat clamp	1			$0.00	$12.00	$12.00	On Order
Bearings	Gardner Bearings	Bearings for forks	1			$0.00	$0.00	$49.98	Arrived
Damper	IMI Norgren	Rotary damper	2			$0.00	$0.00	$105.00	Arrived
Spring	Industrial Springs (SA)	Torsion coils spring for steering	1			$0.00	$0.00	$125.00	On Order
							Sub Total	$467.88	
							Total	$2,520.89	

Items provided in kind by the University	Value
Microstrain 3DM-GX2 IMU	$2,500.00

Further to this not listed are metal/Alluminium costs, nuts and bolts and wire etc.

	Arrived
	Still to order
	On order

Conversion US-AU
0.9

Appendix C.

Risk management and FMEA

C.1. Risk management

Risk Management Level

Result / Likelihood	Insignificant	Minor	Moderate	Major	Catastrophic
	1	2	3	4	5
A- Almost Certain	H	H	E	E	E
B- Likely	M	H	H	E	E
C- Moderate	L	M	H	E	E
D- Unlikely	L	L	M	H	E
E- Rare	L	L	M	H	H

© School of Mechanical Engineering, The University of Adelaide, Australia

Figure C.1.: Risk management level prioritisation level

The Micycle project entails an inherent degree of risk. To manage this and to maximise the chances of the project being a success, standard risk assessment and management techniques were employed.

Key risks were identified during the early stages of the project and prioritised using the risk management level matrix of Figure C.1. The priority codes are generated by weighing the severity of the consequences of a risk against the chance that it will occur. Measures to manage these risks were then developed in order of priority from highest to lowest. Table C.1 lists the key risks identified, ranked in order of their priority, as well as the measures adopted to address them.

The priority codes used in Figure C.1are E = Extreme, H = High, M = Medium and L = Low.

Risk	Likelihood	Severity	Priority	Comments	Current Controls
Underestimating the budget required for the project	Likely	Major	Extreme	Components may be damaged during testing and need to be replaced, or found to be unsatisfactory.	Reserve funds allocated. Possibility of emergency fund-raising.
Superficial or structural damage to Micycle	Likely	Minor	High	It is written in the specifications that the Micycle is to be made aesthetically pleasing.	Rubber bump-stops installed at key points on chassis. Design to withstand the rigors of operation
Personnel illness/injury requiring extended time off	Moderate	Moderate	High	Extended personnel time off due to illness and/or injury	Task timelines design to mitigate this issue.
Issues arising from manufacturing	Unlikely	Moderate	Medium	Extended manufacturing time required	Submission of drawings and discussion of require manufacturing well in advance of deadline
Hardware issues extending the time required for tasks	Moderate	Moderate	High	Components may be damaged or malfunction and need to be replaced.	Timeline structured around these possibilities. The purchasing of equipment in advance and early drawings submitted

Table C.1.: Risks and mitigation measures

C.2. Failure modes and effects analysis (FMEA)

The FMEA, in tabular format, begins on the following page.

Function	Failure Mode	Effect	S[1]	Cause	O[2]	Current Controls	D[3]	CRIT	RPN	Recommendations
Stability Control	Motor controller saturates.	Loss of pitch control. Micycle pitches over and motor continues running. Potentially serious injury to rider, both during fall and subsequent to fall as motor continues to operate.	9	Excessive speed of the Micycle.	7	Maximum speed limited in software. Program triggers soft stop when threshold exceeded. Threshold is set well below the point of non-recoverability, so that the soft stop subroutine can bring about controlled deceleration. Rider equipped with helmet, knee guards and elbow guards.	2	63	126	Implement audio warning to user if design speed exceeded. Description of this audio warning and its implication to be written into SOP.
			9	Excessive pitch angle.	8	Maximum pitch angle limited in software. Program triggers hard stop when threshold exceeded to prevent motor from running after fall.	2	72	144	None.
	General instability condition.	Plant no longer controllable. Micycle may exhibit large-scale oscillatory behaviour. Micycle inevitably pitches over and motor continues to operate at	9	Excessive pitch angular rate. Since the Micycle is intended to be ridden unidirectionally, there is no reason for a large change in	7	Maximum angular rate limited in software. Program triggers hard stop when threshold exceeded, since controlled recovery no longer possible.	2	63	126	None.

1 Severity
2 Occurance
3 Detection rating
4 Criticality rating = S x O
5 Risk Priority Number = S x O x D

Function	Failure Mode	Effect	S[1]	Cause	O[2]	Current Controls	D[3]	CRIT	RPN	Recommendations
		saturation limits of motor controller. Potential for serious injury to rider.		angular rate during normal operation.						
	Large disturbance in control system.	A large spike in plant dynamics may be beyond the ability of the control loop to recover and maintain stability.	8	Micycle hits protuberance in terrain.	5	Maximum motor current limited in software. Program triggers soft stop.	1	45	45	Write into SOP that the Micycle is not designed for rough terrain. Select smooth terrain area for running at exhibition.
		Rider in loop induces oscillations by overcompensating for plant disturbance.	8	Noise spikes in sensor signals. Micycle hits protuberance in terrain.	8	Sensor noise spike should not be an issue using the Microstrain IMU. Low-pass filter implemented in software to eliminate noise spikes in Kalman filter for extension goal IMU implementation. Direct-drive power train eliminates slosh and minimises delay time. Dead man's switch triggers soft stop.	4	64	256	Explicitly warn users to trust in control system and not overcompensate by shifting their balance.

1 Severity
2 Occurance
3 Detection rating
4 Criticality rating = S x O
5 Risk Priority Number = S x O x D

Function	Failure Mode	Effect	S[1]	Cause	O[2]	Current Controls	D[3]	CRIT	RPN	Recommendations
Moving Parts	User's extremities caught in pinch points.	Potential for serious injury to rider.	9	User's appendages come into proximity with moving parts.	5	Spoke-less hub motor design reduces pinch points. Monkey grip located far from moving parts. Steering linkages located behind rider, out of easy reach. Mushroom button cuts power in emergencies.	2	45	45	Write adequate warning about dangers of moving parts into SOP.
Driving	Collision with environment objects.	Potential for serious injury to rider.	8	Obstacles present in operational area.	3	Rider equipped with helmet, knee guards and elbow guards. Mushroom button allows for immediate power kill. Tilt limit in software provides additional fail-safe.	1	24	24	Ensure operational area is clear of obstacles before use.
	Collision with bystanders	Potential for serious injury to bystanders.	7	Bystanders present in operational area.	3	None.	1	21	21	Cordon off operational area during exhibition and make public announcement advising bystanders to stand clear prior to operation.

1 Severity
2 Occurance
3 Detection rating
4 Criticality rating = S x O
5 Risk Priority Number = S x O x D

Function	Failure Mode	Effect	S[1]	Cause	O[2]	Current Controls	D[3]	CRIT	RPN	Recommendations
Battery	Exposed live wire	Potential for electric shock to user. May cause severe discomfort, but unlikely to result in serious injury.	6	Power cables not adequately sheathed. Defective electrical connectors.	3	Wires are routed inside structural members and housing where possible. All wiring fully sheathed or in ribbons.	7	21	147	Ensure precautions against electric shock are written into SOP.
	Battery voltage level drops.	Change in plant dynamics that is invisible to the controller. Without appropriate adjustments to control gains, the plant may become unstable.	7	Voltage level decrease is inevitable and will occur naturally as battery discharges.	10	Battery voltage level monitored. If voltage level drops below design threshold, software will sound audio warning and initiate controlled deceleration and soft stop.	2	70	140	Audio warning for this failure mode should be distinct from excessive speed audio warning. Description of this audio warning and its implication to be written into SOP.
Signals	Communication between IMU and microcontroller interrupted.	Microcontroller would become unresponsive as the program hangs, waiting for a valid reading from the IMU. Motor would continue at constant speed. All control of system would be lost. Motor would continue to run even after the Micycle falls over.	9	IMU returns no value or unexpected value.	6	Program enters exception handling mode: IMU error function halts program operation and generates error code.	7	54	378	Check voltage level of IMU power rail – if nominal, output unique 'IMU communication error' code to 7-seg display. This is the default output code for an IMU error if the three checks below do not yield an error.

1 Severity
2 Occurance
3 Detection rating
4 Criticality rating = S x O
5 Risk Priority Number = S x O x D

Function	Failure Mode	Effect	S[1]	Cause	O[2]	Current Controls	D[3]	CRIT	RPN	Recommendations
			9	Power to IMU lost due to wiring/connection fault.	2	Program enters exception handling mode: IMU error function halts program operation and generates error code.	2	18	36	Check voltage level of IMU power rail – if abnormal, output unique 'IMU power error' code to 7-seg display.
			9	RS232 cable fails.	2	Program enters exception handling mode: IMU error function halts program operation and generates error code.	4	18	72	Check level on DCE pin of RS-232. If 0, output unique 'IMU serial connection interrupted' error code to 7-seg display.
			9	Decoding error.	5	Program enters exception handling mode: IMU error function halts program operation and generates error code.	8	45	360	Use checksum algorithm to diagnose fault. If error detected, output 'IMU decoding error' to 7-seg display.
	Unexpected ADC input.	System exhibits sporadic, unpredictable behaviour, Potential for injury to rider, especially if at high speed.	7	Battery charge indicator signal error due to wiring fault.	4	Out-of-bounds detection built into software. Program triggers soft stop with appropriate error code reported.	6	28	168	All wires to be inspected thoroughly during testing phase and prior to public exhibition.
		The wrong set of controller gains may be applied to the system. Performance degrades.	3	Gain toggle signal error due to wiring fault.	4	Out-of-bounds detection built into software. Program triggers soft stop with appropriate error code	6	12	72	All wires to be inspected thoroughly during testing phase and prior to public exhibition.

1 Severity
2 Occurance
3 Detection rating
4 Criticality rating = S x O
5 Risk Priority Number = S x O x D

Function	Failure Mode	Effect	S[1]	Cause	O[2]	Current Controls	D[3]	CRIT	RPN	Recommendations
		Erroneous controller gain values generated. This will cause performance to degrade and may render the system unstable.	8	Strain gauge signal error due to wiring fault.	4	Out-of-bounds detection built into software. Program triggers soft stop with appropriate error code reported.	6	32	192	All wires to be inspected thoroughly during testing phase and prior to public exhibition.
		No feedback on motor speed. Impossible to measure translational velocity of Micycle. The system will inevitably go unstable.	9	Motor controller monitor signal error due to wiring fault.	4	Out-of-bounds detection built into software. Program triggers soft stop with appropriate error code	6	36	216	All wires to be inspected thoroughly during testing phase and prior to public exhibition.
Motor Controller	Over temperature: Power stage temperature is too high and switched off (disable status).	The motor controller shuts down if temperature limit is exceeded. This may be very hazardous to the rider if the Micycle is travelling at high speed.	8	Power stage temperature exceeds 115°. High ambient temperature. Insufficient convective cooling.	3	Program reads Ready signal from Maxon controller and reports 'General Op' error code to 7-seg display. Open chassis design maximises airflow and convective cooling of electronic components.	2	18	36	Tap off LED lines on Maxon controller and write software driver to diagnose Maxon errors and report to the 7-seg display.

1 Severity
2 Occurance
3 Detection rating
4 Criticality rating = S x O
5 Risk Priority Number = S x O x D

Function	Failure Mode	Effect	S[1]	Cause	O[2]	Current Controls	D[3]	CRIT	RPN	Recommendations
	Invalid Hall Sensor Signals: Invalid Hall sensor pattern detected during power-up. Invalid sequence of Hall sensor signals detected.	Motor controller may shut down in worst case. This may cause the Micycle to lose stability suddenly, which is potentially hazardous to the rider.	8	Incorrect Hall sensor connection. Damaged Hall sensor. EM disturbance of Hall sensor lines. Hall sensor supply voltage on motor side too low.	3	Program reads Ready signal from Maxon controller and reports 'General Op' error code to 7-seg display.	2	18	36	Tap off LED lines on Maxon controller and write software driver to diagnose Maxon errors and report to the 7-seg display. Use shielded cable for Hall sensor signals.
	Overvoltage: Power supply voltage is too high for operation.	Motor controller may shut down in worst case. This may cause the Micycle to lose stability suddenly, which is potentially hazardous to the rider.	8	Supply voltage exceeds 77V. Power supply is not able to buffer fed-back energy.	3	Program reads Ready signal from Maxon controller and reports 'General Op' error code to 7-seg display.	2	18	36	Tap off LED lines on Maxon controller and write software driver to diagnose Maxon errors and report to the 7-seg display.
	Undervoltage: Power supply voltage is too low for operation.	Motor controller may shut down in worst case. This may cause the Micycle to lose stability suddenly, which is potentially hazardous to the rider.	8	Supply voltage is under 9.4V. Supply voltage falls below 9.4V during acceleration.	2	Low battery voltage failsafe built into software provides a guard against this eventuality. Program reads Ready signal from Maxon controller and reports 'General Op' error code to 7-seg display.	2	16	32	Tap off LED lines on Maxon controller and write software driver to diagnose Maxon errors and report to the 7-seg display.

1 Severity
2 Occurance
3 Detection rating
4 Criticality rating = S x O
5 Risk Priority Number = S x O x D

Function	Failure Mode	Effect	S[1]	Cause	O[2]	Current Controls	D[3]	CRIT	RPN	Recommendations
	Overcurrent: Motor winding current is too high.	Motor controller may shut down in worst case. This may cause the Micycle to lose stability suddenly, which is potentially hazardous to the rider. Excessive current may also cause damage to the motor.	8	Motor winding current exceeds 60A peak. Motor winding current exceeds 27.2A for more than 400ms. Current regulator gain too high. Speed regulator gain too high. Damaged power stage.	3	Program reads Ready signal from Maxon controller and reports 'General Op' error code to 7-seg display. Potentiometer P6 can be adjusted to reduce current regulator gain. Potentiometer P5 can be adjusted to reduce speed regulator gain. The software current limit mentioned in the 'Motor controller saturates' failure mode will provide a safeguard against this eventuality.	2	24	48	Tap off LED lines on Maxon controller and write software driver to diagnose Maxon errors and report to the 7-seg display.
	Overspeed: Amplifier speed limit is exceeded	Motor controller may shut down in worst case. This may cause the Micycle to lose stability suddenly, which is potentially hazardous to the rider.	8	Motor speed exceeds 3500pm (for 28 pole pairs)	1	Program reads Ready signal from Maxon controller and reports 'General Op' error code to 7-seg display. The software speed limiter mentioned in the 'Motor controller saturates' failure mode will cut in before this condition can occur.	1	8	8	Tap off LED lines on Maxon controller and write software driver to diagnose Maxon errors and report to the 7-seg display.

1 Severity
2 Occurance
3 Detection rating
4 Criticality rating = S x O
5 Risk Priority Number = S x O x D

Function	Failure Mode	Effect	S[1]	Cause	O[2]	Current Controls	D[3]	CRIT	RPN	Recommendations
Gain Toggle	Change in PID controller gains during operation.	Instantaneous spike in jerk of motor response. Detrimental to ride comfort and controller performance.	2	User toggles gain switch during operation. Scaling of the gains as the voltage drops across the battery.	4	Gains will not be modified in software after initialisation. To update gains the system must be restarted.	3	8	24	Write into SOP that gains will not be reset until a system restart.
	Abrupt change in controller gain during operation.	Gains set to extreme value, potentially rendering system unstable. Gain adjustment no longer affects system, making fault diagnosis difficult.	8	Potentiometer becomes stuck on power rail.	2	Design decision to employ digital toggle rather than potentiometer to adjust gains.	8	16	128	None.
Software	Unknown failure mode.	Unexpected system behaviour. Difficult to identify the source of problem. This issue will occur frequently during initial testing and debugging phase.	5	Program bugs. System enters state not anticipated in software design.	10	Error handling code for each specific error scenario in software. Error code reported to 7-seg display. Allows for easy identification of underlying failure modes in software and electrical systems.	9	50	450	Error handling code to be fully documented during software development.

1 Severity
2 Occurance
3 Detection rating
4 Criticality rating = S x O
5 Risk Priority Number = S x O x D

Function	Failure Mode	Effect	S[1]	Cause	O[2]	Current Controls	D[3]	CRIT	RPN	Recommendations
Start-up	Micycle powered up in an unsafe position.	Sudden movement as controller attempts to establish verticality. The user may not expect sudden, large scale motion and may potentially be seriously injured.	8	Mechanical and control design assumes that Micycle powers up in upright position. There may also be an expectation from the user (based on prior experience with motorcycles and bicycles) that the Micycle will not attempt to balance until they are seated.	6	Software ensures the system will not be fully initialised until it is upright.	1	48	48	Safe start-up procedure to be documented in SOP. Users at public exhibition to be explicitly warned of this behaviour.
	IMU or Maxon do not initialise in time.	Microcontroller unable to communicate with peripheral devices. When subroutines are called that refer to these devices, the system will exhibit unexpected behaviour.	5	Unpredictable start-up times of individual electronic components.	6	Clearly defined boot sequence. Program checks that all systems have been initialised, and throws an error code for whichever system has not. Program triggers hard stop and must be reset.	6	30	180	None.

1 Severity
2 Occurance
3 Detection rating
4 Criticality rating = S x O
5 Risk Priority Number = S x O x D

Function	Failure Mode	Effect	S[1]	Cause	O[2]	Current Controls	D[3]	CRIT	RPN	Recommendations
Steering Mechanism	Rotary damper failure.	Steering becomes rough and prone to fluctuations. More difficult to execute turns. Discomfort to the rider. Not critical to safe operation of Micycle.	2	Rotary dampers impacted heavily during a fall.	2	Two rotary dampers provide an element of redundancy.	2	4	8	None.
	Torsion spring/spring mount failure.	Steering becomes loose and no longer centres automatically. More difficult to execute turns. Not critical to safe operation of Micycle.	2	Spring subject to excessive loading from an extreme weight imbalance between the two foot pegs.	1	Heavy duty spring designed to withstand shock loading.	2	2	4	None.
Structure	Split collar failure.	Structural integrity compromised, rendering Micycle inoperable.	7	Excessive weight loading on Micycle. (Load intensity will be magnified by terrain protuberances)	1	Second split collar provides load-bearing redundancy, meaning structural failure will not be catastrophic. Load-bearing structure rated to 200kg according to FEA. Cushioned seat and cantilevered structure geometry attenuates impulse.	2	7	14	Ensure maximum weight limit is written into SOP.

1 Severity
2 Occurance
3 Detection rating
4 Criticality rating = S x O
5 Risk Priority Number = S x O x D

Function	Failure Mode	Effect	S[1]	Cause	O[2]	Current Controls	D[3]	CRIT	RPN	Recommendations
	Fork assembly failure.	Structural integrity compromised, rendering Micycle inoperable. Structure abruptly unable to support load. Rider falls and may sustain injuries.	10	Excessive weight loading on Micycle. (Load intensity will be magnified by terrain protuberances)	2	Fork assembly made from CRMO steel for increased strength. Load-bearing structure rated to 200kg according to FEA. Cushioned seat and cantilevered structure geometry attenuates impulse.	2	20	40	Ensure maximum weight limit is written into SOP.
	Chassis plate failure.	Structural integrity compromised, rendering Micycle inoperable. Structure abruptly unable to support load. Rider falls and may sustain injuries.	10	Excessive weight loading on Micycle. (Load intensity will be magnified by terrain protuberances)	3	Provision made for additional Al members to link between spars on chassis, increasing strength and rigidity. Load-bearing structure rated to 200kg according to FEA. Cushioned seat and cantilevered structure geometry attenuates impulse.	2	30	60	Ensure maximum weight limit is written into SOP.

1 Severity
2 Occurance
3 Detection rating
4 Criticality rating = S x O
5 Risk Priority Number = S x O x D

Appendix D.

Software flow charts

The flow charts describe the intended software design. They begin on the following page.

Main.c

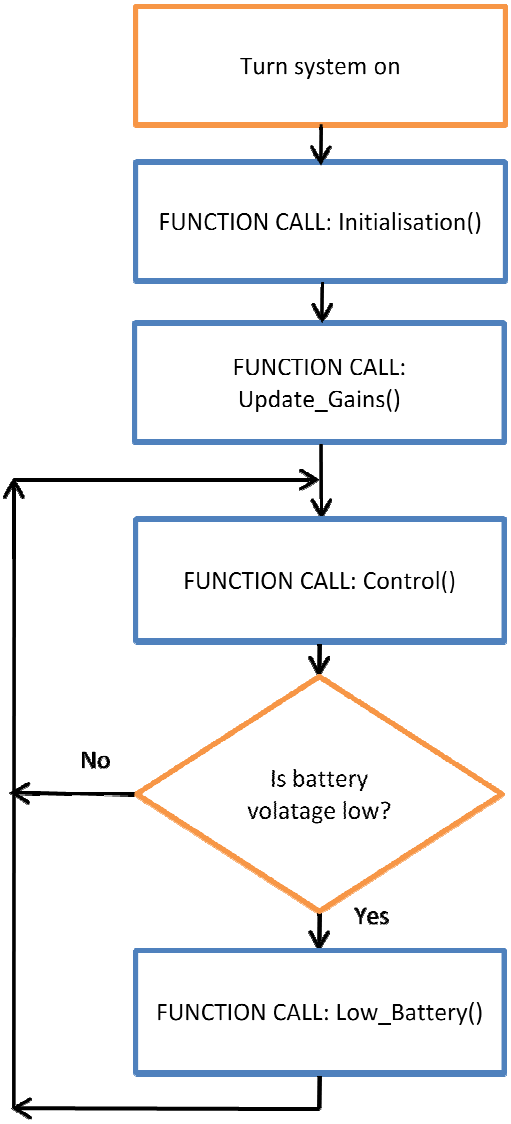
Turn system on
FUNCTION CALL: Initialisation()
FUNCTION CALL: Update_Gains()
FUNCTION CALL: Control()
Is battery volatage low?
No
Yes
FUNCTION CALL: Low_Battery()

FUNCTION: Initialisation()

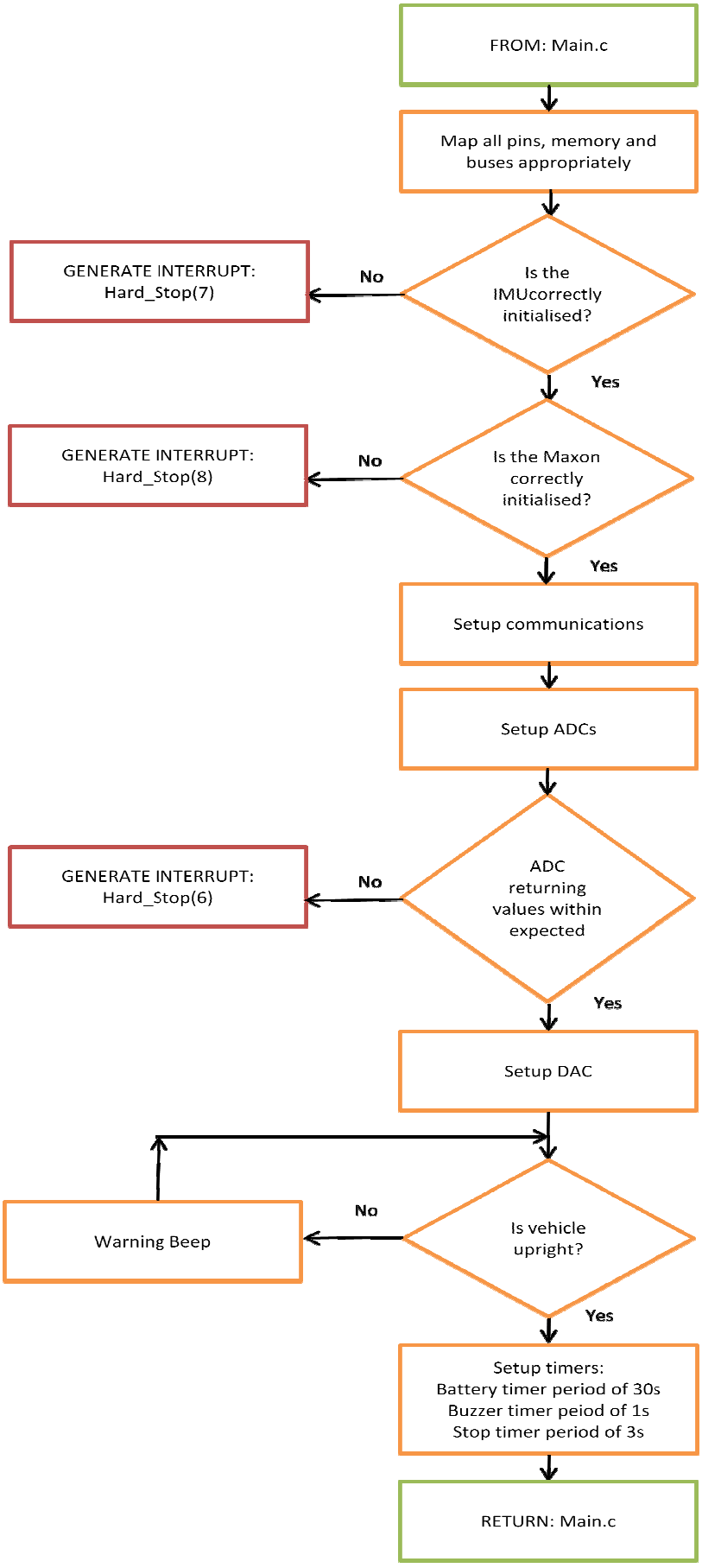

FUNCTION: Control()

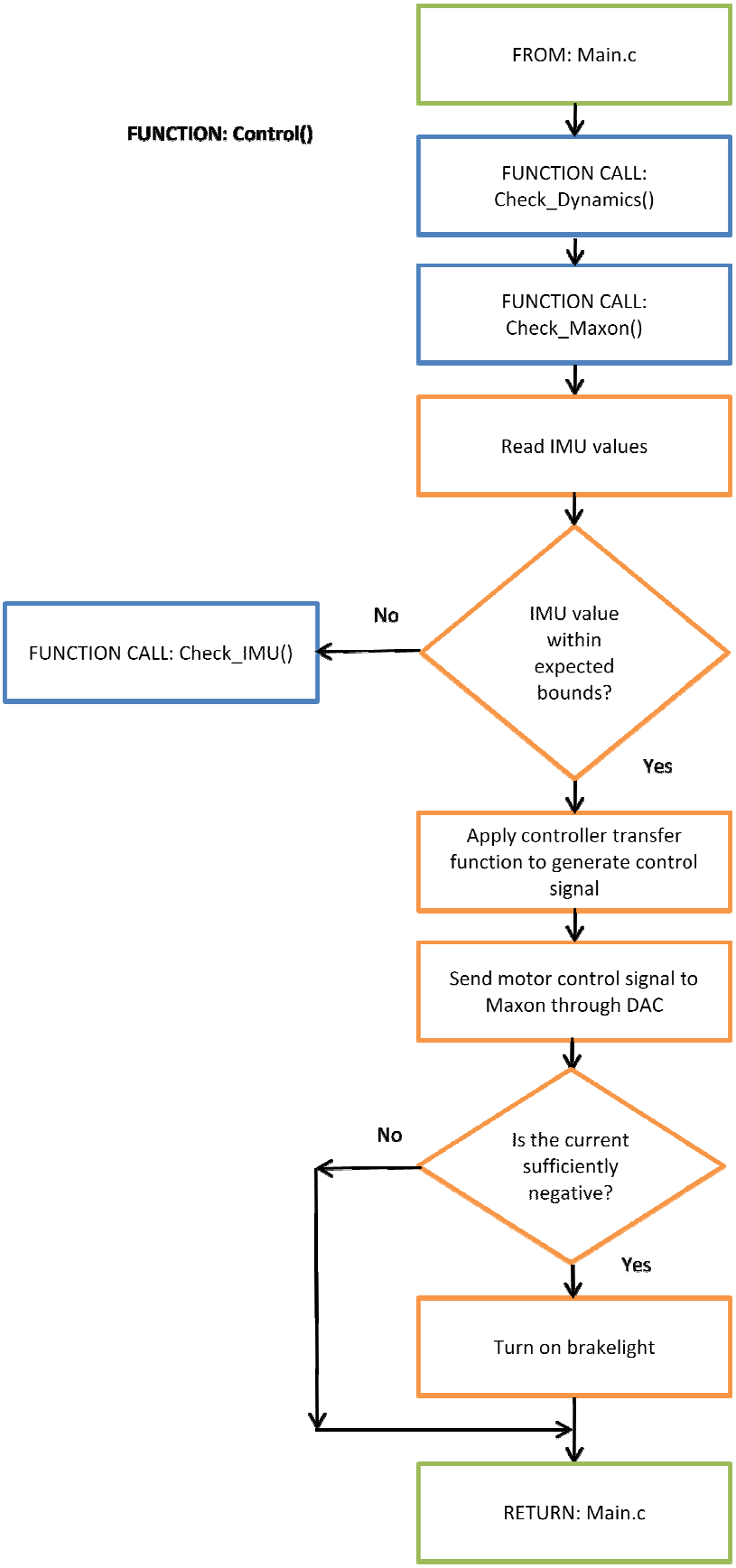

FUNCTION: Check_Dynamics()

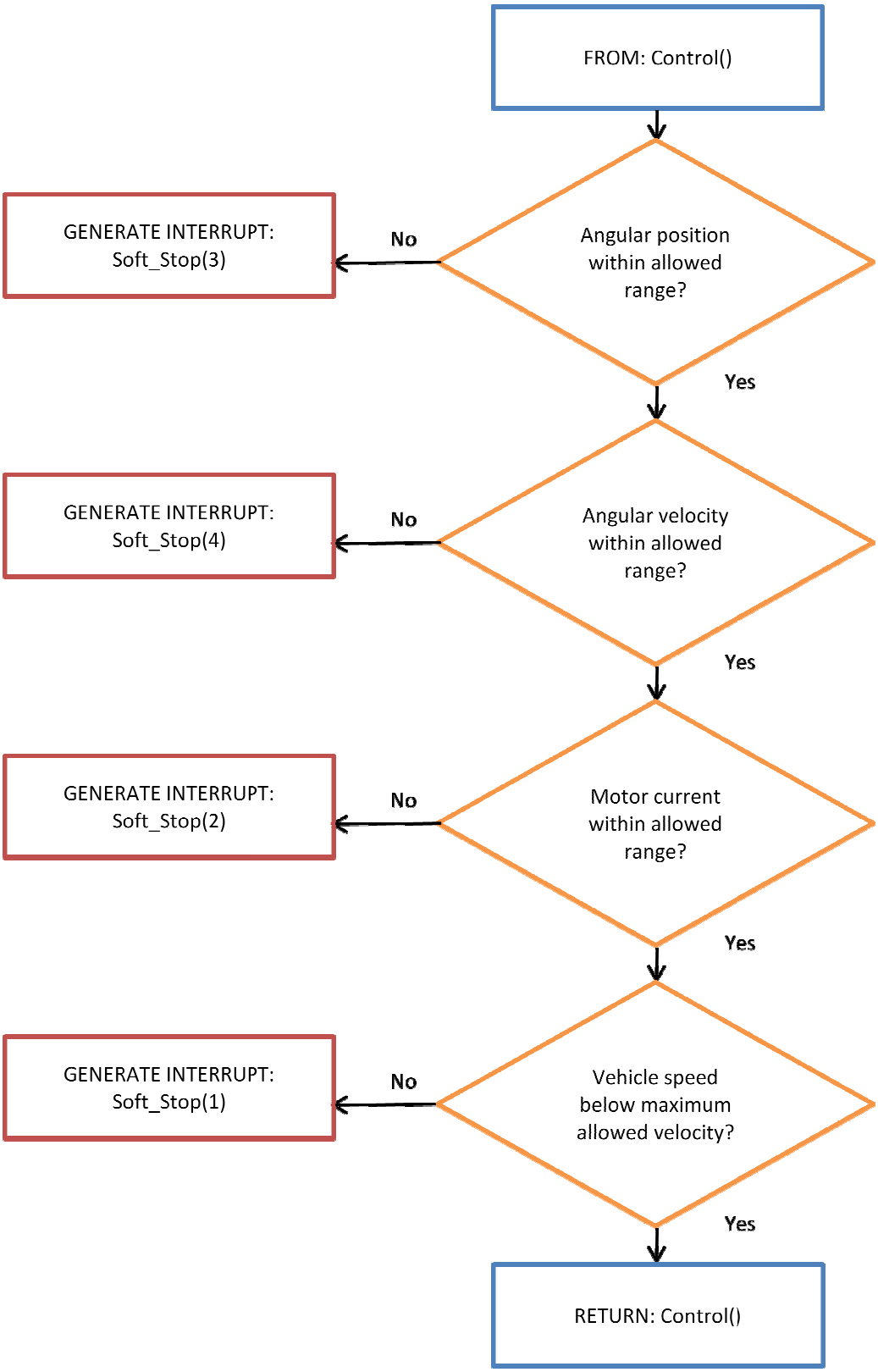

FUNCTION: Check_IMU()

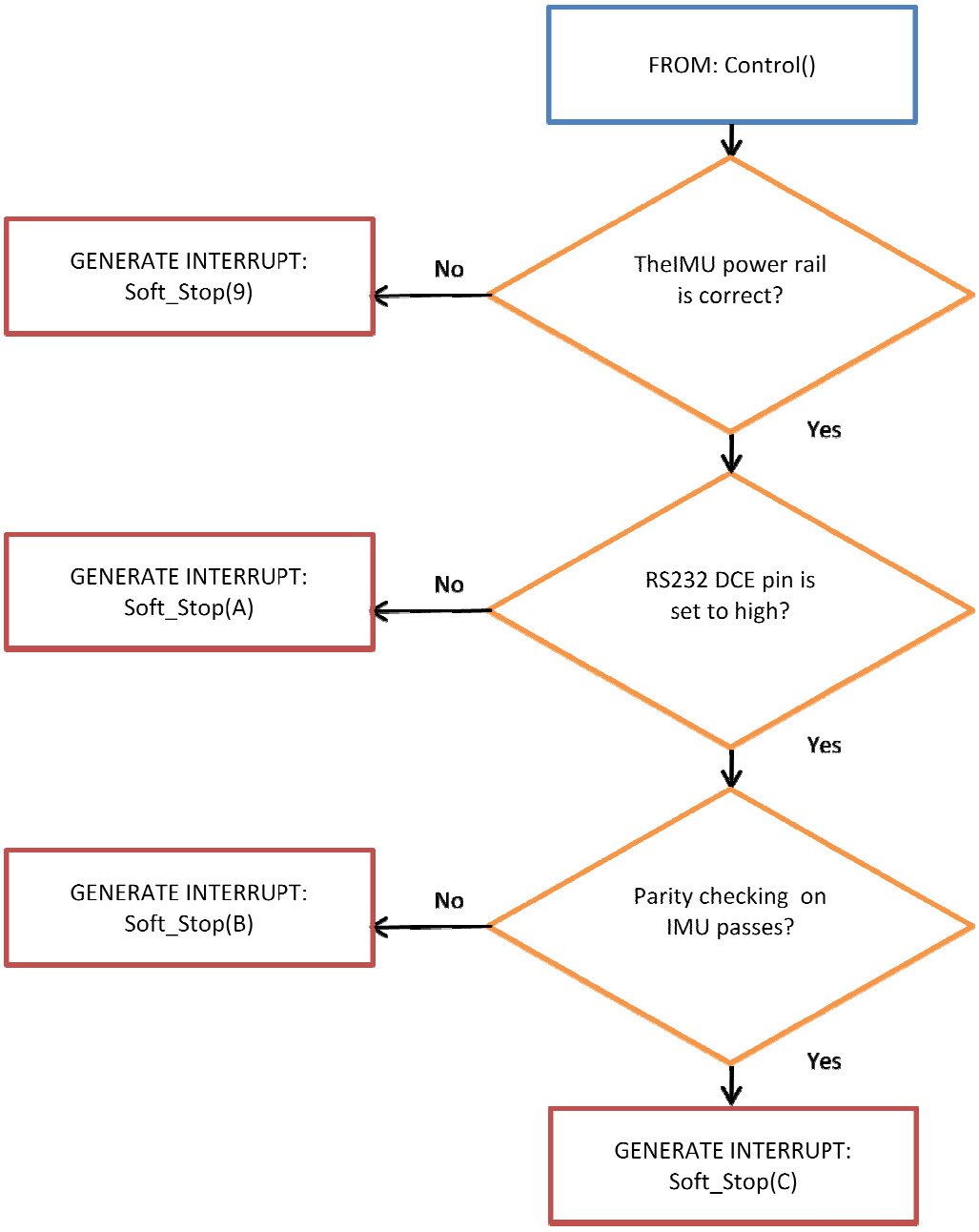

FUNCTION: Check_Maxon()

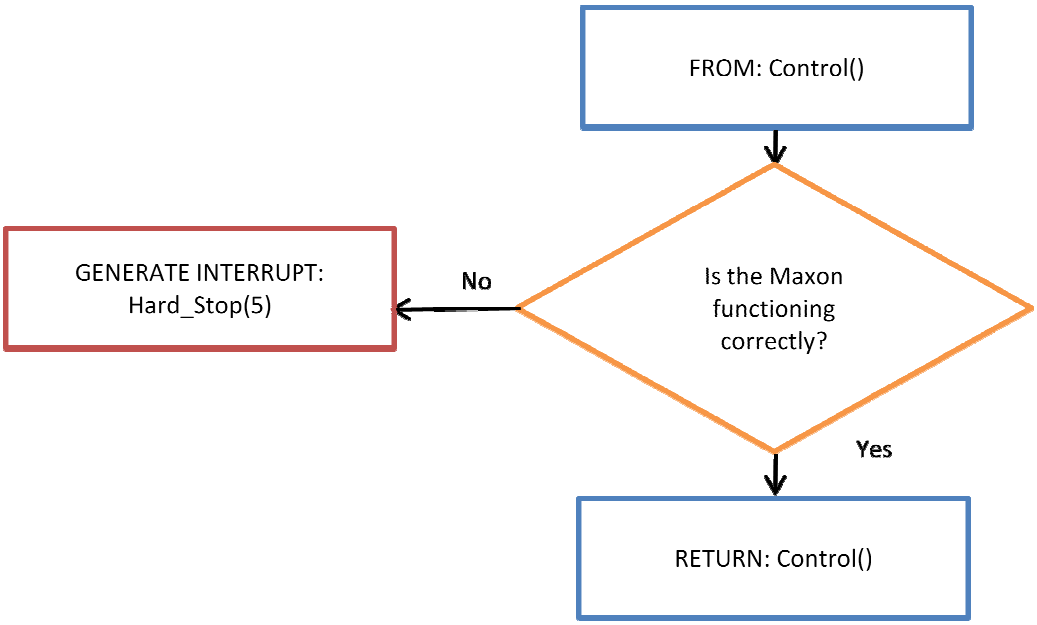

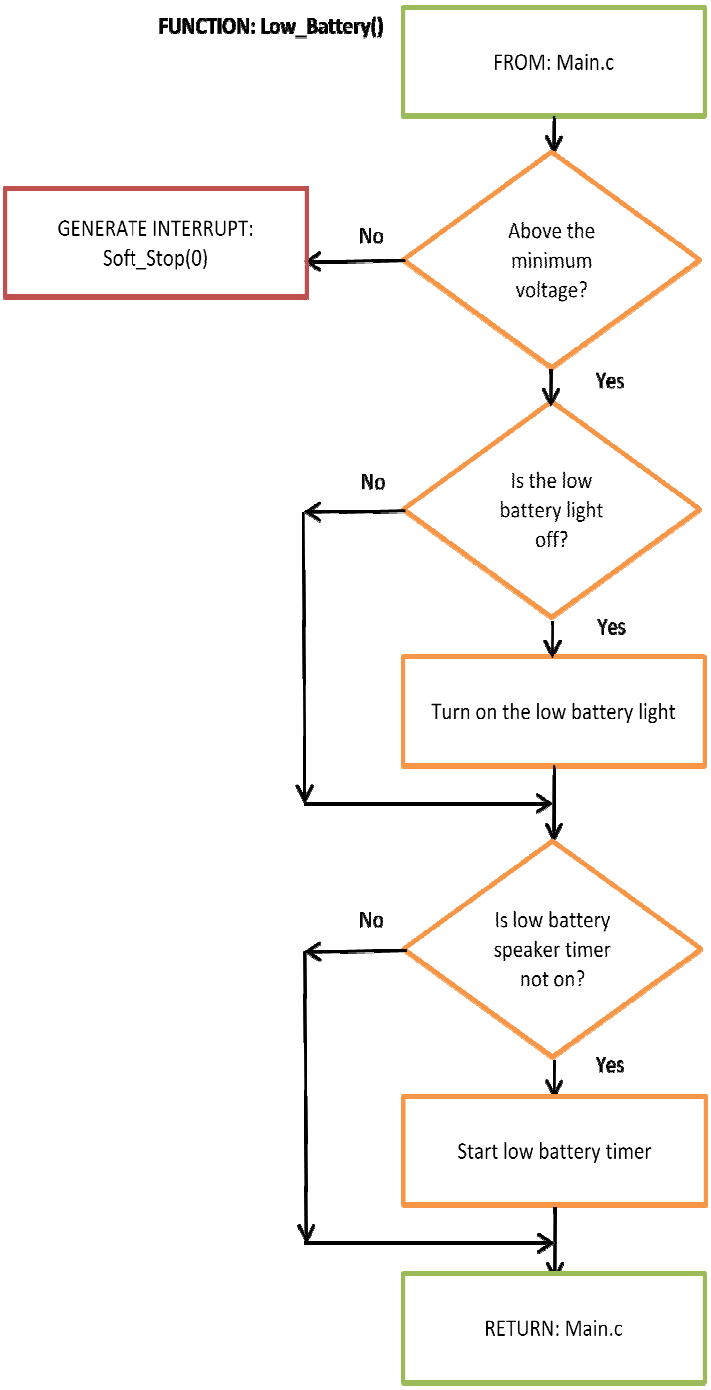
FUNCTION: Low_Battery()
FROM: Main.c
Above the minimum voltage?
No
GENERATE INTERRUPT: Soft_Stop(0)
Yes
Is the low battery light off?
No
Yes
Turn on the low battery light
Is low battery speaker timer not on?
No
Yes
Start low battery timer
RETURN: Main.c

FUNCTION: Update_Gains()

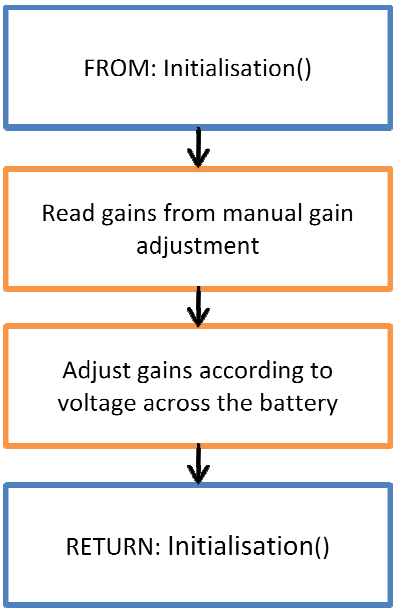
FROM: Initialisation()
Read gains from manual gain adjustment
Adjust gains according to voltage across the battery
RETURN: Initialisation()

INTERRUPT: Hard_Stop(error code)

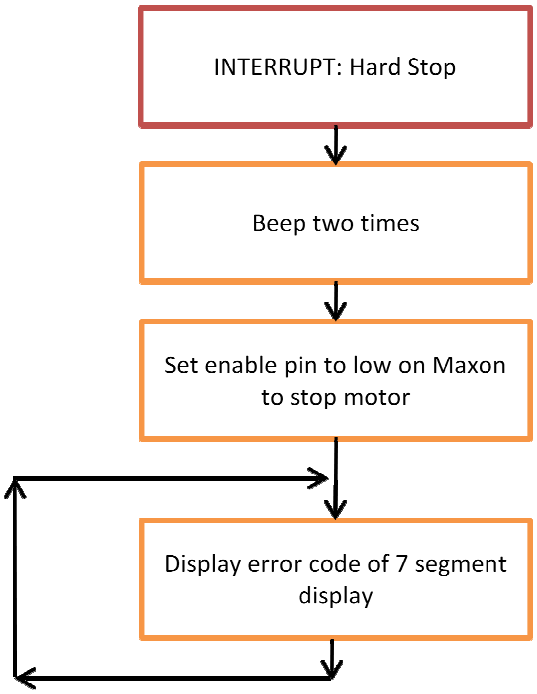

INTERRUPT: Soft_Stop(error code)

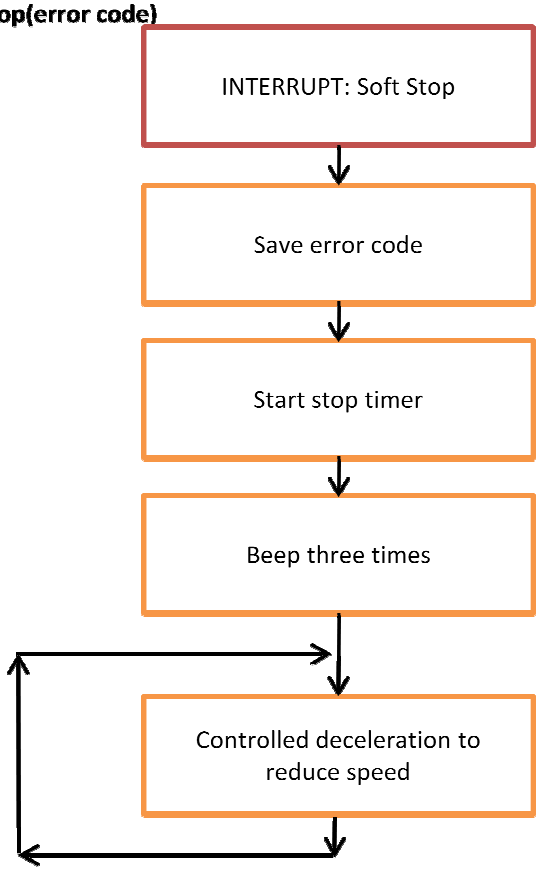

INTERRUPT: Stop_Timer()

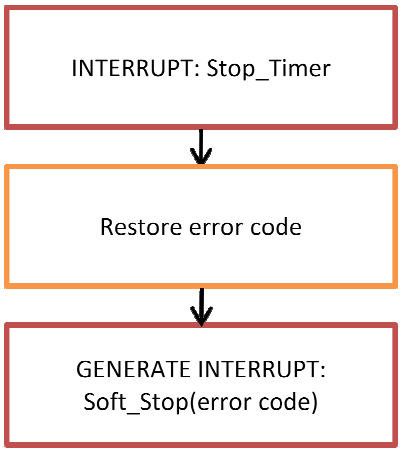

INTERRUPT: Buzzer_Timer()

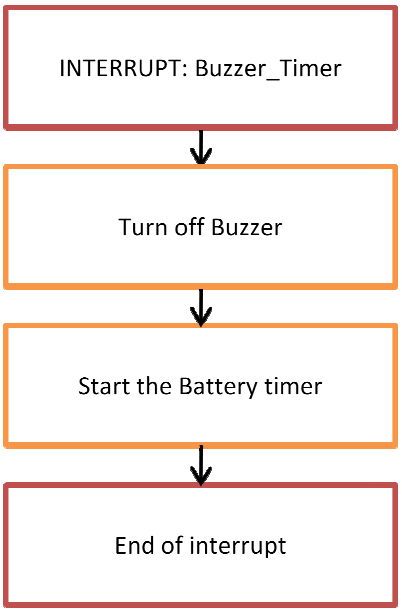

INTERRUPT: Battery_Timer()

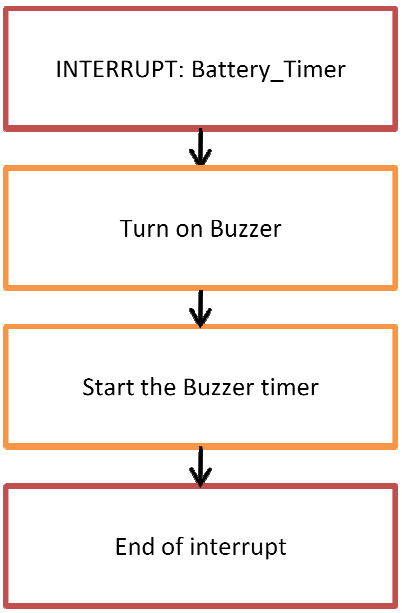

Appendix E.

Code

E.1. Embedded M-file for Simulink block

```
%Declare input outputs for M file block
function [x_dot_dot,theta_dot_dot] =
        System_Dynamics(tau, x_dot, x, theta, theta_dot)

%Constants
g = 9.81;

%Physical properties of the system
rw = 0.16;
rf = 0.7;
mw = 7;
mf = 80;

%Set damping and friction forces
beta = 50;
gamma = 50;

%Calculate Moments of Inertia
Ifg = ( mf*rf.^2 )/3;
Iwg = ( mw*rw.^2 )/2;

%Simplifying terms for equation entry
a = mf + mw + Iwg/rw.^2;
b = mf * rf;
c = mf*rf.^2 + Ifg;
d = 1/( a*c - b.^2*cos(theta ));

%Enter terms of output
a1 = b * c * theta_dot.^2 * sin(theta);
a2 = - b.^2 * g * sin(theta) * cos(theta);
```

```
a3 = tau * ( c-b*rw*cos(theta) )/rw;
a4 = - beta * c * x_dot;
a5 = gamma * b * cos(theta) * theta_dot;

b1 = b * g * a * sin(theta);
b2 = - b.^2 * theta_dot.^2 * sin(theta) * cos(theta);
b3 = tau * ( a*rw - b*cos(theta) )/rw;
b4 = - gamma * a * theta_dot;
b5 = beta * b * cos(theta) * x_dot;

%Enter outputs
x_dot_dot = d*(a1 + a2 + a3 + a4 + a5);
theta_dot_dot = d*(b1 + b2 + b3 + b4 + b5);
```

Appendix F.

Component datasheets

The following component datasheets are included in this appendix (all overleaf).

F.1. ACE FDT70 rotary damper

F.2. MiniDRAGON+2 microcontroller

The schematic diagram of the circuit board is attached.

F.3. Golden Motor Magic Pie

The dimensional drawing is attached.

F.4. Maxon motor controller

The block diagram and dimensional drawing are attached.

F.5. Microstrain 3DM-GX2 IMU

F.6. SparkFun IMU Combo Board

Soft Silent Safety

F70A/FDN-70A Series

RoHS Compliant

Disk Damper [Bi-Directional] [Uni-Directional] Fixed

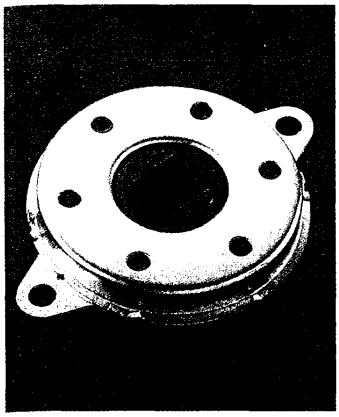

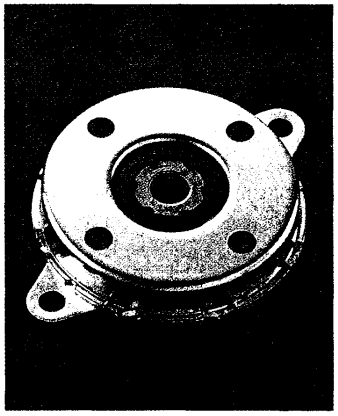

<Specifications>

Model	Rated torque	Damping direction
FDT-70A-903 FDT-70B-903	8.7±0.8 N·m (87±8.0 kgf·cm)	Both directions
FDN-70A-R114	11±1.1 N·m	Clockwise
FDN-70A-L114	(110±11 kgf·cm)	Counter-clockwise

Note) Rated torque is measured at a rotation speed of 20rpm at 23°C±3°C
70B has a slotted rotating shaft opening

*Max. rotation speed	50rpm
*Max. cycle rate	12 cycle/min
*Operating temperature	−10~50°C
*Weight	FDT-70A : 112g, FDN-70A : 136g
*Main body material	Iron (SPFC)
*Rotor (shaft) material	Nylon (with glass)
*Oil type	Silicone oil

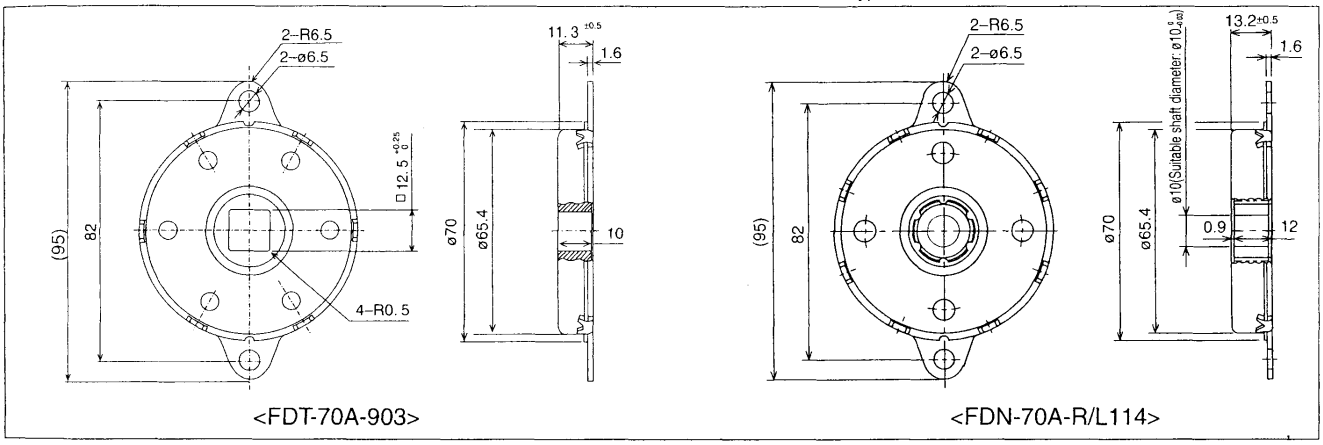

<FDT-70A-903> <FDN-70A-R/L114>

How to Use the Damper

1. Dampers may generate torque in both directions, clockwise, or counter-clockwise.
2. Please make sure that a shaft attached to a damper has a bearing, as the damper itself is not fitted with one.
3. Please refer to the recommended dimensions below when creating a shaft for FDN-70A. Not using the recommended shaft dimensions may cause the shaft to slip out.

Shaft's external dimensions	ø10 0 -0.03
Surface hardness	HRC55 or higher
Quenching depth	0.5mm or higher
Surface roughness	1.0Z or lower
Chamfer end (Damper insertion side)	C0.2-C0.3 (or R0.2-R0.3)

4. To insert a shaft into FDN-70A, insert the shaft while spinning it in the idling direction of the one-way clutch. (Do not force the shaft in from the regular direction. This may damage the one-way clutch.)
5. When using FDT-70A, please ensure that a shaft with specified angular dimensions is inserted in the damper's shaft opening. A wobbling shaft and damper shaft may not allow the lid to slow down properly when closing. Please see the diagrams to the right for the recommended shaft dimensions for a damper.

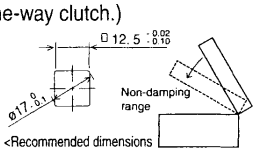

6. A damper shaft connecting to a part with slotted groove is also available. The slotted groove type is excellent for usage with spiral springs.

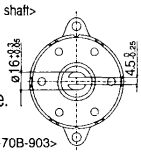

<FDT-70B-903>

Damper Characteristics

1. Speed characteristics

A disk damper's torque varies according to the rotation speed. In general, as shown in the graph to the right, the torque increases as the rotation speed increases, and the torque decreases as the rotation speed decreases. Torque at 20rpm is shown in this catalogue. In a closing lid, the rotation speed is slow when the lid begins to close, resulting in the generation of torque that is smaller than the rated torque.

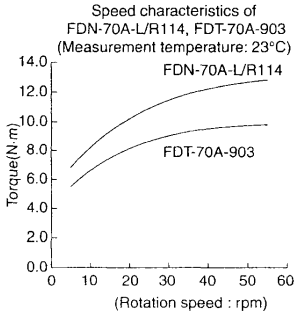

2. Temperature characteristics

Damper torque (rated torque in this catalogue) varies according to the ambient temperature. As the temperature increases, the torque decreases, and as the temperature decreases, the torque increases. This is because the viscosity of the silicone oil inside the damper varies according to the temperature. The graph to the right illustrates the temperature characteristics.

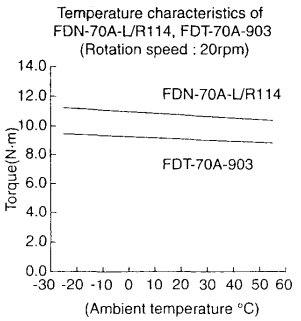

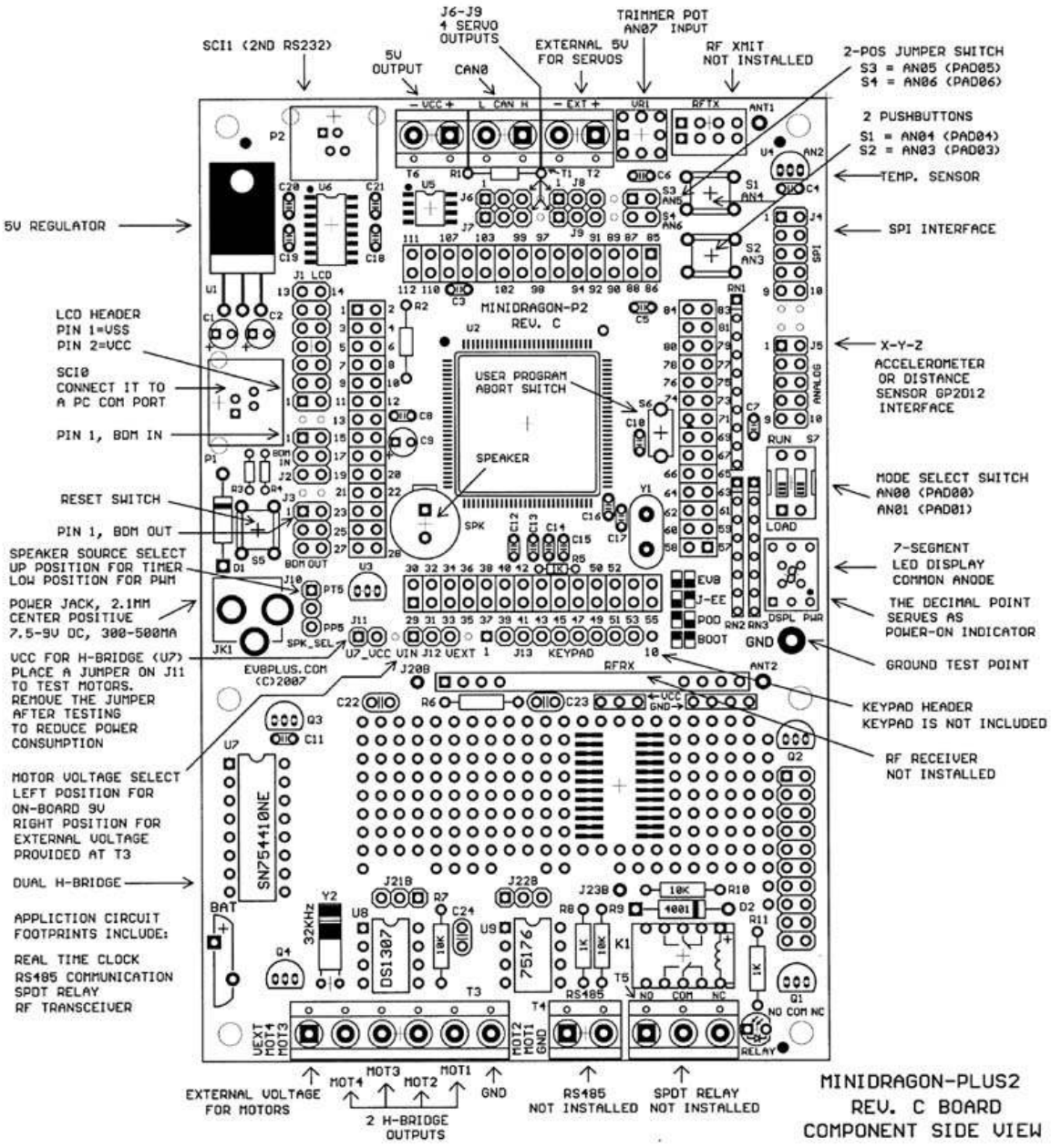
SCI1 (2ND RS232)
5V OUTPUT
CAN0
J6-J9 4 SERVO OUTPUTS
EXTERNAL 5V FOR SERVOS
TRIMMER POT AN07 INPUT
RF XMIT NOT INSTALLED
2-POS JUMPER SWITCH S3 = AN05 (PAD05) S4 = AN06 (PAD06)
2 PUSHBUTTONS S1 = AN04 (PAD04) S2 = AN03 (PAD03)
TEMP. SENSOR
SPI INTERFACE
5V REGULATOR
LCD HEADER PIN 1=VSS PIN 2=VCC
SCI0 CONNECT IT TO A PC COM PORT
PIN 1, BDM IN
RESET SWITCH
PIN 1, BDM OUT
SPEAKER SOURCE SELECT UP POSITION FOR TIMER LOW POSITION FOR PWM
POWER JACK, 2.1MM CENTER POSITIVE 7.5-9V DC, 300-500MA
VCC FOR H-BRIDGE (U7) PLACE A JUMPER ON J11 TO TEST MOTORS. REMOVE THE JUMPER AFTER TESTING TO REDUCE POWER CONSUMPTION
MOTOR VOLTAGE SELECT LEFT POSITION FOR ON-BOARD 9V RIGHT POSITION FOR EXTERNAL VOLTAGE PROVIDED AT T3
DUAL H-BRIDGE
APPLICTION CIRCUIT FOOTPRINTS INCLUDE:
REAL TIME CLOCK
RS485 COMMUNICATION
SPDT RELAY
RF TRANSCEIVER
MINIDRAGON-P2 REV. C
USER PROGRAM ABORT SWITCH
SPEAKER
X-Y-Z ACCELEROMETER OR DISTANCE SENSOR GP2D12 INTERFACE
MODE SELECT SWITCH AN00 (PAD00) AN01 (PAD01)
7-SEGMENT LED DISPLAY COMMON ANODE
THE DECIMAL POINT SERVES AS POWER-ON INDICATOR
GROUND TEST POINT
KEYPAD HEADER KEYPAD IS NOT INCLUDED
RF RECEIVER NOT INSTALLED
EVBPLUS.COM (C)2007
SN754410NE
DS1307
75176
32KHz
EXTERNAL VOLTAGE FOR MOTORS
2 H-BRIDGE OUTPUTS
RS485 NOT INSTALLED
SPDT RELAY NOT INSTALLED
MINIDRAGON-PLUS2 REV. C BOARD COMPONENT SIDE VIEW

Golden Motor MagicPie for 135mm rear fork

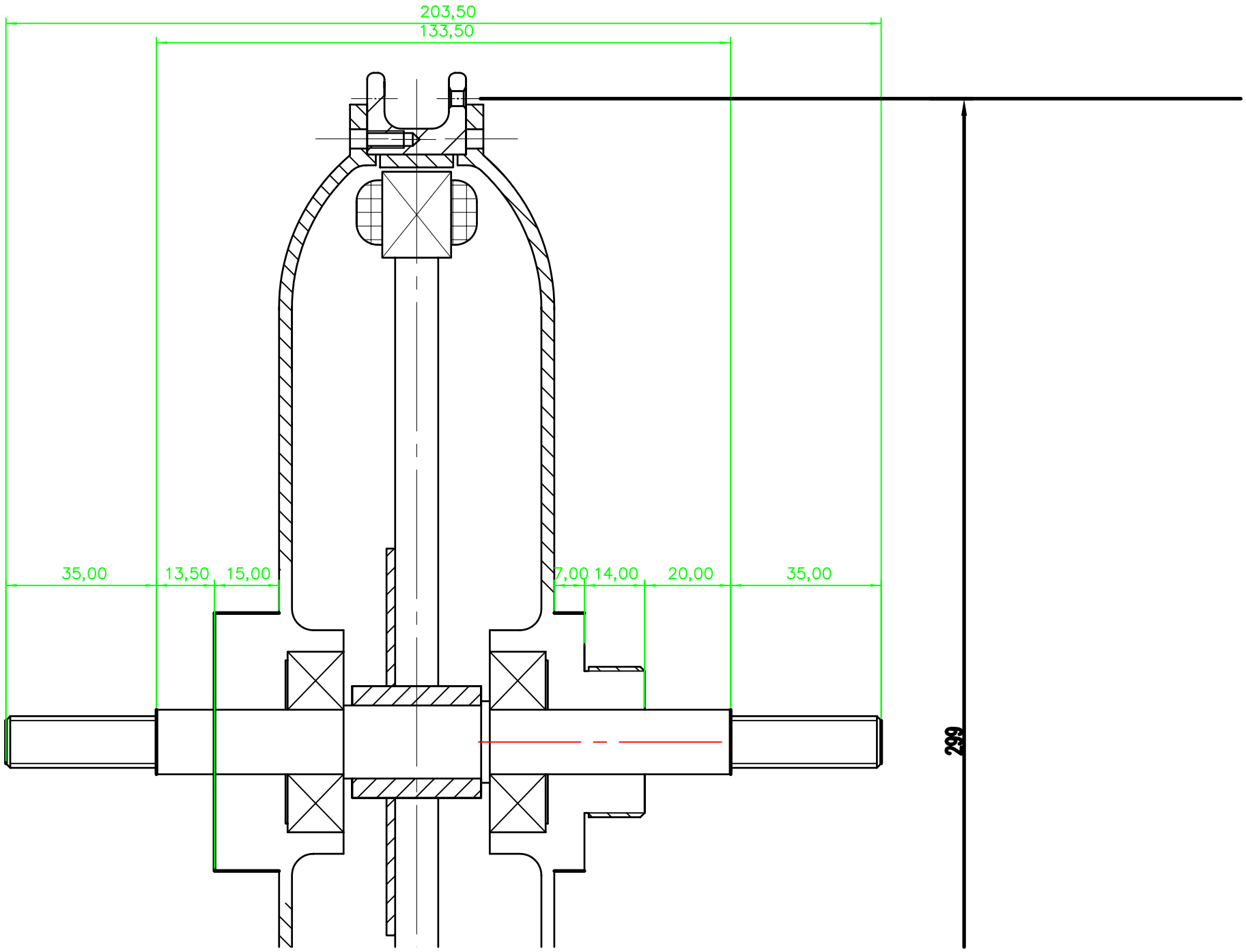

13 Block Diagram

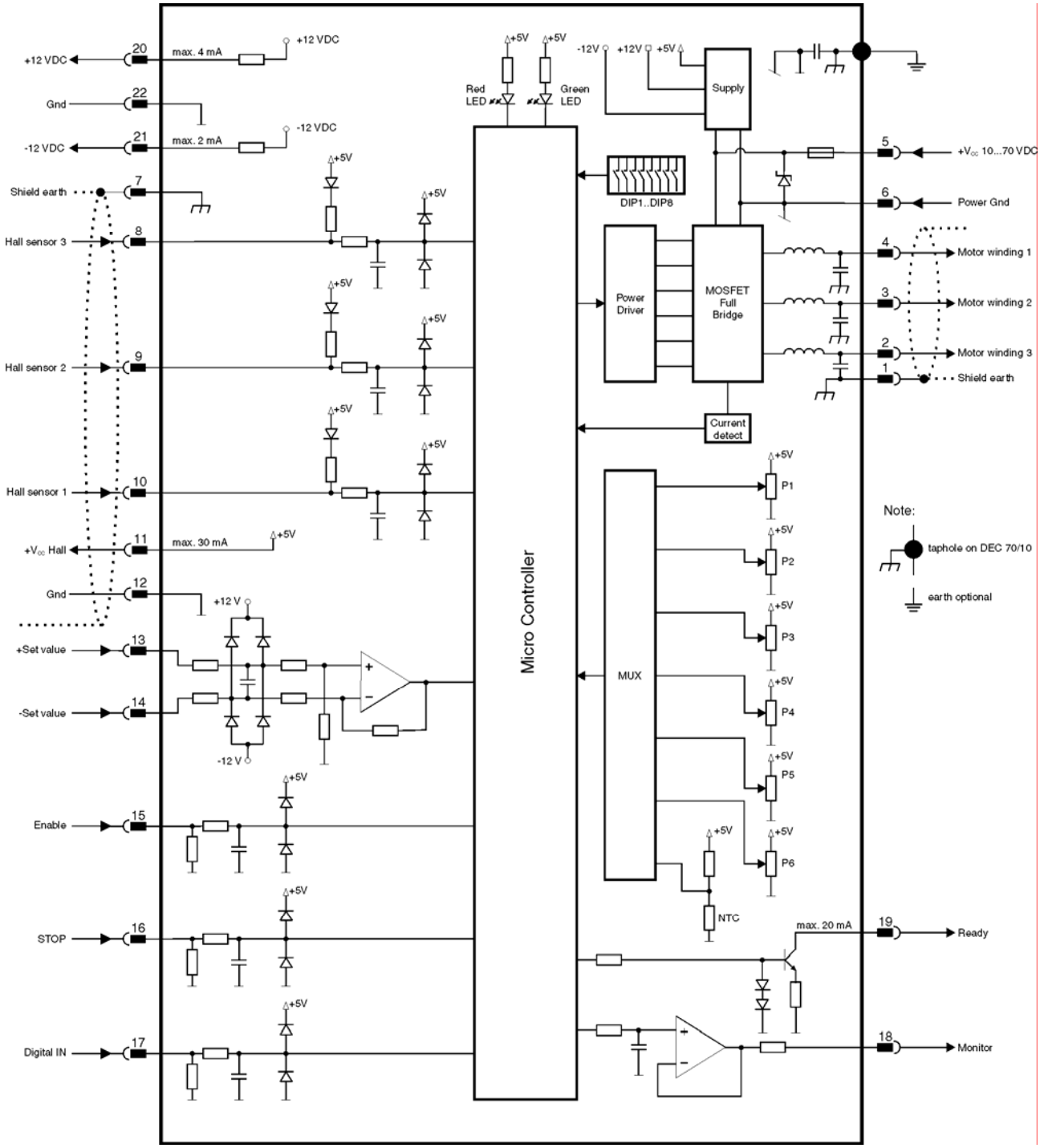

Figure 17: Block diagram

14 Dimension Drawing

Dimensions in [mm]

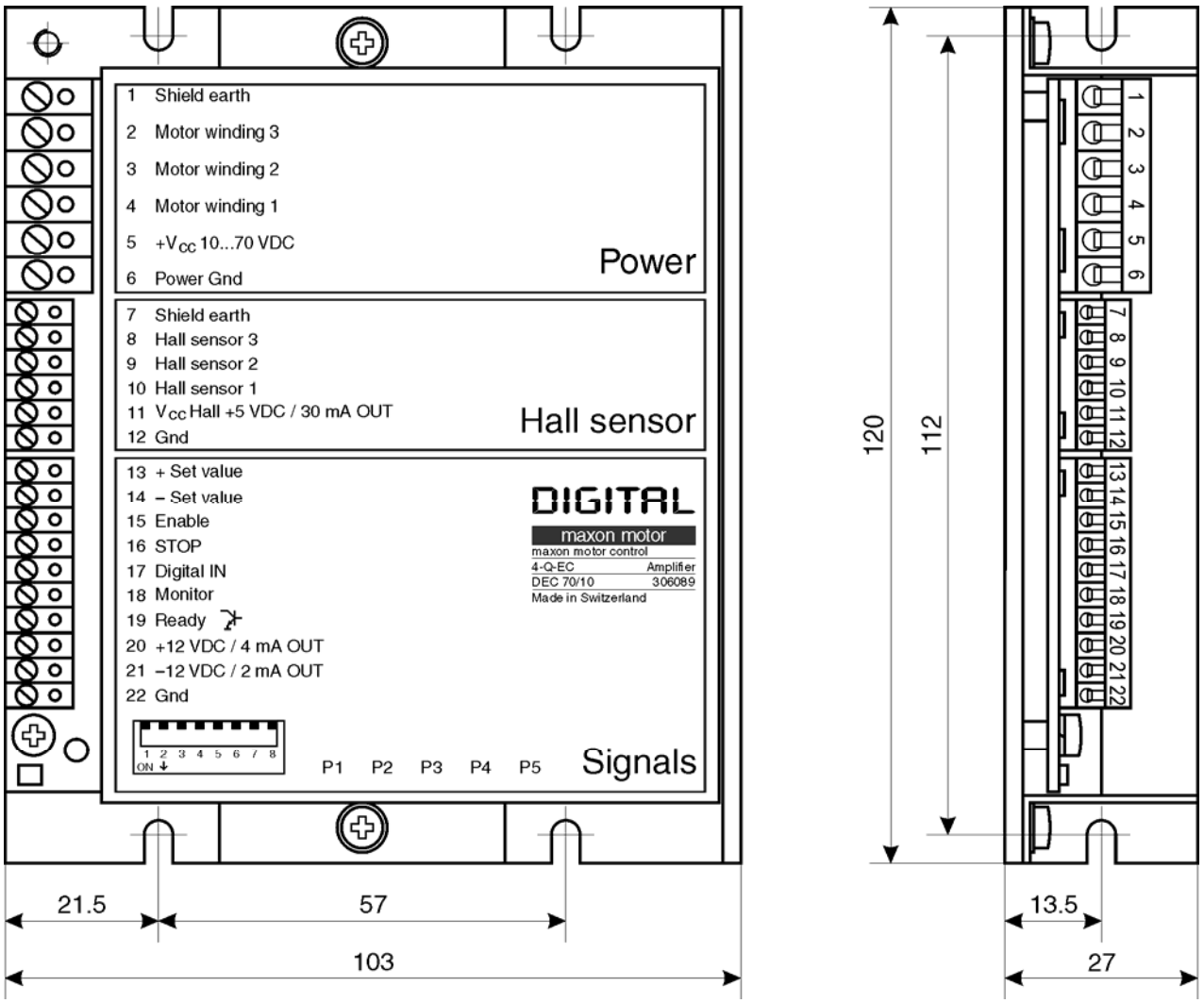

Figure 18: Dimension drawing

15 Spare Parts List

maxon order number	Designation
312176	6 pole pluggable terminal block pitch 5.0 mm labelled 1…6
312178	6 pole pluggable terminal block pitch 3.5 mm labelled 7…12
312179	10 pole pluggable terminal block pitch 3.5 mm labelled 13…22

Technical Product Overview

3DM-GX2™

Gyro Enhanced Orientation Sensor

Introduction

3DM-GX2™ is a high-performance gyro enhanced orientation sensor which utilizes miniature MEMS sensor technology. It combines a triaxial accelerometer, triaxial gyro, triaxial magnetometer, temperature sensors, and an on-board processor running a sophisticated sensor fusion algorithm.

3DM-GX2™ offers a range of output data quantities from fully calibrated inertial measurements (acceleration, angular rate and magnetic field or deltaAngle & deltaVelocity vectors) to computed orientation estimates (pitch & roll or rotation matrix). All quantities are fully temperature compensated and corrected for sensor misalignment. The angular rate quantities are further corrected for G-sensitivity and scale factor non-linearity to third order.

3DM-GX2's communications interface hardware is contained in a separable module, and can therefore be easily customized. Currently available interface modules include a wireless transceiver, USB 2.0, RS232 and RS422. An OEM version is available without the communications interface enabling the sensor to be integrated directly into a host system's circuitboard, providing a very compact sensing solution.

Features & Benefits

- small, light-weight, low-power design ideal for size-sensitive applications including wearable devices
- fully temperature compensated over entire operational range
- calibrated for sensor misalignment, gyro G-sensitivity, and gyro scale factor non-linearity
- simultaneous sampling for improved time integration performance
- available with wireless and USB communication interfaces
- user adjustable data rate (1 to 250Hz) and sensor bandwith (1 to 100Hz)
- outputs include Euler angles, rotation matrix, deltaAngle & deltaVelocity, acceleration and angular rate vectors

Applications

- inertial aiding INS and GPS, location tracking
- unmanned vehicles, robotics – navigation, artificial horizon
- computer science, biomedical – animation, linkage free tracking/control
- platform stabilization
- antenna and camera pointing

BEST OF sensors expo CHICAGO 2005 GOLD

The system architecture has been carefully designed to substantially eliminate common sources of error such as hysteresis induced by temperature changes and sensitivity to supply voltage variations. The use of six independent Delta-Sigma A/D converters (one for each sensor) ensures that all sensors are sampled simultaneously, and that the best possible time integration results are achieved. On-board coning and sculling compensation allows for use of lower data output rates while maintaining performance of a fast internal sampling rate.
3DM-GX2 incorporates an integral triaxial magnetometer; optionally, the magnetometer can be located remotely to reduce hard and soft iron interference.

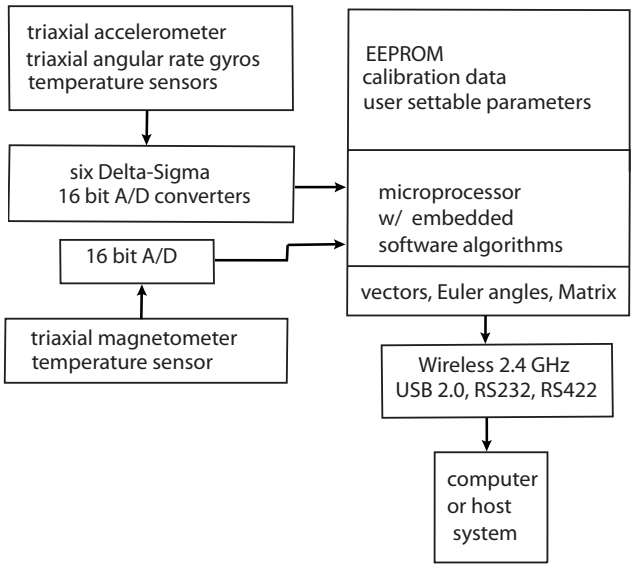

Specifications

Orientation range (pitch, roll, yaw)	360° about all axes
Accelerometer range	accelerometers: ± 5 *g* standard ± 10 *g* and ± 2 *g* also available
Accelerometer bias stability	± 0.010 *g* for ± 10 *g* range ± 0.005 *g* for ± 5 *g* range ± 0.003 *g* for ± 2 *g* range
Accelerometer nonlinearity	0.2%
Gyro range	gyros: ± 300°/sec standard, ± 1200°/sec, ± 600°/sec, ± 150°/sec, ± 75°/sec also available
Gyro bias stability	± 0.2°/sec for ± 300°/sec
Gyro nonlinearity	0.2%
Magnetometer range	± 1.2 Gauss
Magnetometer nonlinearity	0.4%
Magnetometer bias stability	0.01 Gauss
A/D resolution	16 bits
Orientation Accuracy	± 0.5° typical for static test conditions ± 2.0° typical for dynamic (cyclic) test conditions & for arbitrary orientation angles
Orientation resolution	<0.1° minimum
Repeatability	0.20°
Output modes	acceleration and angular rate, deltaAngle and deltaVelocity, Euler angles, rotation matrix
Interface options	RS232, RS422, USB 2.0 and wireless - 2.45 GHz IEEE 802.15.4 direct sequence spread spectrum, license free worldwide (2.450 to 2.490 GHz) - 16 channels
Wireless communication range	70 m
Digital output rates	1 to 250 Hz with USB interface 1 to 100 Hz with wireless interface
Serial data rate	115200 bps
Supply voltage	5.2 to 9.0 volts
Power consumption	90 mA
Connectors	micro DB9
Operating temp.	-40 to +70°C with enclosure -40 to +85°C without enclosure
Dimensions	41 mm x 63 mm x 32 mm with enclosure 32 mm x 36 mm x 24 mm without enclosure
Weight	39 grams with enclosure, 16 grams without enclosure
Shock limit	1000 *g* (unpowered), 500*g* (powered)

MicroStrain®
MicroStrain Inc.
310 Hurricane Lane, Unit 4
Williston, VT 05495 USA
www.microstrain.com
ph: 800-449-3878
fax : 802-863-4093
sales@microstrain.com

Patent Pending

Copyright © 2007 MicroStrain Inc.
3DM-GX2 is a trademark of MicroStrain Inc. Specifications are subject to change without notice.
Updated July 13, 2007

IMU Combo Board

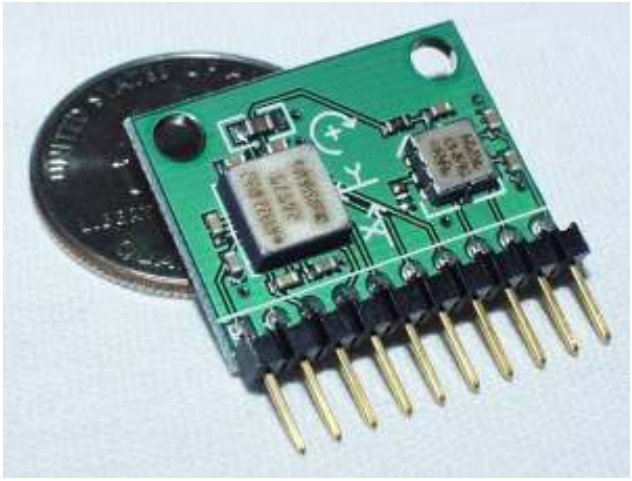

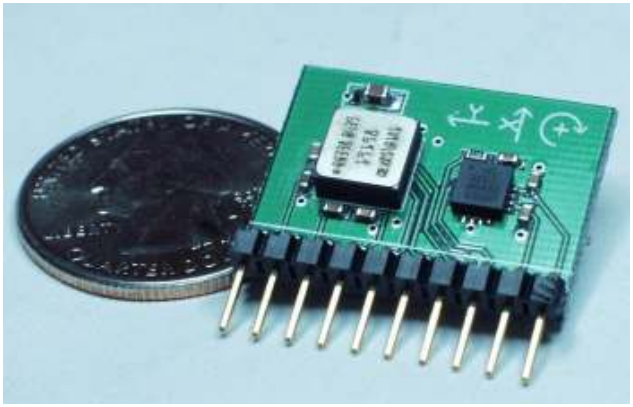

2 Degree of Freedom Gyroscope/ Accelerometer Combination
4/12/2005

1 Overview

The new ADXRS Gyro and ADXL Tilt sensors from Analog Devices are great new MEMs technology sensors. This module was developed to get these great sensors into the hands of hobbyists, engineers, and students. The footprint was made as small as possible, while retaining the most raw form of output from the sensors allowing the module to be used for any purpose the imagination can fathom. This module is ideal for reverse pendulum robots (the Segway is a perfect example) or with Unmanned Aerial Vehicle control (detect the roll of a plane for aileron correction).

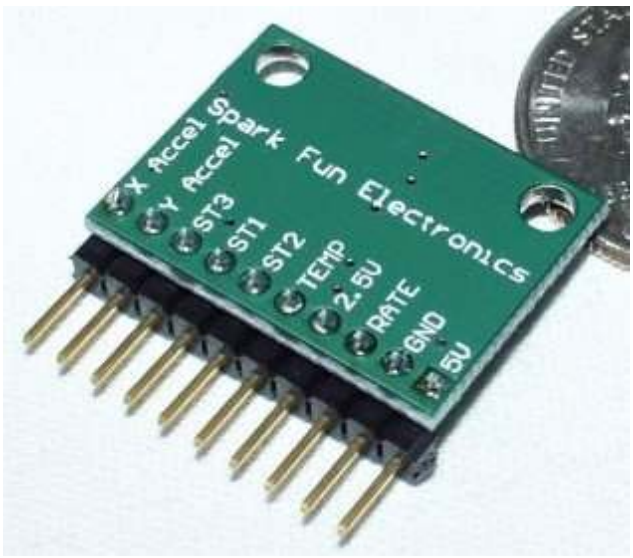

2 Interface Specifications

Both sensors output an analog voltage representing the relative reading.

1. **5V** : 5 volt regulated power
2. **GND** : Ground Connection
3. **Rateout** : Gyro analog output
4. **2.5V Out** : Internal 2.5V precision output
5. **Temp** : Internal precision temperature
6. **ST2** : Self test 2 (Gyro)
7. **ST1** : Self test 1 (Gyro)

© 2005 www.sparkfun.com

8. **ST3** : Self test 3 (Accelerometer)
9. **Y Accel** : Y axis acceleration output
10. **X Accel** : X axis acceleration output

3 Pin Definitions

Rateout : The ADXRS401 outputs 15mV/°/s or 15mV per degree per second. The ADXRS will output 2.5V on the Rateout pin while sitting still. When you rotate the module, this pin will fluctuate around 2.5V depending on how fast you rotate it. With a good ADC, you will be able to detect very small rotations/fluctuations.

2.5V Out : This pin connects to the internal precision 2.5V reference. Use this reference to compare it to your ADC readings to increase accuracy.

Temp : The ADXRS401 includes a precision temperature sensor for temperature compensation for increased accuracy. The Temp pin will output 2.5V at 27°C and will vary 8.4mV°/C.

ST2 : Used to internally self-test the gyro.

ST1 : Used to internally self-test the gyro.

ST3 : Used to internally self-test the accelerometer.

Y-Accel : This pin will output 2.5V when laying flat on a table - perpendicular to the earth's surface. The output will change 312mV/g for the ADXL320 and 1000mV/g for the ADXL203. That is, for every gravity of acceleration on the Y axis, you will see a 312mV (or 1000mV) change on the 2.5V output.

X-Accel : Identical to Y-Accel, but in the perpendicular X axis. When perpendicular to the earth's surface, the ADXL320 X Accel pin (or similarly the Y Accel pin) will output 2.188V or 2.812 depending on orientation (+/- 180 degrees of tilt). Based on these values and the performance of your ADC, you will be able to very accurately detect tilt to a fraction of a degree. The ADXL203 has a much higher swing voltage of 1000mV/g (1.5V at –1g and 3.5V at +1g) and will provide greater resolution compared to the ADXL320 on the same ADC.

Of course you should always read the datasheets specific to the ADXRS and ADXL sensors on your IMU Combo Board for more detailed information on the output specifications.

4 Increasing ADC Performance

The accuracy of your system will depend completely on your ADC. The higher the number of bits, the better resolution you can achieve. For instance, if you have a 10-bit ADC (common on most PICs/AVRs) you can detect

```
5V / 1024 = 4.88mV per bit
```

4.88mV changes. If you have a 12-bit ADC

```
5V / 4096 = 1.22mV per bit
```

or 1.22mV changes. Obviously you will be hindered greatly if your system is noisy or poorly decoupled. Use low noise voltage regulators and lots of decoupling capacitors.

4.1 Decreasing the ADC Window

One common trick to increasing performance is by shrinking the window on which the Analog to Digital Converter operates. For instance, the PIC16F88 has two pins that serve as Vref- and Vref+. These are the upper and lower limits of the Voltage Reference on the ADC. You will need to read heavily into the datasheet for your specific micro, not all micros have both upper and lower Vref pins. The 16F88 can be set within specs to 1.5V and 3.5V. This gives us a *much* smaller window thus a more accurate measurement system:

```
2V / 1024 = 1.95mV per bit
```

We effectively improved the performance of the ADC simply by decreasing the window in which we are measuring.

You will need to consider that you will saturate the ADC if you try to do an ADC on voltages that are less than 1.5V or greater than 3.5V, but just keep this in the back of your mind. Using

© 2005 www.sparkfun.com

the Gyro and Accelerometer for reverse pendulum or UAV applications, you will need to detect very minute changes many times a second. Therefore, the firmware should be able to take care of special cases where the ADC saturates (the 'uh-oh' function should be called).

To set the Vref+/- pins, a simple resistor divider circuit can be used:

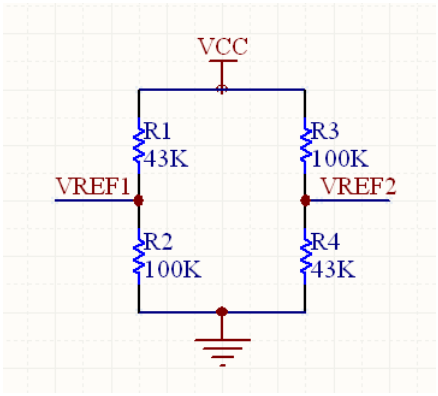

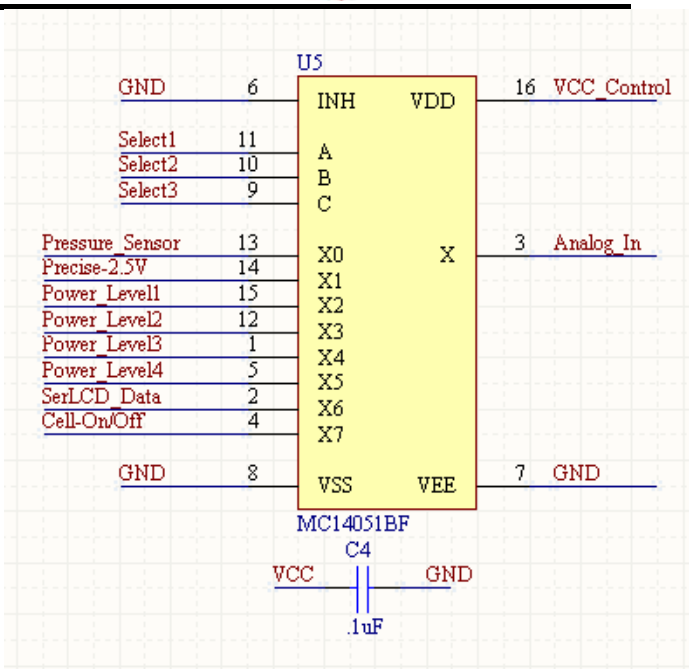

4.2 Finding more ADC Channels

Many micros only have 3-4 ADC channels. Some PICs have as many as 8. But what do you do if you need more? There are devices called Analog Multiplexers that allow you to expand one ADC channel to 8 ADC channels. The 4051 IC (search Digikey "4051 dip mux") allows you to multiplex one ADC channel to 8 different sources using 3 control pins. You get to read 8 ADC devices while only needing 1 ADC pin and 3 control pins (8 for the price of 4!).

4.3 Amplifying the Outputs

The analog signals can be amplified using a simple, single-supply opamp. Search Digikey for "OPA340 DIP". It is a TI opamp that is sufficient for signal amplification and ADC interfacing.

© 2005 www.sparkfun.com

Appendix G.

Mechanical drawings

The drawing list, bill of materials and drawings begin on the following page.

DRG NO	DESCRIPTION	VERSION	DATE
0.1.0	MICYCLE COMPLETE	0	07/05/2010
1.0.0	STEERING ASSEMBLY	0	07/05/2010
1.1.X	LEVER ASSEMBLY	0	07/05/2010
1.1.1	LEVER ARM	0	07/05/2010
1.1.2	SPRING MOUNT LEVER	0	07/05/2010
1.2.1	BEARING SLEEVE	0	07/05/2010
1.3.1	LOWER SPLIT RING COLLAR	0	07/05/2010
1.4.1	UPPER SPLIT RING COLLAR	0	07/05/2010
1.5.1	DAMPER BRACKET	0	07/05/2010
1.6.1	SPRING MOUNT	0	07/05/2010
1.7.1	REAR BRACKET	0	07/05/2010
2.1.X	FORK ASSEMBLY	0	07/05/2010
2.1.1	SPINDLE	0	07/05/2010
2.1.2	FORK HORIZONTAL	0	07/05/2010
2.1.3	FORK LEG	0	07/05/2010
2.1.4	FORK TAB LEFT	0	07/05/2010
2.1.5	FORK TAB RIGHT	0	07/05/2010
2.1.6	FORK CAP	0	07/05/2010
3.0.0	PLATE ASSEMBLY	0	07/05/2010
3.2.1	CHASSIS BACK	0	07/05/2010
3.3.X	POLE SLEEVE ASSEMBLY	0	07/05/2010
3.3.1	POLE SLEEVE TUBE	0	07/05/2010
3.3.2	POLE SLEEVE TAB	0	07/05/2010
3.4.1	SPAR 25mm	0	07/05/2010
3.6.1	SPAR 20mm	0	07/05/2010
3.7.1	COVER PLATE, RIGHT	0	07/05/2010
3.8.1	COVER PLATE, LEFT	0	07/05/2010
3.9.1	BATTERY BRACKET	0	07/05/2010
4.0.0	WHEEL ASSEMBLY	0	07/05/2010
4.1.0	FOOT PEG SLEEVE	0	07/05/2010

DO NOT SCALE

All dimensions in mm unless otherwise stated. surfaces finishes as stated

3rd Angle

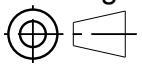

Drawn By: A J Edwards Date: 7/5/10

Checked By: M. Riese Date: 07/05/2010

Authorised By: B. Cazzolato Date: 07/05/2010

Version: 0

Scale: -------

MICYCLE. 980

Part Name: DRAWING LIST

Material: ----------

Part No: 0.1.0

Qty: ------

Size: A4

Sheet:3 of 3

DRG NO	DESCRIPTION	QTY	SOURCE
---	ISO 4762 - M8 x 35	3	OFF-THE-SHELF
---	ISO 4762 - M6 x 30	1	OFF-THE-SHELF
---	ISO 4762 - M8 x 60	2	OFF-THE-SHELF
---	ISO 4762 - M8 x 45	4	OFF-THE-SHELF
---	ISO 4762 - M6 x 20	6	OFF-THE-SHELF
---	ISO 4762 - M6 x 45	2	OFF-THE-SHELF
---	ISO 4762 - M3 x 15	4	OFF-THE-SHELF
---	ISO 10642 - M5 x 20 HEX SOCKET	2	OFF-THE-SHELF
---	ISO 10642 - M5 x 40 HEX SOCKET	12	OFF-THE-SHELF
---	ISO 4027 - M5 x 10 SET SCREW	2	OFF-THE-SHELF
---	ISO 7040 - M8 NUT	4	OFF-THE-SHELF
---	ISO 7040 - M6 NUT	2	OFF-THE-SHELF
---	ISO 4032 - M20 NUT	1	OFF-THE-SHELF
---	ISO 7091 - 20 WASHER	1	OFF-THE-SHELF
---	ISO 7092 - 6 WASHER	7	OFF-THE-SHELF
---	ISO 7092 - 8 WASHER	13	OFF-THE-SHELF
---	50mm M8 THREAD BAR	6	OFF-THE-SHELF
---	MAGIC PIE HUB MOTOR W/ TYRE	1	SUPPLIED
---	CPR 4067-CAS FOOT PEG	2	SUPPLIED
---	SCHWALBE NIMBUS	1	SUPPLIED
---	22.2mm SADDLE POLE COLLAR	1	SUPPLIED
---	TORSION SPRING	1	SUPPLIED
---	FDT-70 ROTARY DAMPER	2	SUPPLIED
---	619062RS1 BALL BEARING	1	SUPPLIED
---	619052RS1 BALL BEARING	1	SUPPLIED
---	RUBBER BUMP-STOP	16	SUPPLIED
---	MAXON DEC 70/10 CONTROLLER	1	SUPPLIED

DRG NO	DESCRIPTION	QTY	SOURCE
1.1.1	LEVER ARM	1	MANUFACTURE
1.1.2	SPRING MOUNT LEVER	1	MANUFACTURE
1.2.1	BEARING SLEEVE	1	MANUFACTURE
1.3.1	LOWER SPLIT RING COLLAR	1	MANUFACTURE
1.4.1	UPPER SPLIT RING COLLAR	1	MANUFACTURE
1.5.1	DAMPER BRACKET	1	MANUFACTURE
1.6.1	SPRING MOUNT	1	MANUFACTURE
1.7.1	REAR BRACKET	1	MANUFACTURE
2.1.1	SPINDLE	1	MANUFACTURE
2.1.2	FORK HORIZONTAL	1	MANUFACTURE
2.1.3	FORK LEG	2	MANUFACTURE
2.1.4	FORK TAB LEFT	1	MANUFACTURE
2.1.5	FORK TAB RIGHT	1	MANUFACTURE
2.1.6	FORK CAP	2	MANUFACTURE
---	ELLIPTICAL END CAP	2	MANUFACTURE
3.2.1	CHASSIS BACK	1	MANUFACTURE
3.3.1	POLE SLEEVE TUBE	1	MANUFACTURE
3.3.2	POLE SLEEVE TAB	4	MANUFACTURE
3.4.1	SPAR 25mm	10	MANUFACTURE
3.6.1	SPAR 20mm	2	MANUFACTURE
3.7.1	COVER PLATE, RIGHT	1	MANUFACTURE
3.8.1	COVER PLATE, LEFT	1	MANUFACTURE
3.9.1	BATTERY BRACKET	2	MANUFACTURE
4.1.0	FOOT PEG SLEEVE	2	MANUFACTURE
---	FOOT PEG SPACER (t = 7mm)	2	MANUFACTURE

DO NOT SCALE

All dimensions in mm unless otherwise stated. surfaces finishes as stated

3rd Angle

Drawn By: A J Edwards Date: 4/5/10

Checked By: M. Riese Date: 07/05/2010

Authorised By: B. Cazzolato Date: 07/05/2010

Version: 0

Scale: -------

MICYCLE. 980

Part Name: BILL OF MATERIALS

Material: ----------

Part No: 0.1.0

Qty: -----

Size: A4

ITEM	DRG/PART NO	DESCRIPTION	QTY
1	1.0.0	STEERING ASSEMBLY	1
2	2.1.X	FORK ASSEMBLY	1
3	3.0.0	PLATE ASSEMBLY	1
4	4.0.0	WHEEL ASSEMBLY	1
5	-------	SCHWALBE NIMBUS	1

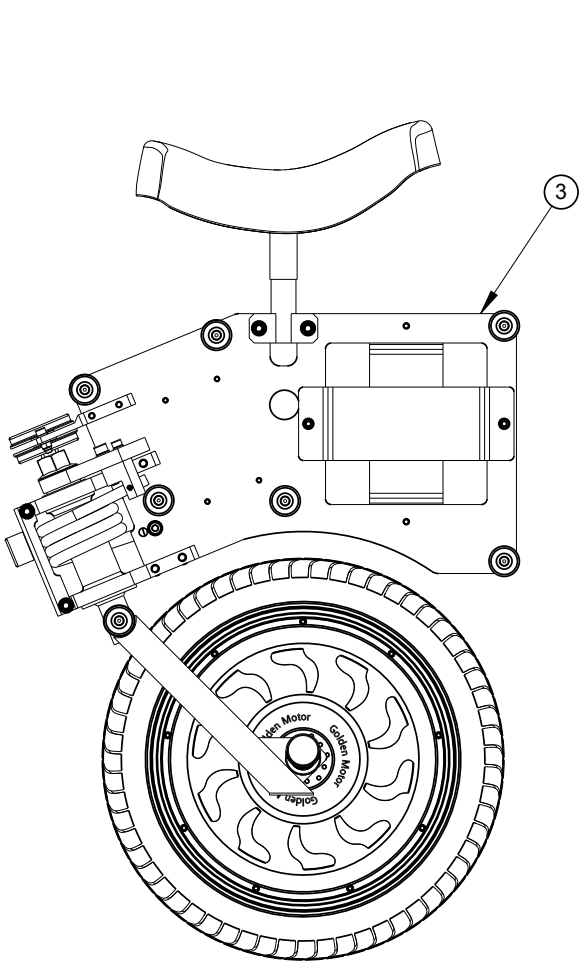

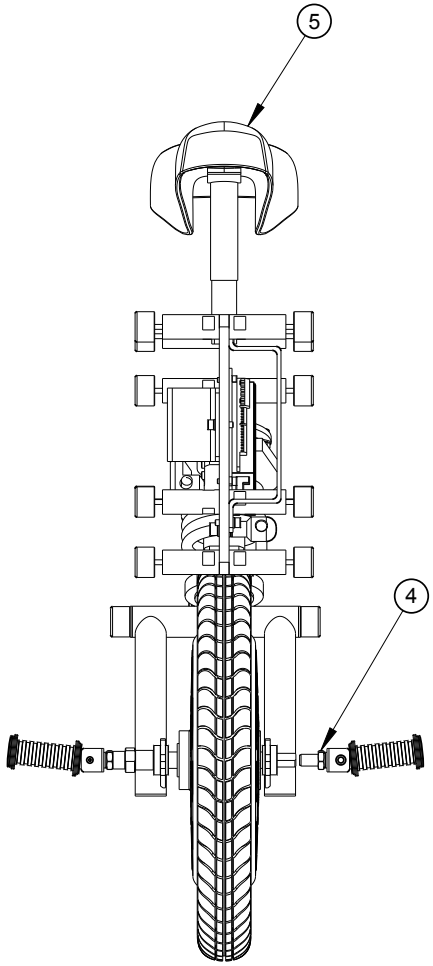

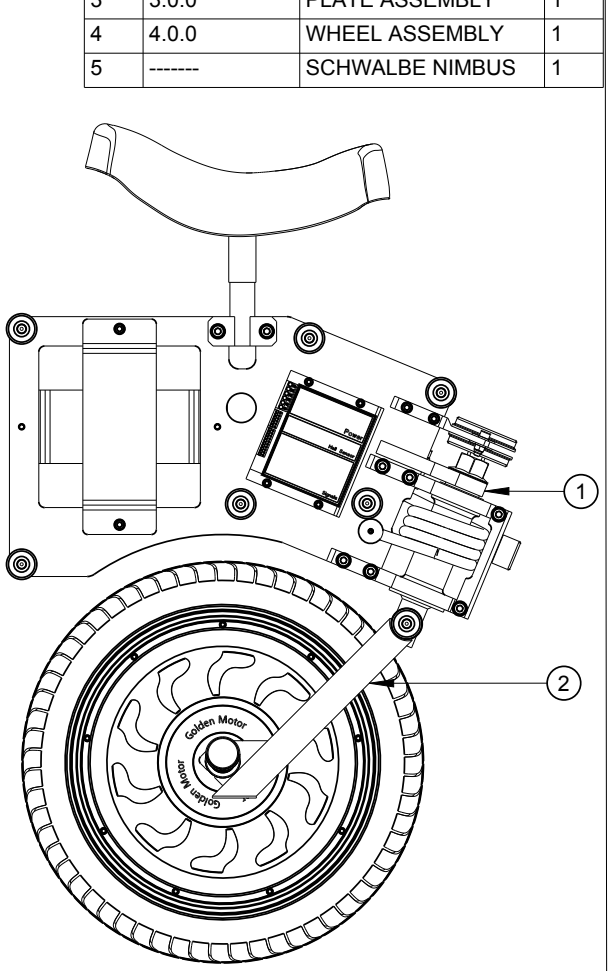

DO NOT SCALE

All dimensions in mm unless otherwise stated . All surfaces finishes as stated	Drawn By: M Jerbic	Date: 4/05/2010	MICYCLE. 980				
	Checked By: M. Riese	Date: 07/05/10	Part Name: MICYCLE COMPLETE				
3rd Angle	Authorised By: B. Cazzolato	Date: 07/05/10	Material: ----------				
	Version: 0	Scale: 1:2	Part No: 0.1.0	Qty: 1	Size A3	Sheet:1 of 3	

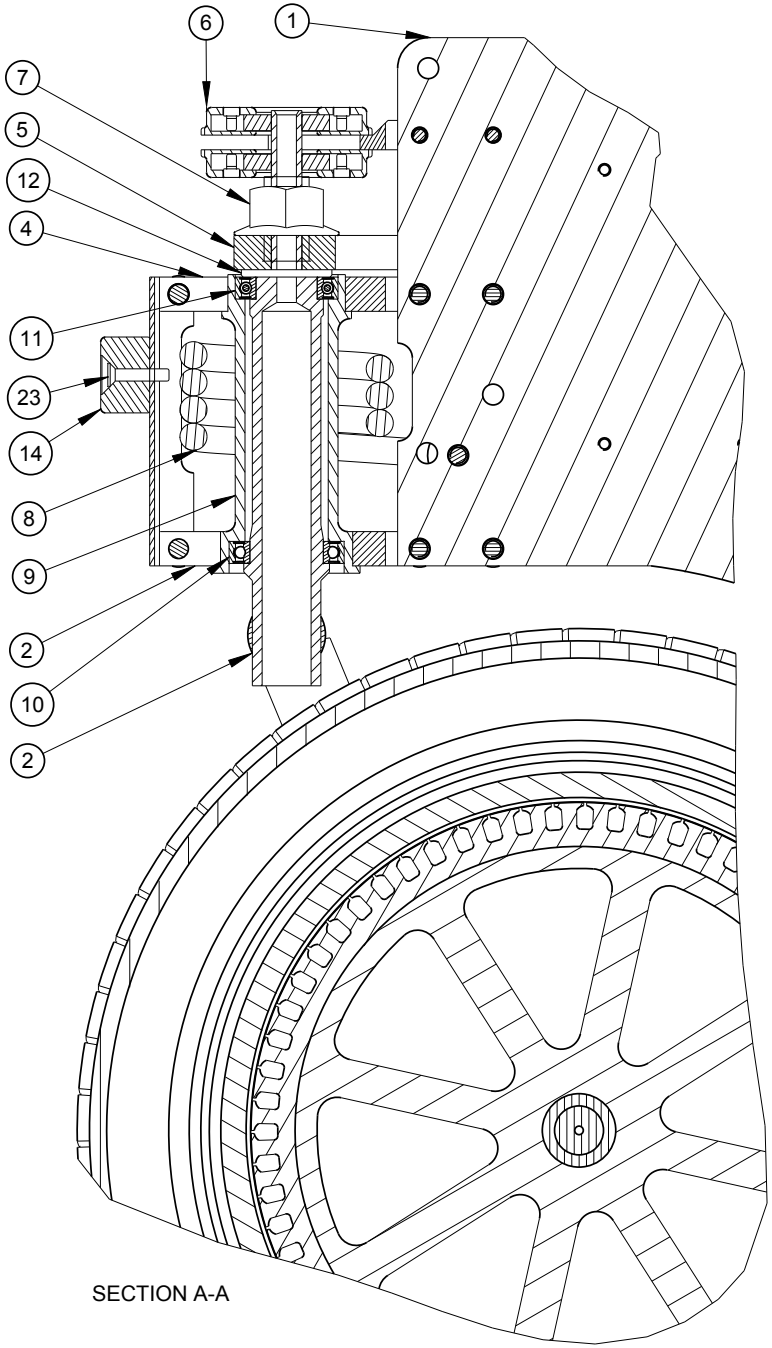

SECTION A-A

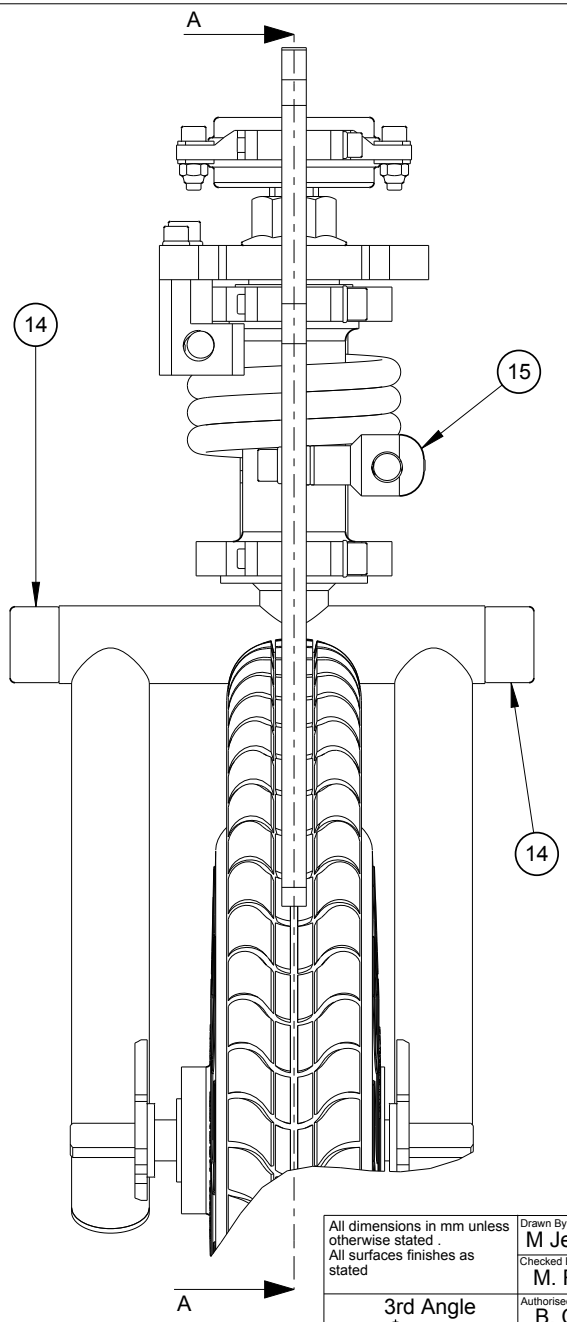

DO NOT SCALE

ITEM	DWG/PART NO	DESCRIPTION	QTY
1	3.2.1	CHASSIS BACK	1
2	2.1.X	FORK ASSEMBLY	1
3	1.3.1	LOWER SPLIT RING	1
4	1.4.1	UPPER SPLIT RING	1
5	1.1.X	LEVER ARM ASSEMBLY	1
6	-------	FDT-70	2
7	-------	ISO 4032-20 NUT	1
8	-------	TORSION SPRING	1
9	1.2.1	BEARING SLEEVE	1
10	-------	619062RS1 BALL BEARING	1
11	-------	619052RS1 BALL BEARING	1
12	-------	ISO 7091-20	1
13	1.7.1	REAR BRACKET	1
14	-------	BUMPSTOP	3
15	1.6.1	SPRING MOUNT	1
16	-------	IS0 4027-M5X10 SET SCREW	1
17	-------	ISO 4762-M8 X 60	2
18	-------	ISO 7040-M8 NUT	2
19	-------	ISO 4762-M8 X 45	4
20	-------	ISO 7092-8 WASHER	8
21	-------	ISO 4762-M6 X 20	2
22	-------	ISO 7040-M6 NUT	2
23	-------	ISO 10642-M5 X 25 HEX SOCKET	2
24	-------	ISO 4762-M6 X 45	2
25	-------	ISO 7092-6 WASHER	2

All dimensions in mm unless otherwise stated .
All surfaces finishes as stated

3rd Angle

Drawn By: M Jerbic	Date: 21/04/2010	MICYCLE. 980	
Checked By: M. Riese	Date: 07/05/10	Part Name:	STEERING SUB-ASSEMBLY
Authorised By: B. Cazzolato	Date: 07/05/10	Material:	REFER TO PART DRAWINGS
Version: 0	Scale: 1:2	Part No: 1.0.0 / Qty: 1 / Size: A3	Sheet: 1 of 2

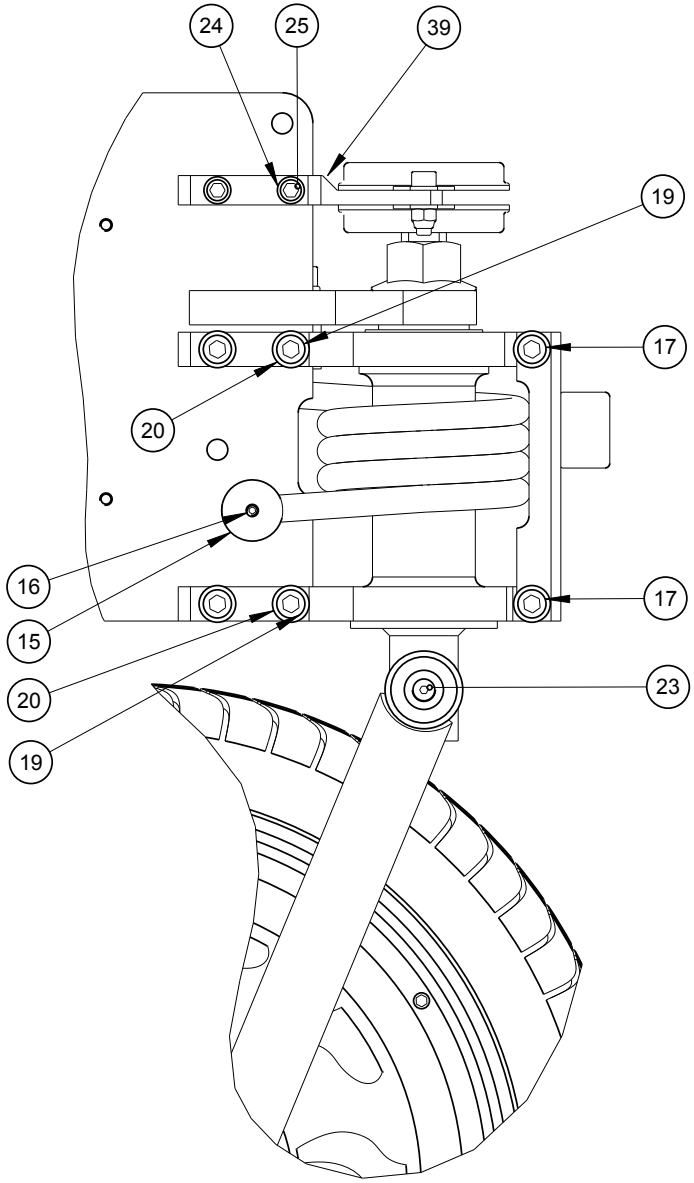

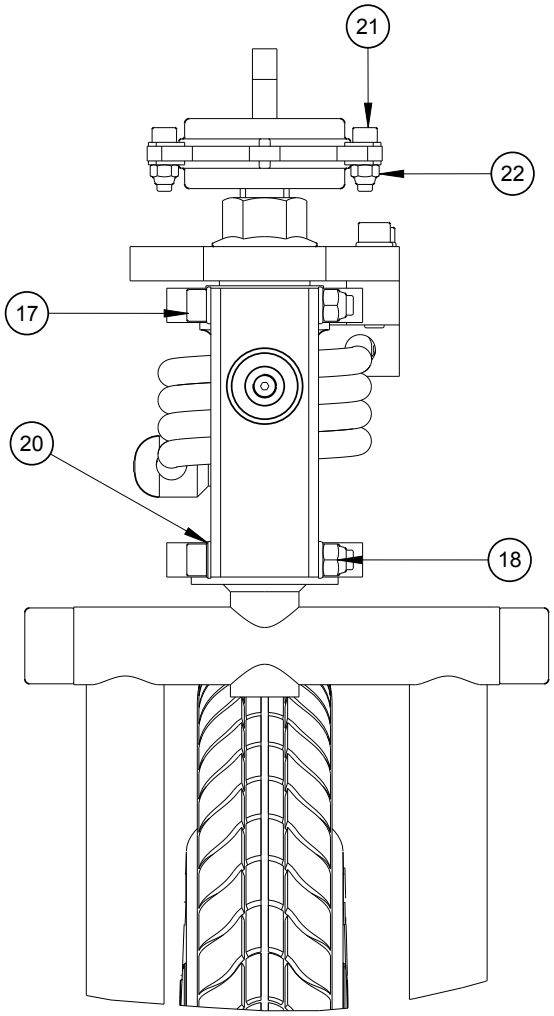

ITEM	DWG/PART NO	DESCRIPTION	QTY
1	3.2.1	CHASSIS BACK	1
2	2.1.X	FORK ASSEMBLY	1
3	1.3.1	LOWER SPLIT RING	1
4	1.4.1	UPPER SPLIT RING	1
5	1.1.X	LEVER ARM ASSEMBLY	1
6	-------	FDT-70	2
7	-------	ISO 4032-20 NUT	1
8	-------	TORSION SPRING	1
9	1.2.1	BEARING SLEEVE	1
10	-------	619062RS1 BALL BEARING	1
11	-------	619052RS1 BALL BEARING	1
12	-------	ISO 7091-20	1
13	1.7.1	REAR BRACKET	1
14	-------	BUMPSTOP	3
15	1.6.1	SPRING MOUNT	1
16	-------	IS0 4027-M5X10 SET SCREW	1
17	-------	ISO 4762-M8 X 60	2
18	-------	ISO 7040-M8 NUT	2
19	-------	ISO 4762-M8 X 45	4
20	-------	ISO 7092-8 WASHER	8
21	-------	ISO 4762-M6 X 20	2
22	-------	ISO 7040-M6 NUT	2
23	-------	ISO 10642-M5 X 25 HEX SOCKET	2
24	-------	ISO 4762-M6 X 45	2
25	-------	ISO 7092-6 WASHER	2
39	1.5.1	DAMPER BRACKET	1

DO NOT SCALE

All dimensions in mm unless otherwise stated .
All surfaces finishes as stated

3rd Angle

Drawn By: M Jerbic Date: 21/04/2010
Checked By: M. Riese Date: 07/05/10
Authorised By: B. Cazzolato Date: 07/05/10
Version: 0
Scale: 1:2

MICYCLE. 980
Part Name: STEERING SUB-ASSEMBLY
Material: REFER TO PART DRAWINGS
Part No: 1.0.0
Qty: 1
Size A3
Sheet: 2 of 2

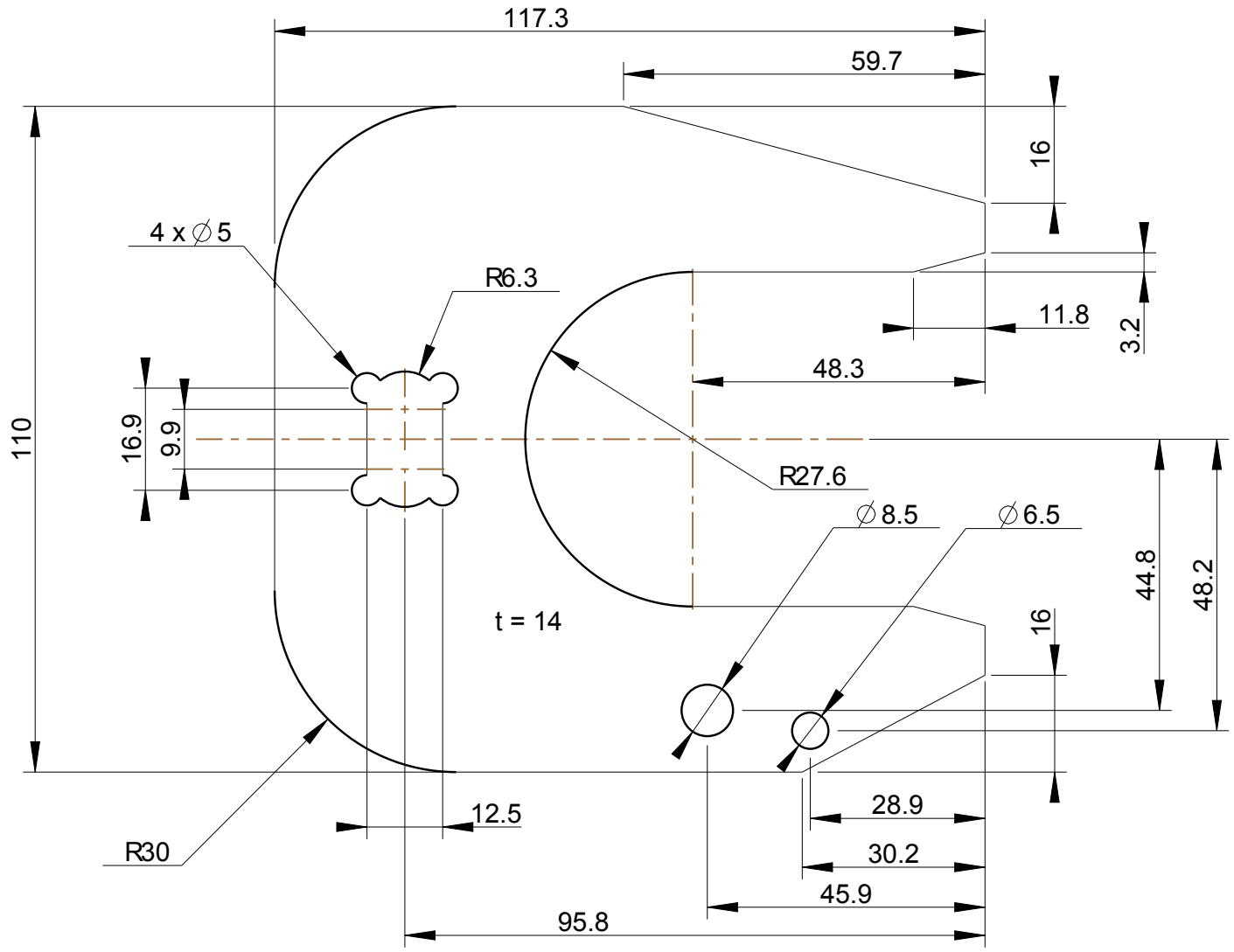

ISO 2768-m

dim	tol
0.5<3	±0.1
3<6	±0.1
6<30	±0.2
30<120	±0.3
120<400	±0.5

NOTE:

1) 0.8 ALL OVER

BREAK ALL EDGES

DO NOT SCALE

All dimensions in mm unless otherwise stated. surfaces finishes as stated

3rd Angle

Drawn By: A J Edwards	Date: 27/4/10	MICYCLE. 980			
Checked By: M. Riese	Date: 07/05/10	Part Name: SPRING LEVER			
Authorised By: B. Cazzolato	Date: 07/05/10	Material: 5005 ALUMINIUM			
Version: 0	Scale: 1:1	Part No: 1.1.1	Qty: 1	Size: A4	Sheet:1 of 1

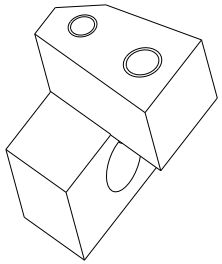

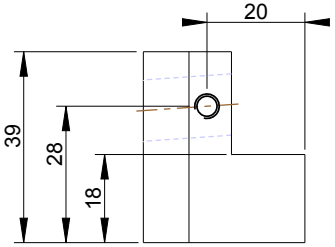

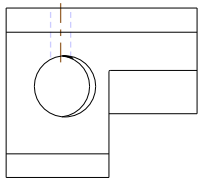

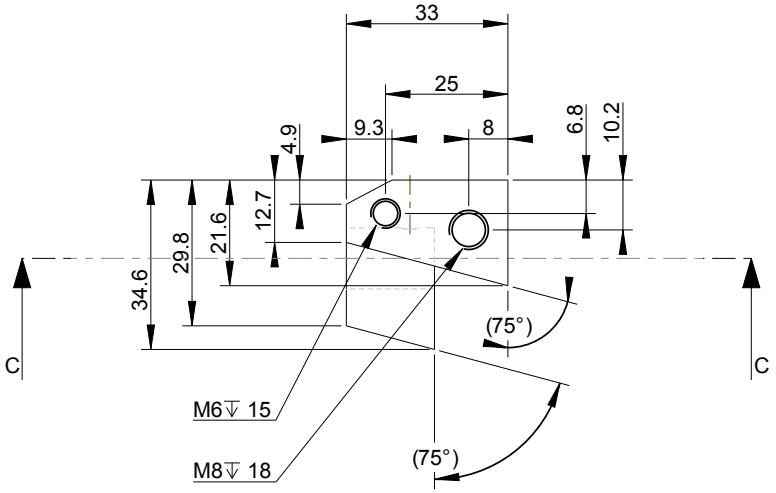

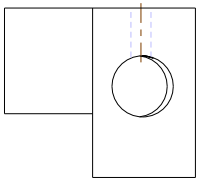

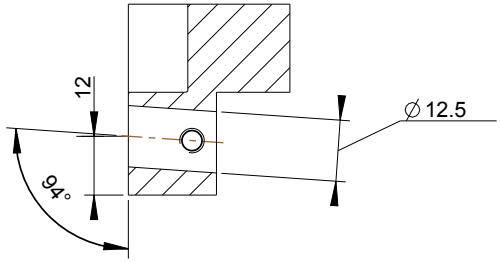

SECTION C-C

ISO 2768-m

dim	tol
0.5<3	±0.1
3<6	±0.1
6<30	±0.2
30<120	±0.3
120<400	±0.5

NOTE:

1) 3.2 ALL OVER UNLESS OTHERWISE STATED

BREAK ALL EDGES

DO NOT SCALE

All dimensions in mm unless otherwise stated .
All surfaces finishes as stated

3rd Angle

Drawn By: M Jerbic	Date: 25/04/2010	MICYCLE. 980	
Checked By: M. Riese	Date: 07/05/10	Part Name: SPRING MOUNT LEVER	
Authorised By: B. Cazzolato	Date: 07/05/10	Material: MILD STEEL	
Version: 0	Scale: 1:1	Part No: 1.1.2	Qty: 1	Size A3	Sheet: 1 of 1

ITEM	DRG/PART NO	DESCRIPTION	QTY
1	1.1.1	LEVER ARM	1
2	1.1.2	SPRING MOUNT	1
3	-------	IS0 4762 - M8 x 35 - 8.8	1
4	-------	ISO 7092-8 WASHER	1
5	-------	ISO 4762 - M6 x 30 - 8.8	1
6	-------	ISO 7092-6 WASHER	1
7	-------	ISO 4027 - M5 x 10	1

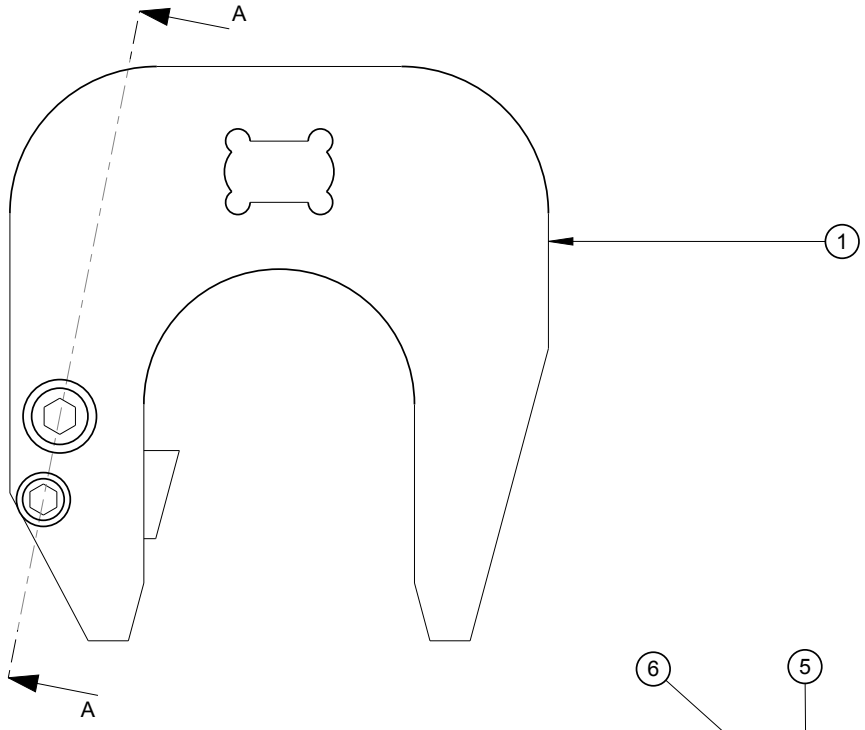

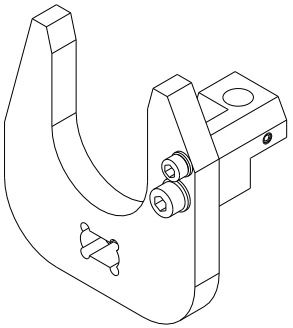

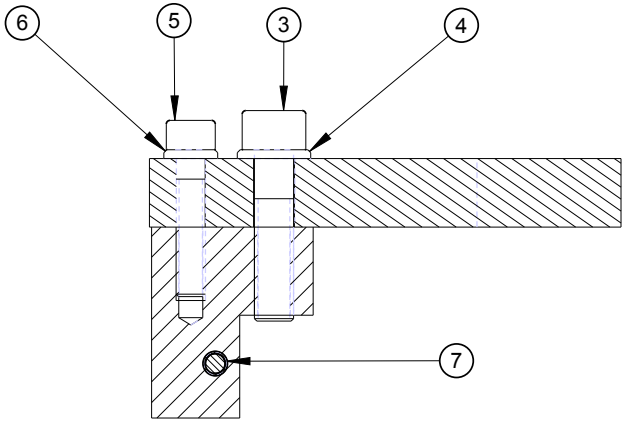

SECTION A-A

DO NOT SCALE

All dimensions in mm unless otherwise stated . All surfaces finishes as stated	Drawn By: M Jerbic	Date: 25/04/2010	MICYCLE. 980				
	Checked By: M. Riese	Date: 07/05/10	Part Name: LEVER ASSEMBLY				
3rd Angle	Authorised By: B. Cazzolato	Date: 07/05/10	Material: REFER TO PART DRAWINGS				
	Version: 0	Scale: 1:1	Part No: 1.1.X	Qty: 1	Size A3	Sheet: 1 of 1	

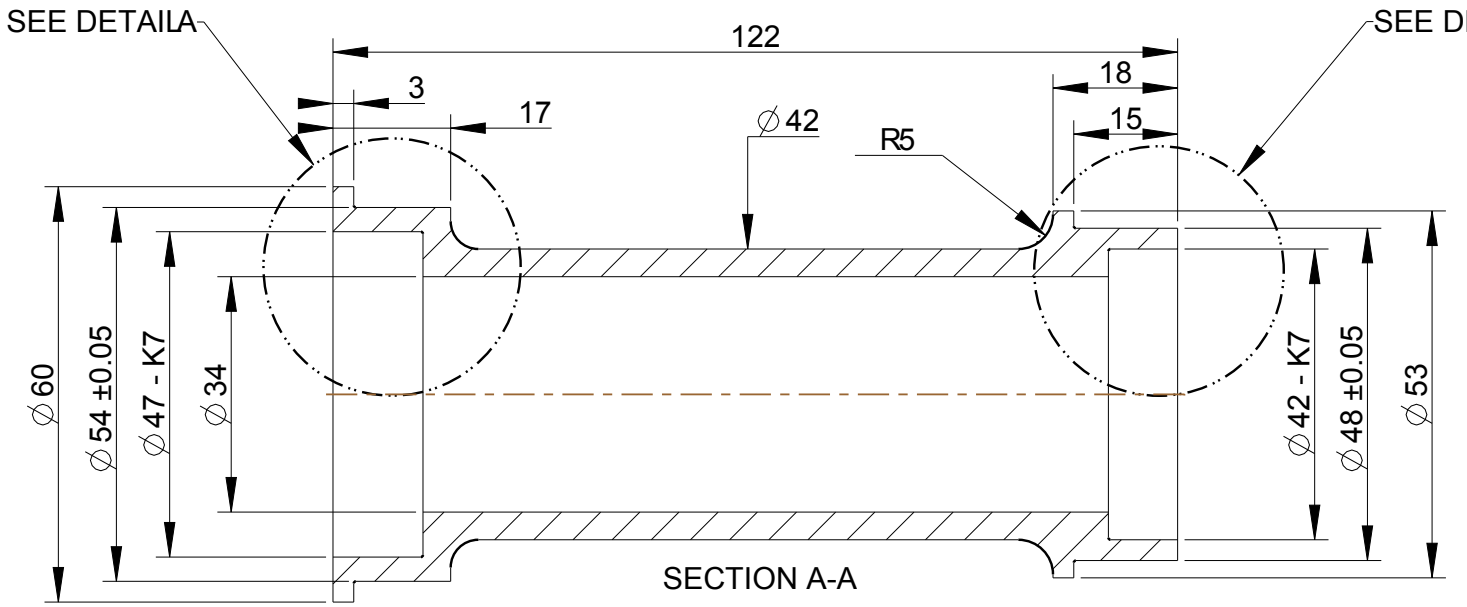

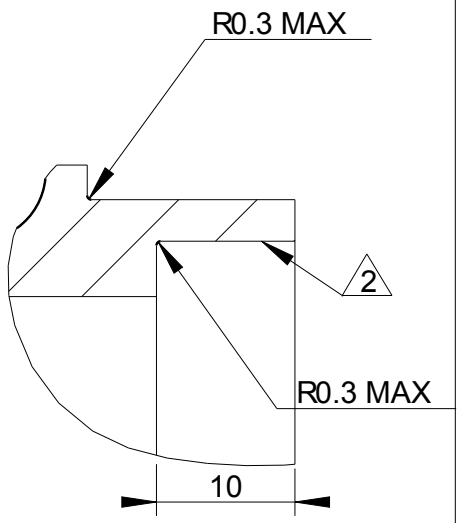

DETAIL B

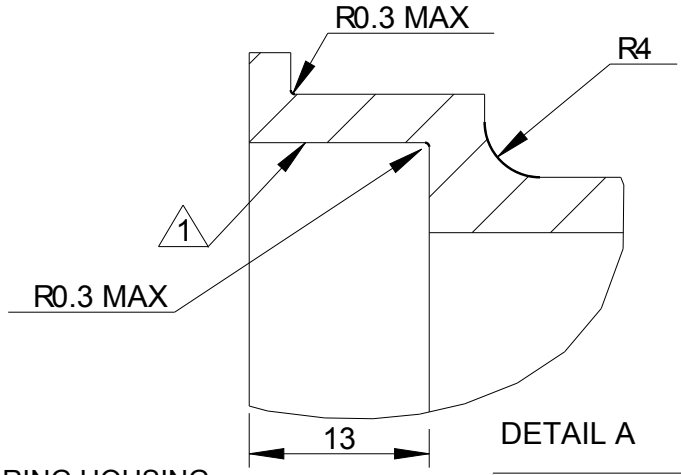

DETAIL A

ISO 2768-m

dim	tol
0.5<3	±0.1
3<6	±0.1
6<30	±0.2
30<120	±0.3
120<400	±0.5

NOTE:

1. 619062RS1 BEARING HOUSING
2. 619052RS1 BEARING HOUSING
3) ALL CHAMFERS ARE 0.3 X 45°
4) 1.6 ALL OVER

BREAK ALL EDGES
DO NOT SCALE

All dimensions in mm unless otherwise stated. surfaces finishes as stated

3rd Angle

Drawn By: M Jerbic	Date: 20/04/2010	MICYCLE. 980			
Checked By: M. Riese	Date: 07/05/10	Part Name: BEARING SLEAVE			
Authorised By: B. Cazzolato	Date: 07/05/10	Material: 5005 ALUMINIUM			
Version: 0	Scale: 1:1	Part No: 1.2.1	Qty: 1	Size: A4	Sheet: 1 of 1

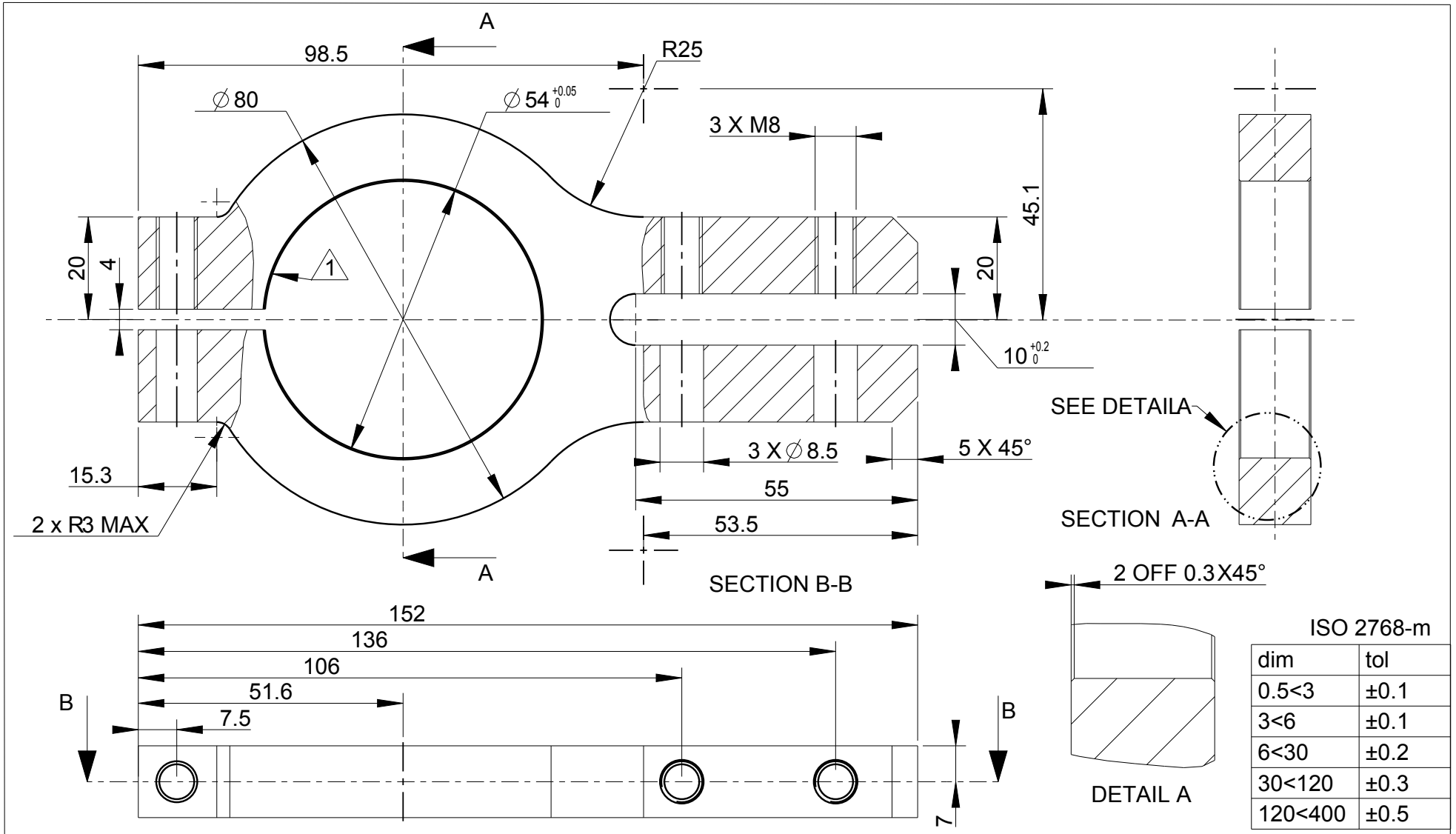

ISO 2768-m

dim	tol
0.5<3	±0.1
3<6	±0.1
6<30	±0.2
30<120	±0.3
120<400	±0.5

NOTE:

1. TO FIT ON BEARING SLEEVE (PART NO 1.2.1)
2. 0.8 ALL OVER

BREAK ALL EDGES
DO NOT SCALE

All dimensions in mm unless otherwise stated. surfaces finishes as stated

3rd Angle

Drawn By: M Jerbic	Date: 19/04/2010	MICYCLE. 980			
Checked By: M. Riese	Date: 07/05/10	Part Name: LOWER SPLIT RING COLLAR			
Authorised By: B. Cazzolato	Date: 07/05/10	Material: 5005 ALUMINIUM			
Version: 0	Scale: 1:1	Part No: 1.3.1	Qty: 1	Size: A4	Sheet: 1 of 1

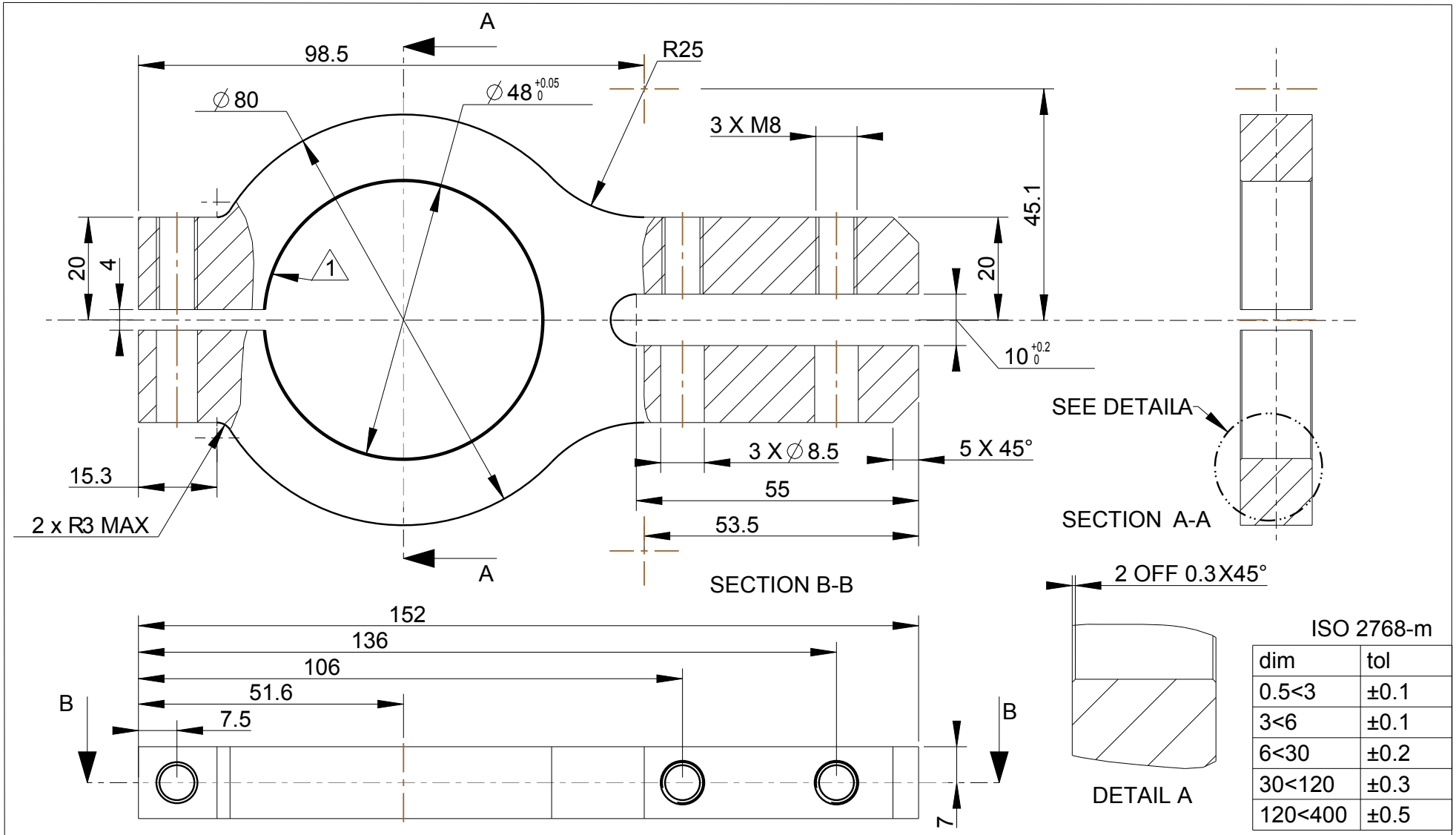

ISO 2768-m

dim	tol
0.5<3	±0.1
3<6	±0.1
6<30	±0.2
30<120	±0.3
120<400	±0.5

NOTE:

1 TO FIT ON BEARING SLEEVE (PART NO 1.2.1)

2) 0.8 ALL OVER

BREAK ALL EDGES
DO NOT SCALE

All dimensions in mm unless otherwise stated. surfaces finishes as stated

3rd Angle

Drawn By: M Jerbic	Date: 19/04/2010	MICYCLE. 980				
Checked By: M. Riese	Date: 07/05/10	Part Name: UPPER SPLIT RING COLLAR				
Authorised By: B. Cazzolato	Date: 07/05/10	Material: 5005 ALUMINIUM				
Version: 0	Scale: 1:1	Part No: 1.4.1	Qty: 1	Size: A4	Sheet: 1 of 1	

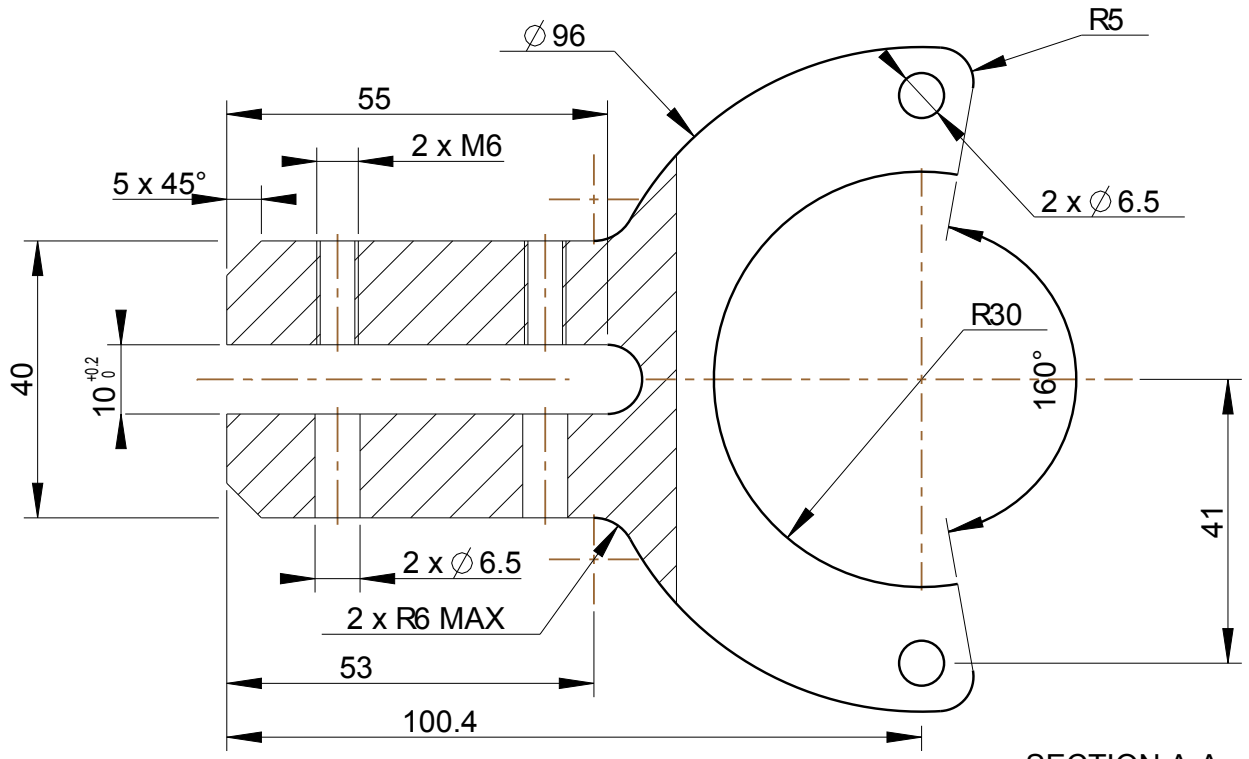

SECTION A-A

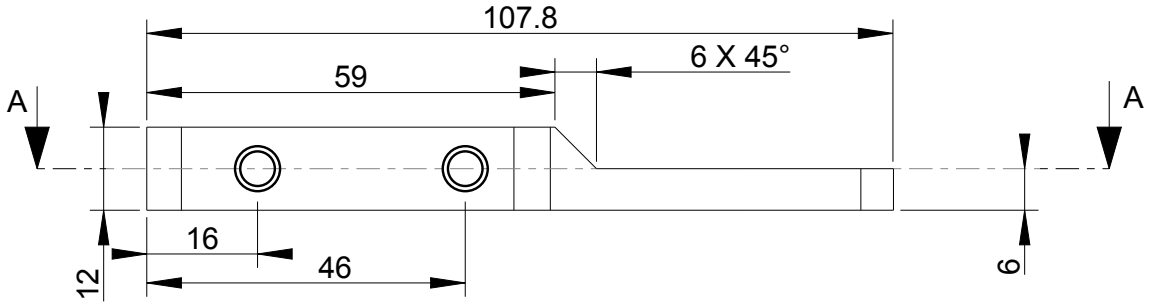

ISO 2768-m

dim	tol
0.5<3	±0.1
3<6	±0.1
6<30	±0.2
30<120	±0.3
120<400	±0.5

NOTE:

1) 0.8 ALL OVER

BREAK ALL EDGES

DO NOT SCALE

All dimensions in mm unless otherwise stated. surfaces finishes as stated

3rd Angle

Drawn By: A J Edwards	Date: 19/4/10	MICYCLE. 980			
Checked By: M. Riese	Date: 07/05/10	Part Name: DAMPER BRACKET			
Authorised By: B. Cazzolato	Date: 07/05/10	Material: 5005 ALUMINIUM			
Version: 0	Scale: 1:1	Part No: 1.5.1	Qty: 1	Size: A4	Sheet: 1 of 1

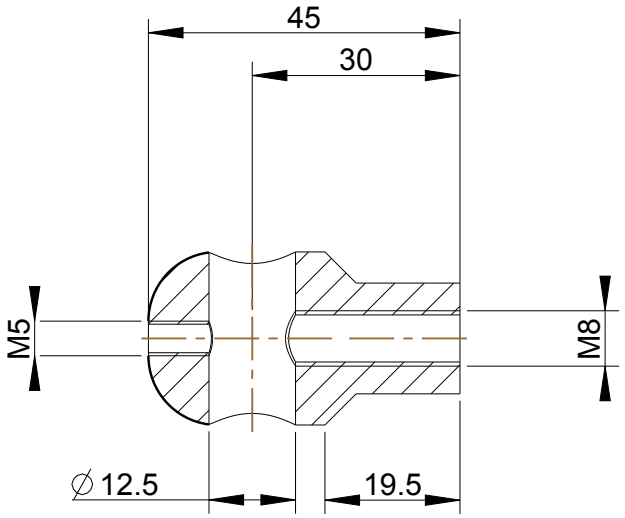

SECTION A-A

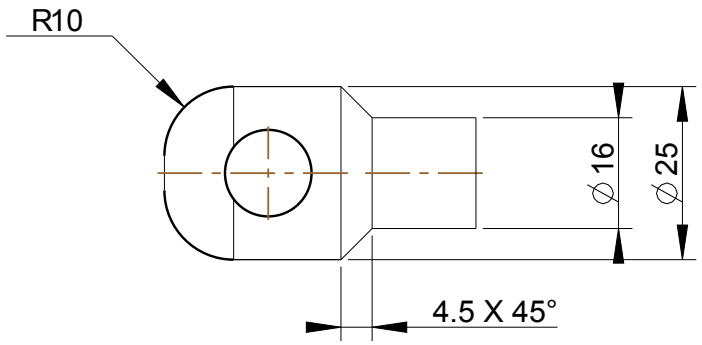

ISO 2768-m

dim	tol
0.5<3	±0.1
3<6	±0.1
6<30	±0.2
30<120	±0.3
120<400	±0.5

NOTE:

1) 3.2 ALL OVER UNLESS OTHERWISE STATED

BREAK ALL EDGES

DO NOT SCALE

All dimensions in mm unless otherwise stated. surfaces finishes as stated

3rd Angle

Drawn By: M Jerbic	Date: 26/04/2010	MICYCLE. 980	
Checked By: M. Riese	Date: 07/05/10	Part Name: SPRING MOUNT	
Authorised By: B. Cazzolato	Date: 07/05/10	Material: MILD STEEL	
Version: 0	Scale: 1:1	Part No: 1.6.1	Qty: 1	Size: A4	Sheet: 1 of 1

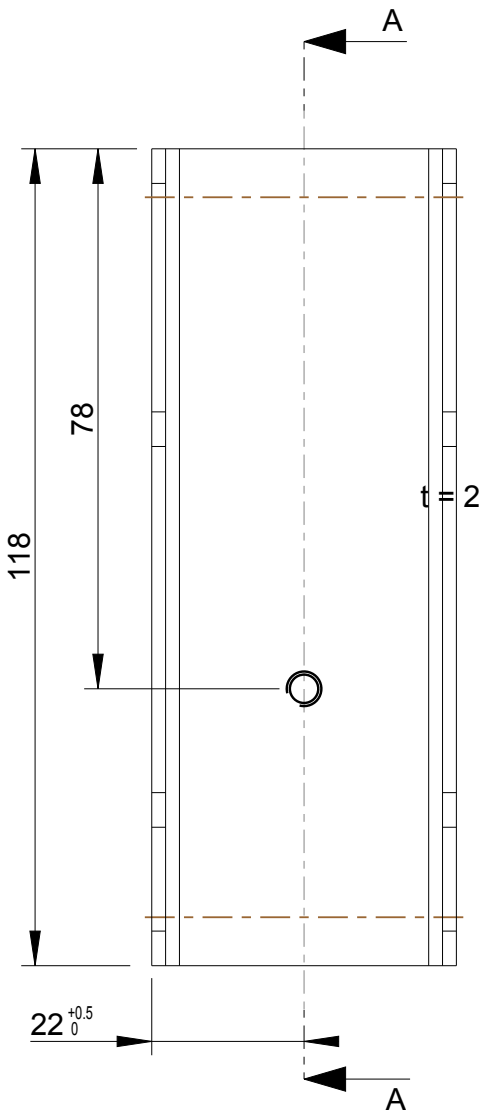

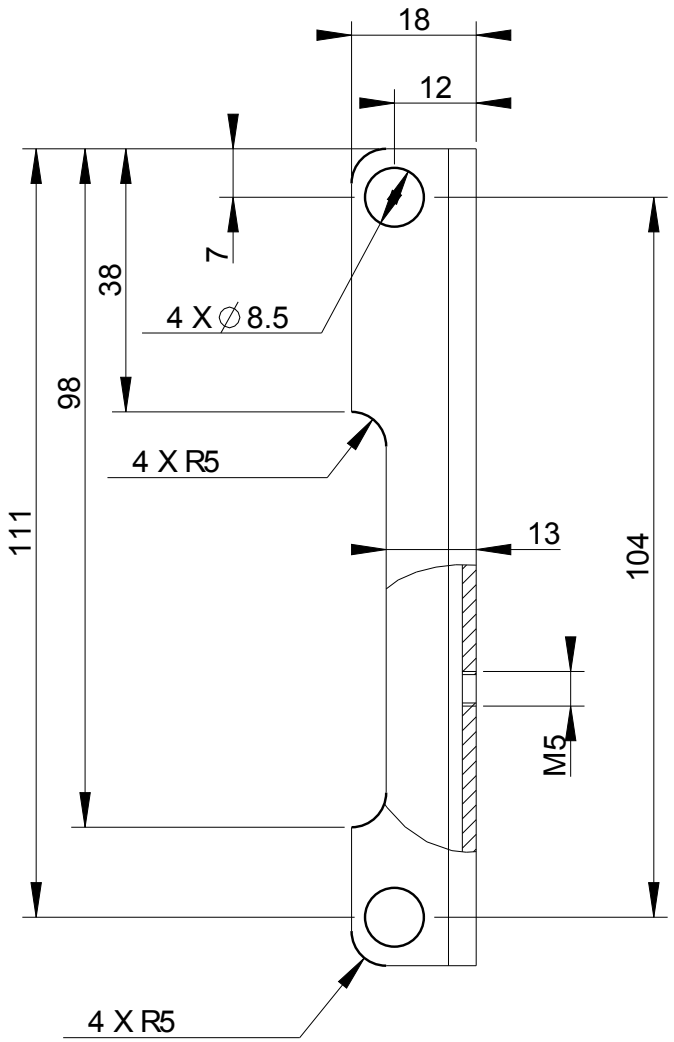

SECTION A-A

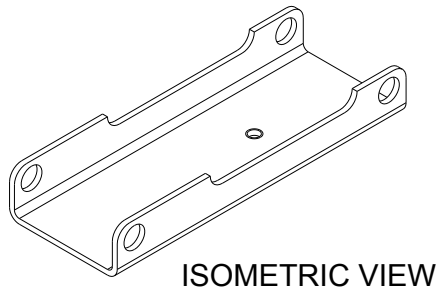

ISOMETRIC VIEW

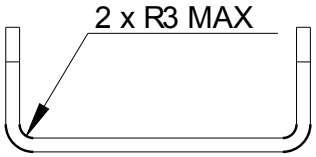

BREAK ALL EDGES

DO NOT SCALE

ISO 2768-m

dim	tol
0.5<3	±0.1
3<6	±0.1
6<30	±0.2
30<120	±0.3
120<400	±0.5

All dimensions in mm unless otherwise stated. surfaces finishes as stated

3rd Angle

Drawn By: M Jerbic	Date: 27/04/2010	MICYCLE. 980	
Checked By: M. Riese	Date: 07/05/10	Part Name: REAR BRACKET	
Authorised By: B. Cazzolato	Date: 07/05/10	Material: MILD STEEL	
Version: 0	Scale: 1:1	Part No: 1.7.1	Qty: 1	Size: A4	Sheet: 1 of 1

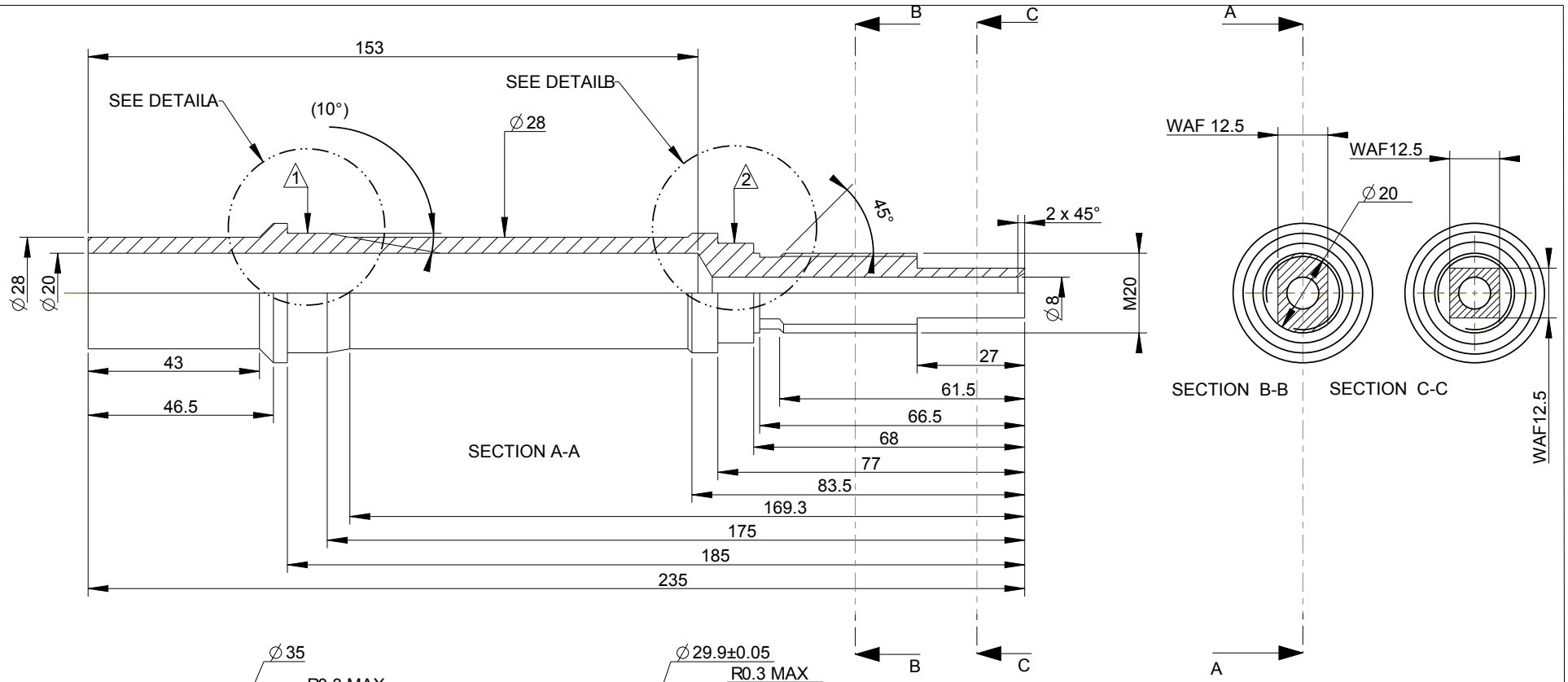

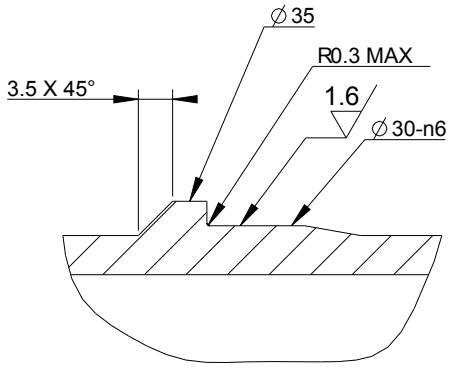

DETAIL A

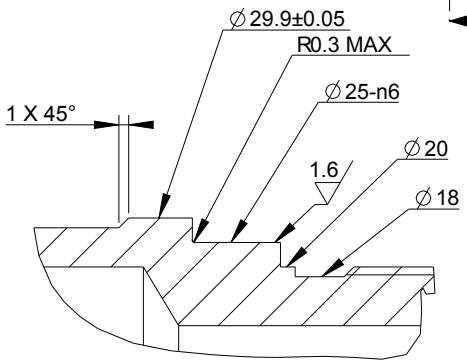

DETAIL B

ISO 2768-m

dim	tol
0.5<3	±0.1
3<6	±0.1
6<30	±0.2
30<120	±0.3
120<400	±0.5

NOTE:

1 619062RS1 BEARING SHAFT

2 619052RS1 BEARING SHAFT

3) 6.3 FOR ALL SURFACES EXCEPT BEARING SURFACE REFER TO SPECIFIC FINISH

BREAK ALL EDGES

DO NOT SCALE

All dimensions in mm unless otherwise stated . All surfaces finishes as stated	Drawn By: M Jerbic	Date: 20/04/2010	MICYCLE. 980			
	Checked By: M. Riese	Date: 07/05/10	Part Name: SPINDLE			
3rd Angle	Authorised By: B. Cazzolato	Date: 07/05/10	Material: 4130N			
	Version: 0	Scale: 1:1	Part No: 2.1.1	Qty: 1	Size A3	Sheet: 1 of 1

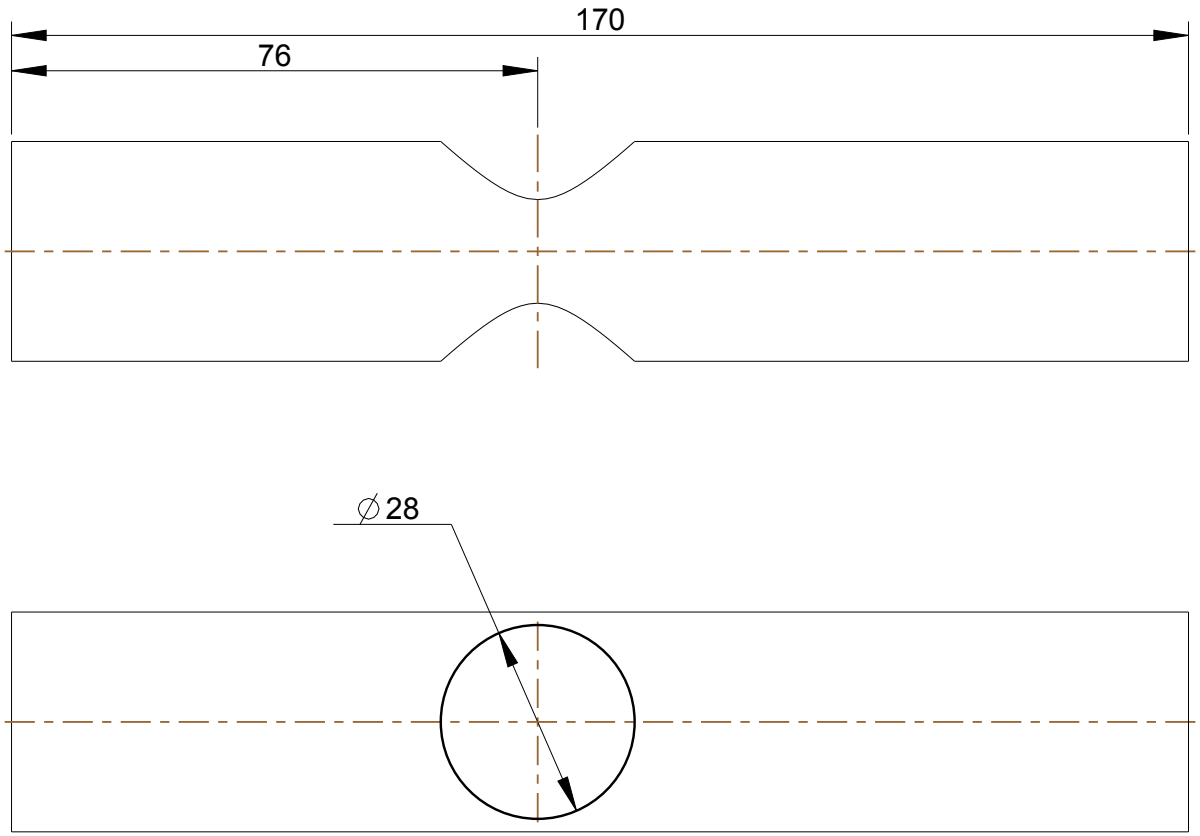

ISO 2768-m

dim	tol
0.5<3	±0.1
3<6	±0.1
6<30	±0.2
30<120	±0.3
120<400	±0.5

All dimensions in mm unless otherwise stated. surfaces finishes as stated

BREAK ALL EDGES

DO NOT SCALE

3rd Angle

Drawn By: M Haynes	Date: 20/04/2010	MICYCLE. 980	
Checked By: M. Riese	Date: 07/05/10	Part Name: FORK HORIZONTAL	
Authorised By: B. Cazzolato	Date: 07/05/10	Material: 4130N ∅ 1 1/4" x .083 CHS	
Version: 0	Scale: 1:1	Part No: 2.1.2	Qty: 1	Size: A4	Sheet: 1 of 1

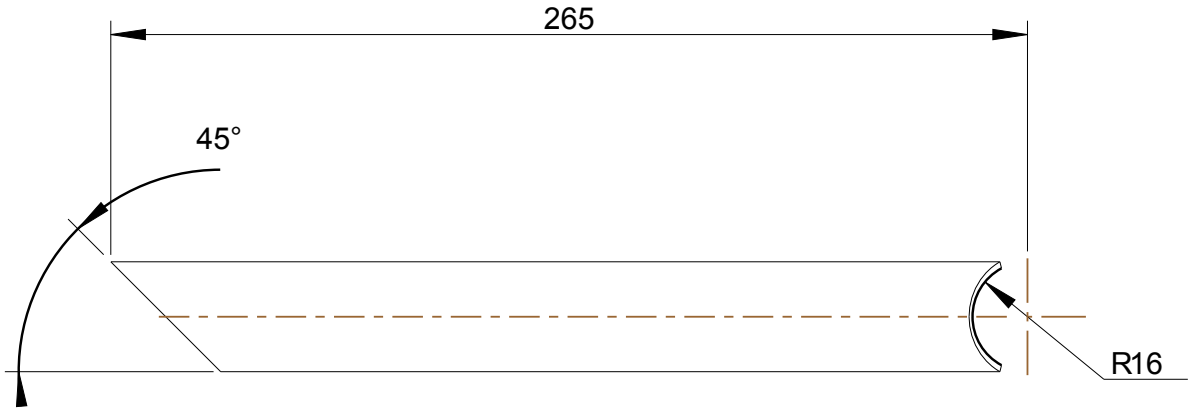

ISO 2768-m

dim	tol
0.5<3	±0.1
3<6	±0.1
6<30	±0.2
30<120	±0.3
120<400	±0.5

All dimensions in mm unless otherwise stated. surfaces finishes as stated

3rd Angle

BREAK ALL EDGES
DO NOT SCALE

Drawn By: D Caldecott	Date: 17/04/2010	MICYCLE. 980			
Checked By: M. Riese	Date: 07/05/10	Part Name: FORK LEG			
Authorised By: B. Cazzolato	Date: 07/05/10	Material: 4130N ∅ 1 1/4" x .083 CHS			
Version: 0	Scale: 1:2	Part No: 2.1.3	Qty: 2	Size: A4	Sheet: 1 of 1

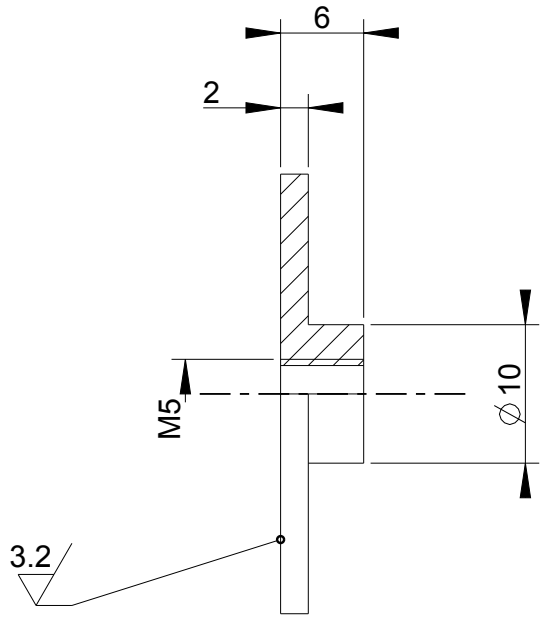

SECTION A-A

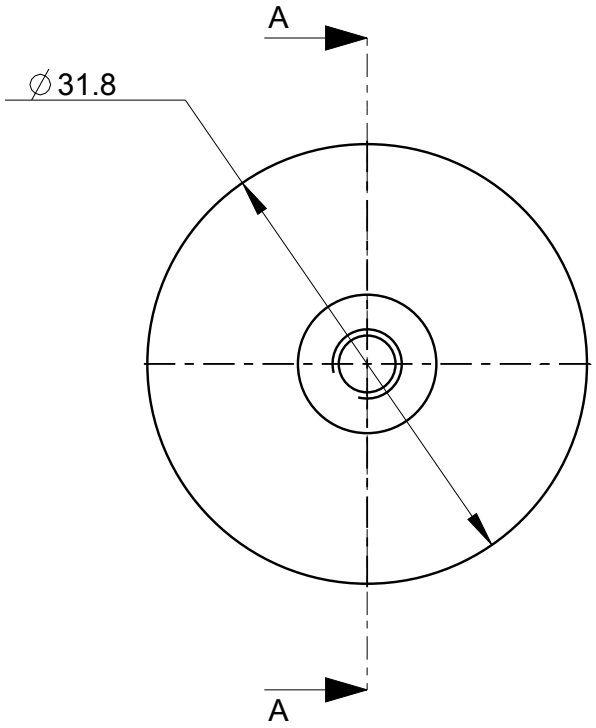

ISO 2768-m

dim	tol
0.5<3	±0.1
3<6	±0.1
6<30	±0.2
30<120	±0.3
120<400	±0.5

BREAK ALL EDGES
DO NOT SCALE

All dimensions in mm unless otherwise stated. surfaces finishes as stated

3rd Angle

Drawn By: M Jerbic	Date: 27/04/2010	MICYCLE. 980			
Checked By: M. Riese	Date: 07/05/10	Part Name: FORK CAP			
Authorised By: B. Cazzolato	Date: 07/05/10	Material: 4130N			
Version: 0	Scale: 1:2	Part No: 2.1.6	Qty: 2	Size: A4	Sheet: 1 of 1

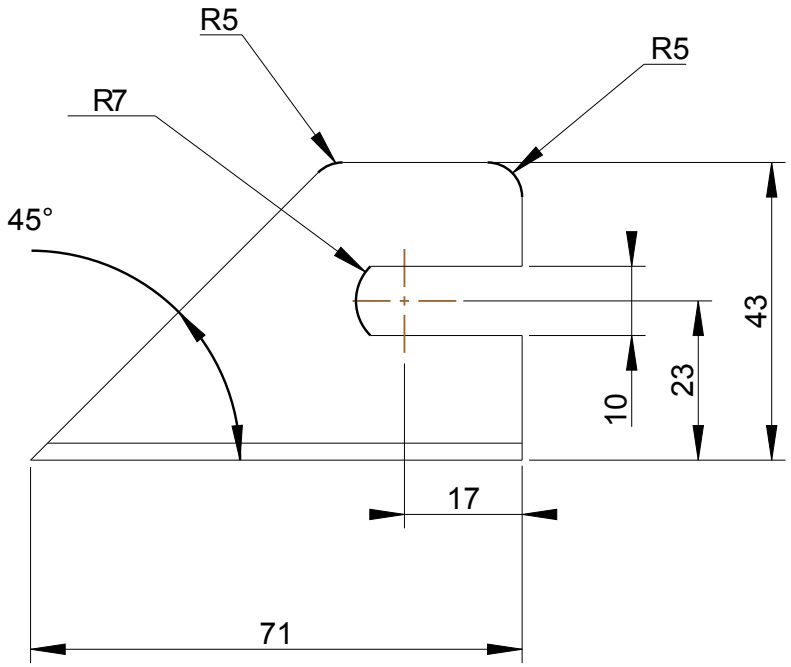

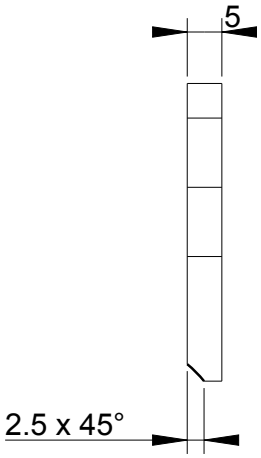

2-OFF MIRROR IMAGE

ISO 2768-m

dim	tol
0.5<3	±0.1
3<6	±0.1
6<30	±0.2
30<120	±0.3
120<400	±0.5

BREAK ALL EDGES
DO NOT SCALE

All dimensions in mm unless otherwise stated. surfaces finishes as stated

3rd Angle

Drawn By: A Kadis	Date: 21/04/2010	MICYCLE. 980	
Checked By: M. Riese	Date: 07/05/10	Part Name: FORK TABS LEFT & RIGHT	
Authorised By: B. Cazzolato	Date: 07/05/10	Material: 4130N	
Version: 0	Scale: 1:1	Part No: 2.1.4 2.1.5	Qty: 1 OF EACH
Size: A4	Sheet: 1 of 1		

ITEM	DRG/PART NO	DESCRIPTION	QTY
1	2.1.1	SPINDLE	1
2	2.1.2	FORK HORIZONTAL	1
3	2.1.6	FORK CAP	2
4	2.1.3	FORK LEG	2
5	2.1.5	FORK TAB RIGHT	1
6	2.1.4	FORK TAB LEFT	1
7	----------	ELLIPTICAL END CAP	2

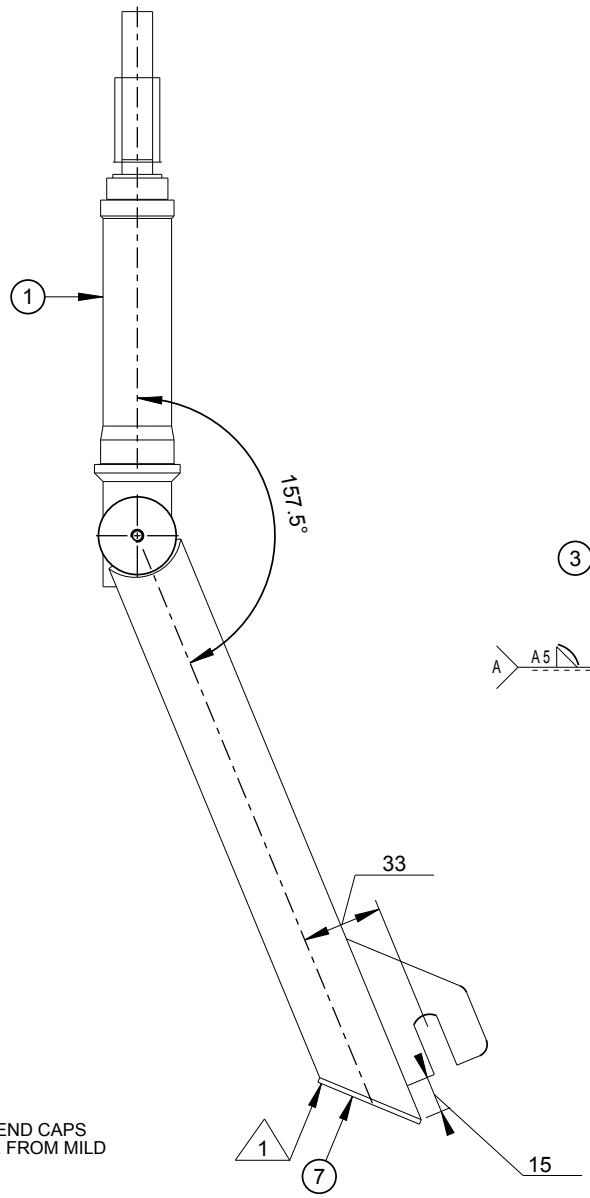

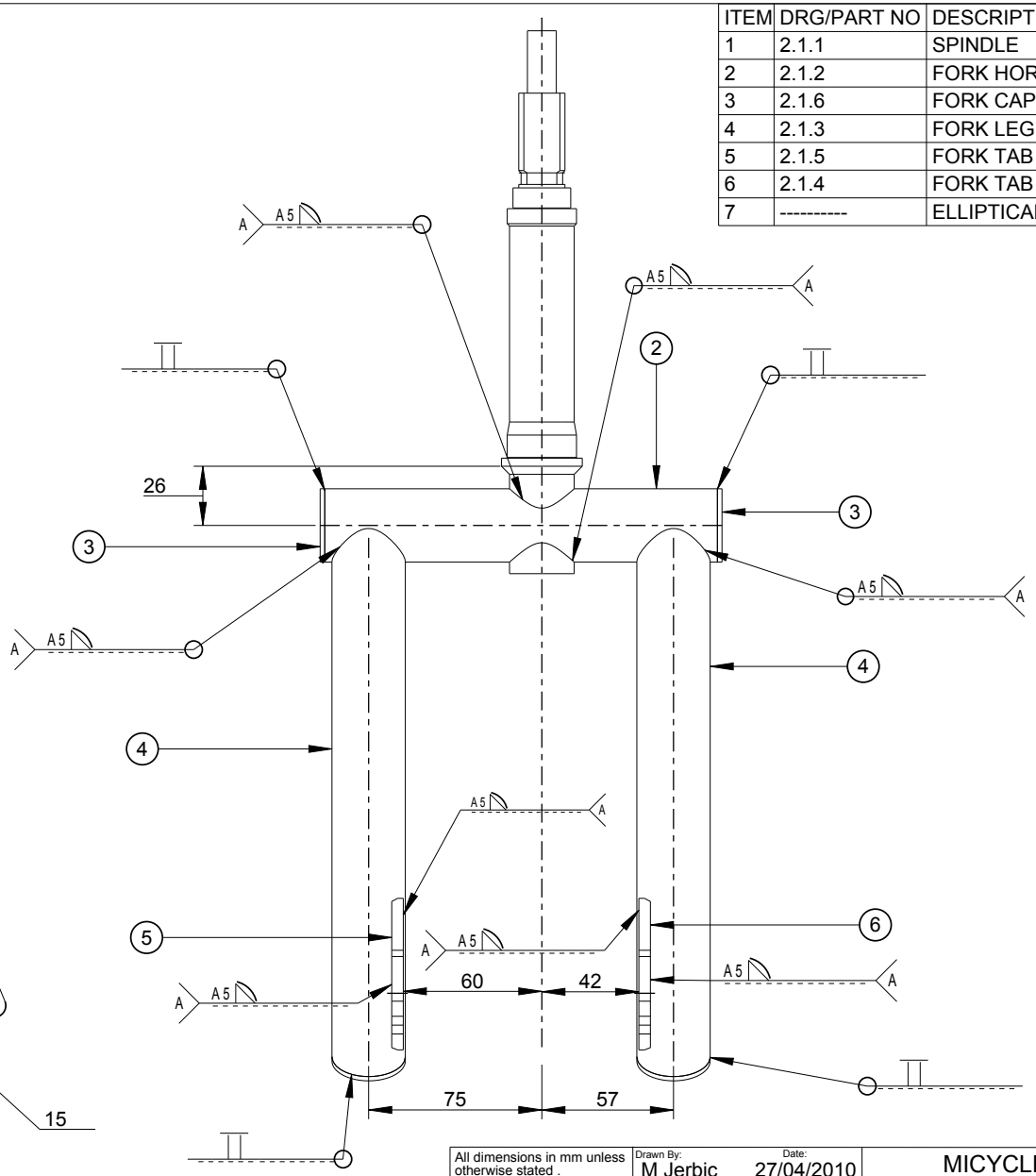

NOTE:

1. ELLIPTICAL END CAPS TO BE MADE FROM MILD STEEL t = 2

2) A 5 A — WELDING PROCESS A ISO 4063-151

3) WELDING PROCESS ISO 4063-131 WELDS TO BE GROUND FLUSH

DO NOT SCALE

All dimensions in mm unless otherwise stated . All surfaces finishes as stated	Drawn By: M Jerbic	Date: 27/04/2010	MICYCLE. 980				
	Checked By: M. Riese	Date: 07/05/10	Part Name: FORK SUBASSEMBLY				
3rd Angle	Authorised By: B. Cazzolato	Date: 07/05/10	Material: REFER TO PART DRAWINGS				
	Version: 0	Scale: 1:2	Part No: 2.1.X	Qty: 1	Size A3	Sheet: 1 of 1	

ITEM	DRG/PART NO	DESCRIPTION	QTY
1	3.2.1	CHASSIS BACK	1
14	-------	BUMPSTOP	12
21	-------	ISO 4762-M6 X 20	4
25	-------	ISO 7092-6 WASHER	4
26	3.3.X	POLE SLEAVE	1
27	3.4.1	SPAR 25mm	10
28	3.6.1	SPAR 20mm	2
29	-------	ISO 4762-M8 X 35	2
30	-------	ISO 7092-8 WASHER	4
31	-------	ISO 7040-M8 NUT	2
32	3.9.1	BATTERY BRACKET	2
33	-------	MAXON DEC 70/10	1
34	--------	ISO 4762-M3 X 15	4
37	3.7.1	COVER PLATE. RIGHT	1
38	3.8.1	COVER PLATE. LEFT	1

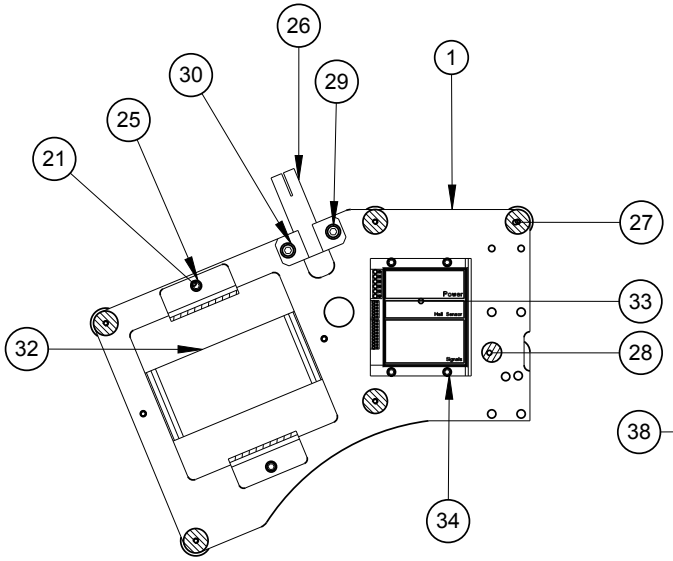

SECTION D-D

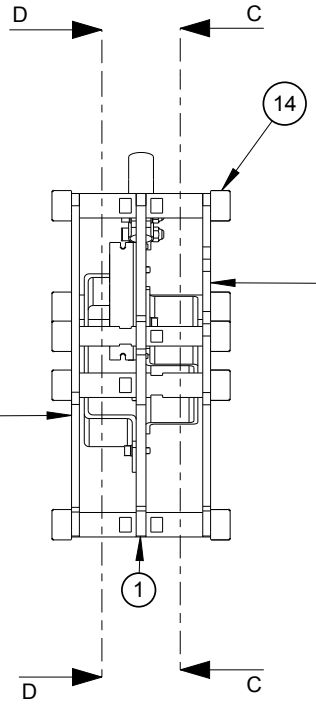

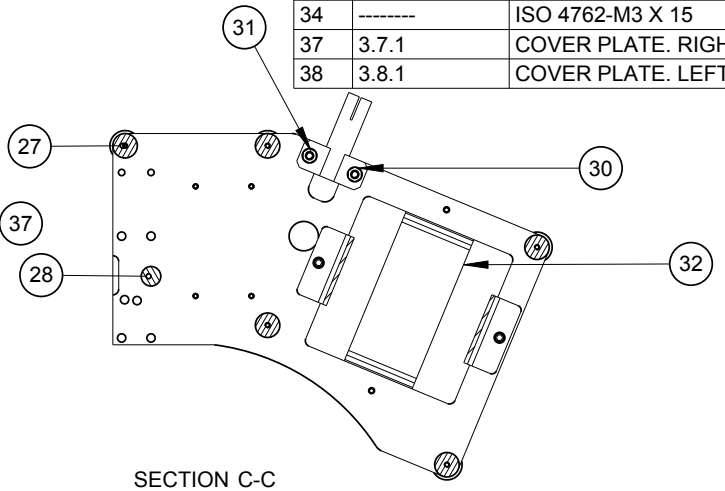

SECTION C-C

DO NOT SCALE

All dimensions in mm unless otherwise stated . All surfaces finishes as stated	Drawn By: M Jerbic	Date: 3/05/2010	MICYCLE. 980				
	Checked By: M. Riese	Date: 07/05/10	Part Name: PLATE ASSEMBLY A				
3rd Angle	Authorised By: B. Cazzolato	Date: 07/05/10	Material: REFER TO PART DRAWINGS				
	Version: 0	Scale: 1:5	Part No: 3.0.0	Qty: 1	Size A3	Sheet: 1 of 2	

ITEM	DRG/PART NO	DESCRIPTION	QTY
1	3.2.1	CHASSIS BACK	1
14	------	BUMPSTOP	12
21	------	ISO 4762-M6 X 20	4
25	------	ISO 7092-6 WASHER	4
26	3.3.1	POLE SLEEVE	1
27	3.4.1	SPAR 25mm	10
32	3.9.1	BATTERY BRACKET	2
35	------	50mm M8 THREAD BAR	6
36	------	ISO 10642-M5 X 40 HEX SOCKET	12
37	3.7.1	COVER PLATE, RIGHT	1
38	3.8.1	COVER PLATE, LEFT	1

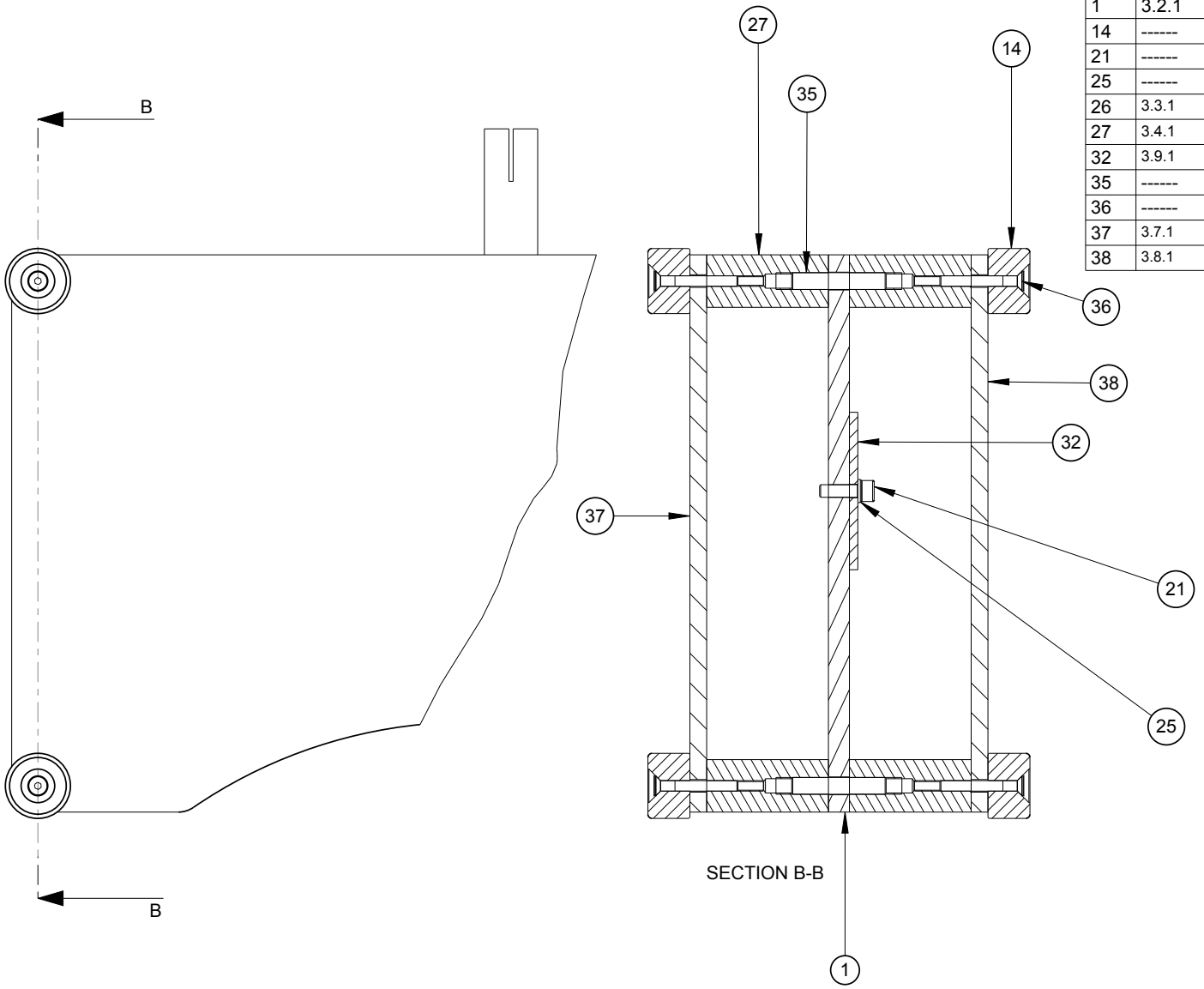

DO NOT SCALE

All dimensions in mm unless otherwise stated .
All surfaces finishes as stated

3rd Angle

Drawn By: M Jerbic	Date: 3/05/2010	MICYCLE. 980					
Checked By: M. Riese	Date: 07/05/10	Part Name: PLATE ASSEMBLY - B					
Authorised By: B. Cazzolato	Date: 07/05/10	Material: REFER TO PART DRAWINGS					
Version: 0	Scale: 1:2	Part No: 3.0.0	Qty: 1	Size A3	Sheet: 2 of 2		

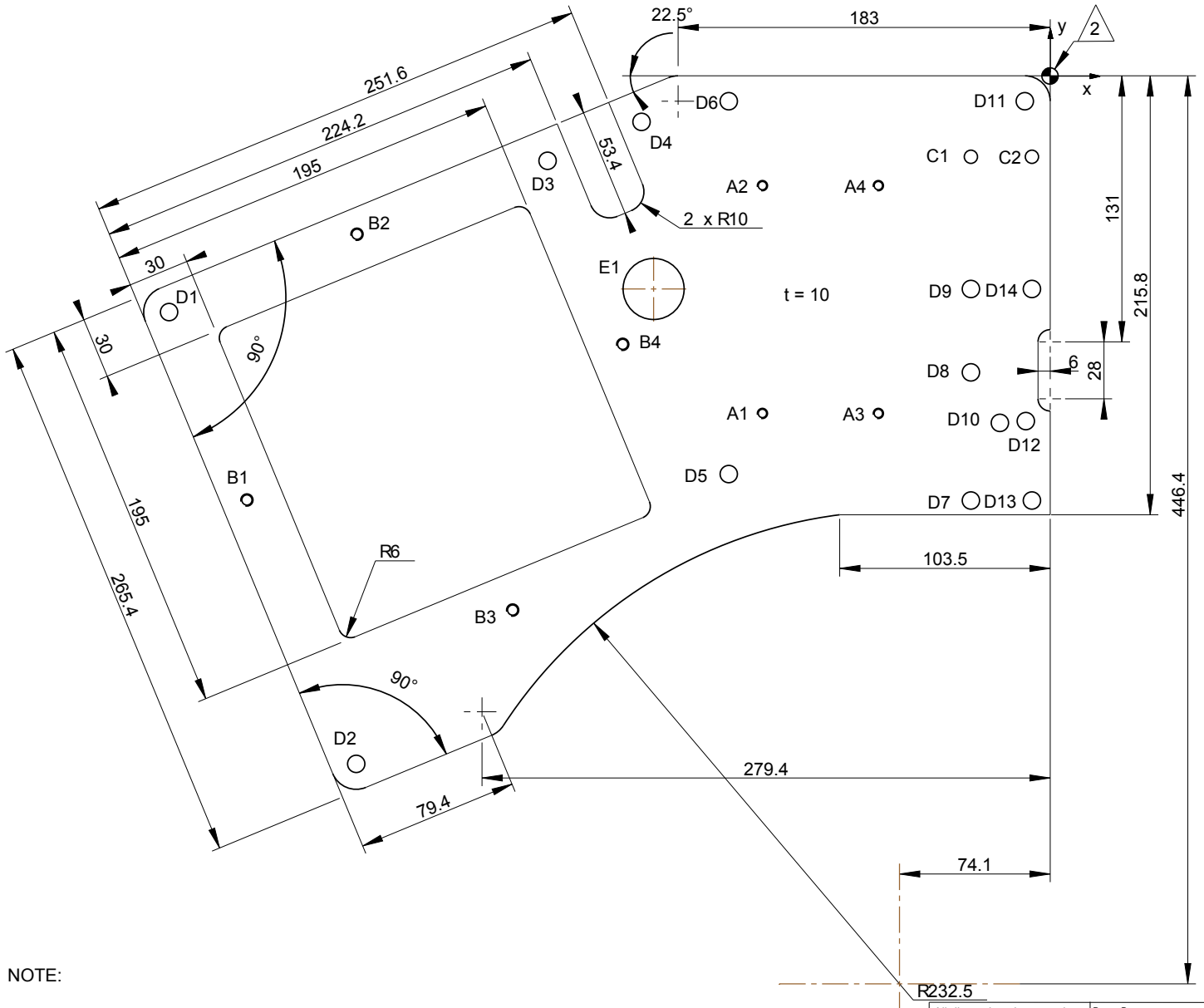

HOLE NO	X	Y	∅	THREAD
A1	-141.5	-166.0	4.1	M3
A2	-141.5	-54.0	4.1	M3
A3	-84.5	-166.0	4.1	M3
A4	-84.5	-54.0	4.1	M3
B1	-395.0	-208.6	5.0	M6
B2	-340.8	-77.9	5.0	M6
B3	-264.3	-262.7	5.0	M6
B4	-210.2	-132.0	5.0	M6
C1	-39.0	-39.8	6.5	-
C2	-9.0	-39.8	6.5	-
D1	-433.2	-116.2	8.5	-
D2	-341.2	-338.3	8.5	-
D3	-247.1	-41.8	8.5	-
D4	-200.9	-22.7	8.5	-
D5	-158.1	-195.8	8.5	-
D6	-158.1	-12.5	8.5	-
D7	-39.0	-208.8	8.5	-
D8	-39.0	-145.8	8.5	-
D9	-39.0	-104.8	8.5	-
D10	-24.7	-170.6	8.5	-
D11	-12.5	-12.5	8.5	-
D12	-12.0	-169.8	8.5	-
D13	-9.0	-208.8	8.5	-
D14	-9.0	-104.8	8.5	-
E1	-195.0	-104.8	30.0	-

ISO 2768-m

dim	tol
0.5<3	±0.1
3<6	±0.1
6<30	±0.2
30<120	±0.3
120<400	±0.5

NOTE:

1) ALL ROUNDS R12.5 UNLESS STATED OTHERWISE

△2 REFERENCE FOR HOLE DIMENSION ONLY

BREAK ALL EDGES

DO NOT SCALE

All dimensions in mm unless otherwise stated .
All surfaces finishes as stated

3rd Angle

Drawn By: A J Edwards Date: 28/4/10

Checked By: M. Riese Date: 07/05/10

Authorised By: B. Cazzolato Date: 07/05/10

Version: 0

Scale: 1:2

MICYCLE. 980

Part Name: CHASSIS BACK

Material: Al 5005

Part No: 3.2.1

Qty: 1

Size A3

Sheet: 1 of 1

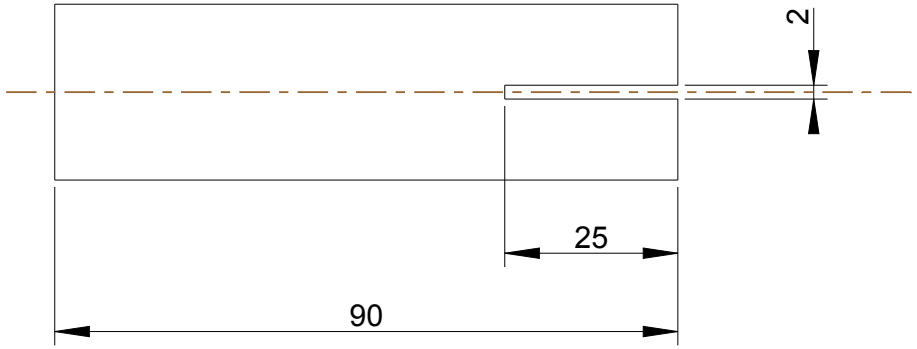

ISO 2768-m

dim	tol
0.5<3	±0.1
3<6	±0.1
6<30	±0.2
30<120	±0.3
120<400	±0.5

BREAK ALL EDGES

DO NOT SCALE

All dimensions in mm unless otherwise stated. surfaces finishes as stated

3rd Angle

Drawn By: A J Edwards	Date: 30/4/10	MICYCLE. 980			
Checked By: M. Riese	Date: 07/05/10	Part Name: POLE SLEEVE TUBE			
Authorised By: B. Cazzolato	Date: 07/05/10	Material: MILD STEEL∅ 1" x .058 CHS			
Version: 0	Scale: 1:1	Part No: 3.3.1	Qty: 1	Size: A4	Sheet: 1 of 1

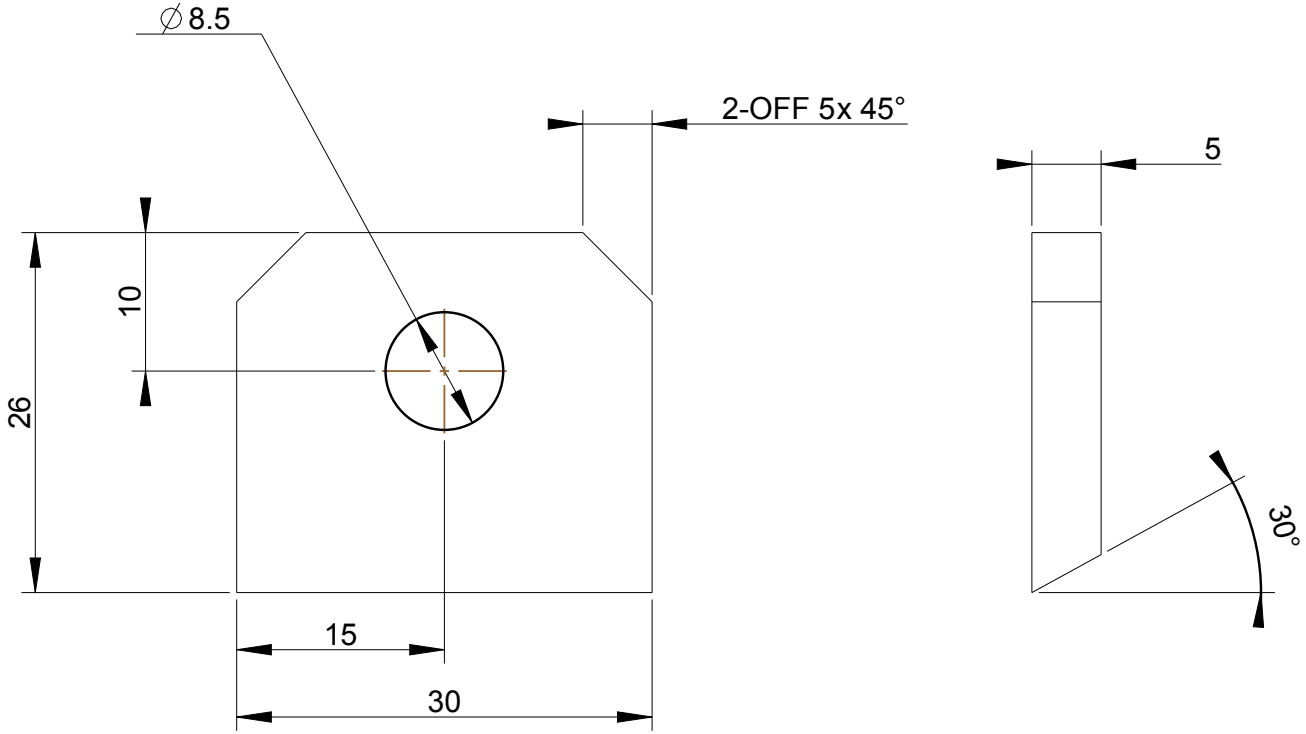

ISO 2768-m

dim	tol
0.5<3	±0.1
3<6	±0.1
6<30	±0.2
30<120	±0.3
120<400	±0.5

BREAK ALL EDGES

DO NOT SCALE

All dimensions in mm unless otherwise stated. surfaces finishes as stated

3rd Angle

Drawn By: A J Edwards	Date: 30/4/10	MICYCLE. 980				
Checked By: M. Riese	Date: 07/05/10	Part Name: POLE SLEEVE TAB				
Authorised By: B. Cazzolato	Date: 07/05/10	Material: MILD STEEL				
Version: 0	Scale: 2:1	Part No: 3.3.2	Qty: 4	Size: A4	Sheet: 1 of 1	

ITEM	DRG/PART NO	DESCRIPTION	QTY
1	3.3.1	POLE SLEEVE TUBE	1
2	3.3.2	POLE SLEEVE TAB	4

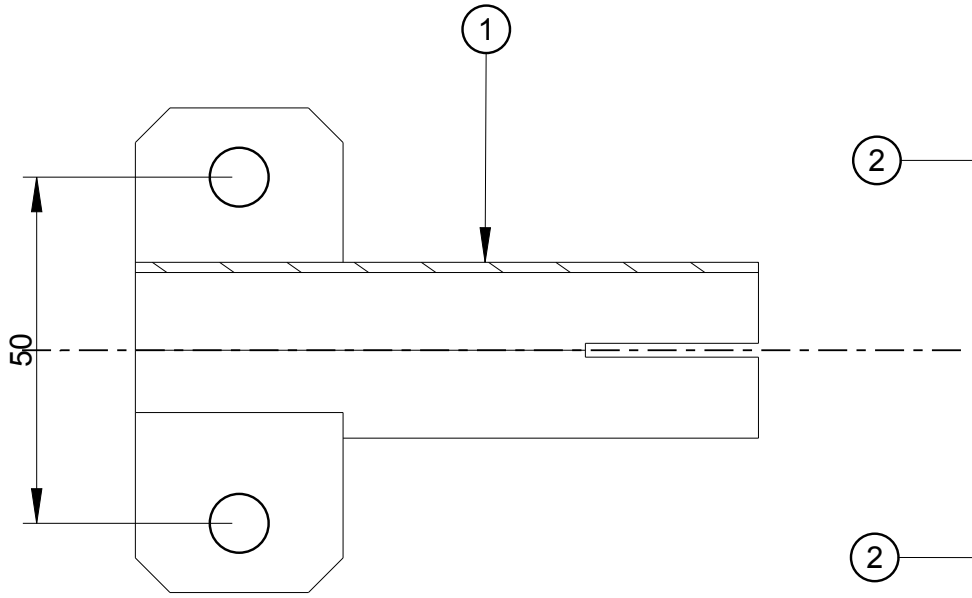

SECTION A-A

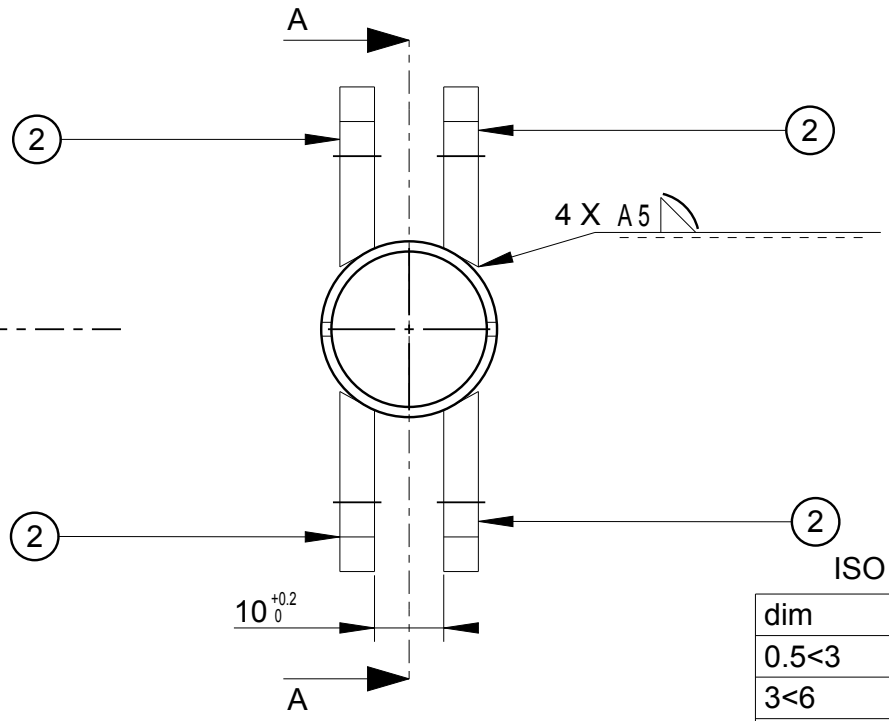

ISO 2768-m

dim	tol
0.5<3	±0.1
3<6	±0.1
6<30	±0.2
30<120	±0.3
120<400	±0.5

BREAK ALL EDGES
DO NOT SCALE

3rd Angle

All dimensions in mm unless otherwise stated. surfaces finishes as stated

Drawn By: M Jerbic	Date: 27/04/2010	MICYCLE. 980			
Checked By: M. Riese	Date:	Part Name: POLE SLEEVE			
Authorised By: B. Cazzolato	Date:	Material: REFER TO PART DRAWINGS			
Version: 0	Scale: 1:1	Part No: 3.3.x	Qty: 1	Size: A4	Sheet: 1 of 1

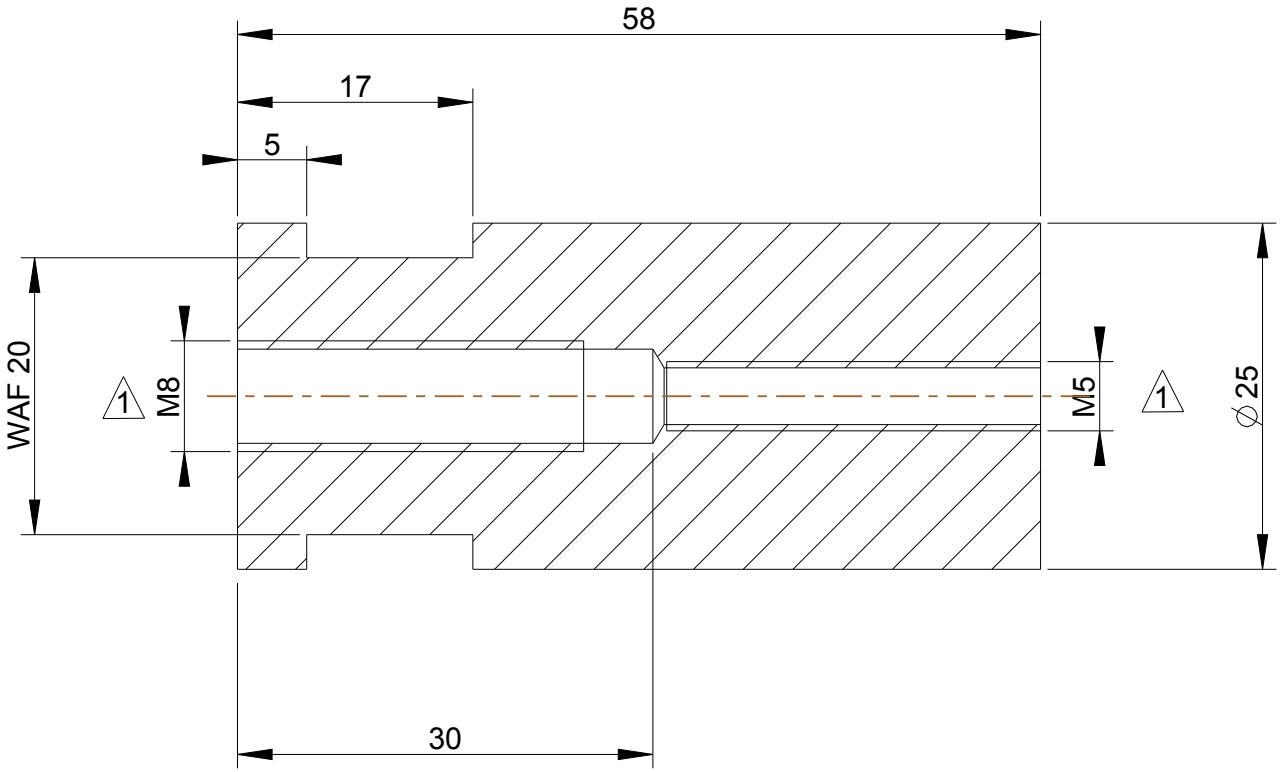

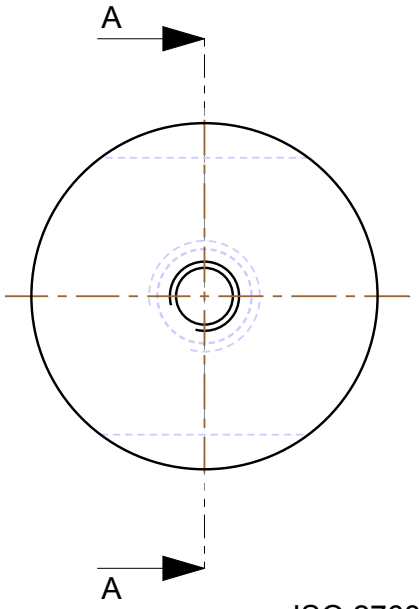

SECTION A-A

ISO 2768-m

dim	tol
0.5<3	±0.1
3<6	±0.1
6<30	±0.2
30<120	±0.3
120<400	±0.5

NOTE:

1 TAP THREADS TO MAXIMUM LENGTH

2) 0.8 ALL OVER

BREAK ALL EDGES

DO NOT SCALE

All dimensions in mm unless otherwise stated. surfaces finishes as stated

3rd Angle

Drawn By: D Caldecott	Date: 19/04/2010	MICYCLE. 980			
Checked By: M. Riese	Date: 07/05/10	Part Name: SPAR 25mm			
Authorised By: B. Cazzolato	Date: 07/05/10	Material: 5005 ALUMINIUM			
Version: 0	Scale: 2:1	Part No: 3.4.1	Qty: 10	Size: A4	Sheet: 1 of 1

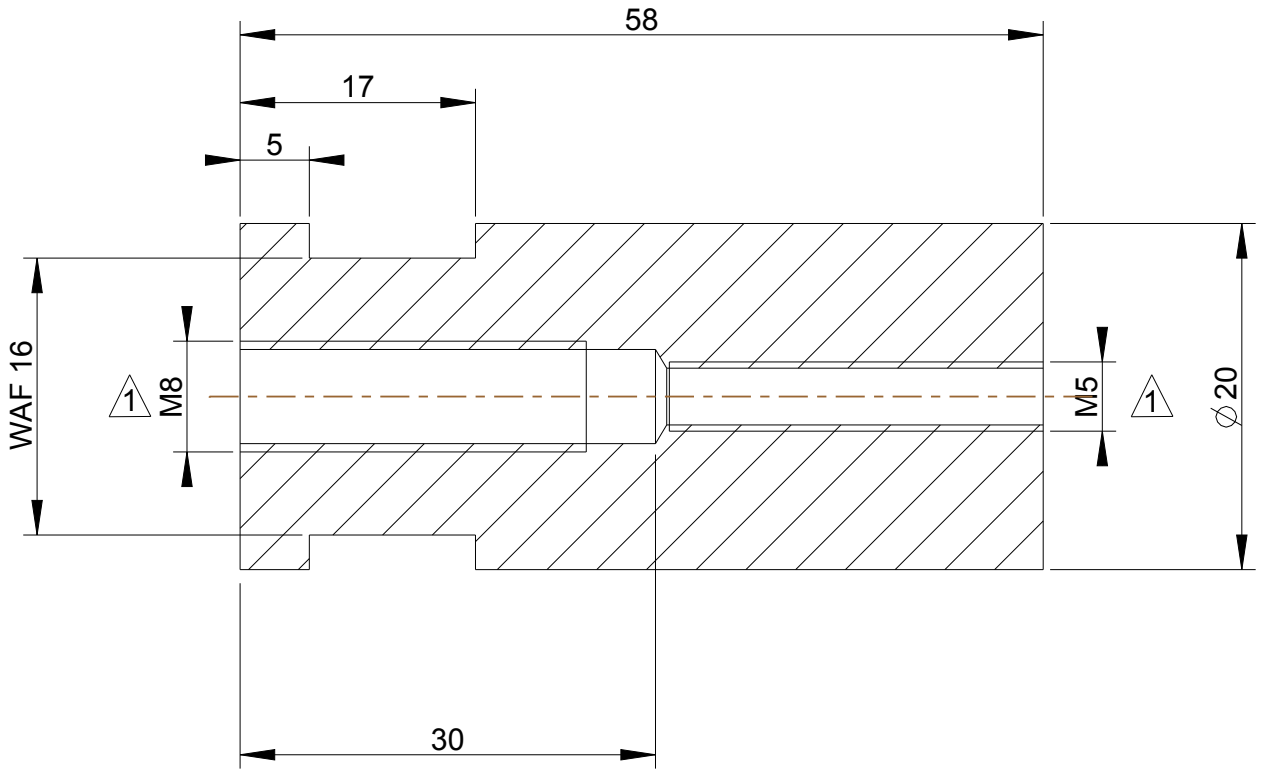

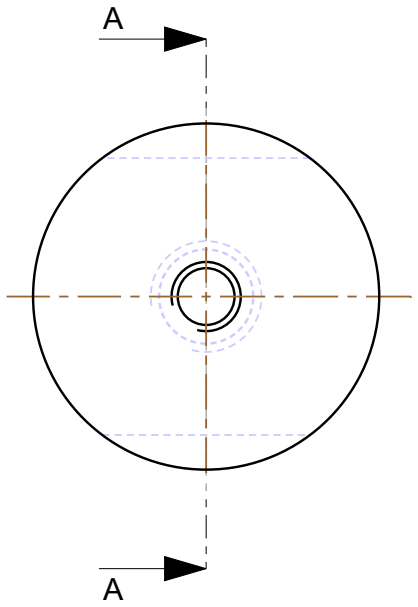

SECTION A-A

ISO 2768-m

dim	tol
0.5<3	±0.1
3<6	±0.1
6<30	±0.2
30<120	±0.3
120<400	±0.5

NOTE:

1 TAP THREADS TO MAXIMUM LENGTH

2) 0.8 ALL OVER

BREAK ALL EDGES

DO NOT SCALE

All dimensions in mm unless otherwise stated. surfaces finishes as stated

3rd Angle

Drawn By: D Caldecott	Date: 19/04/2010	MICYCLE. 980			
Checked By: M. Riese	Date: 07/05/10	Part Name: SPAR 20mm			
Authorised By: B. Cazzolato	Date: 07/05/10	Material: 5005 ALUMINIUM			
Version: 0	Scale: 2:1	Part No: 3.6.1	Qty: 2	Size: A4	Sheet: 1 of 1

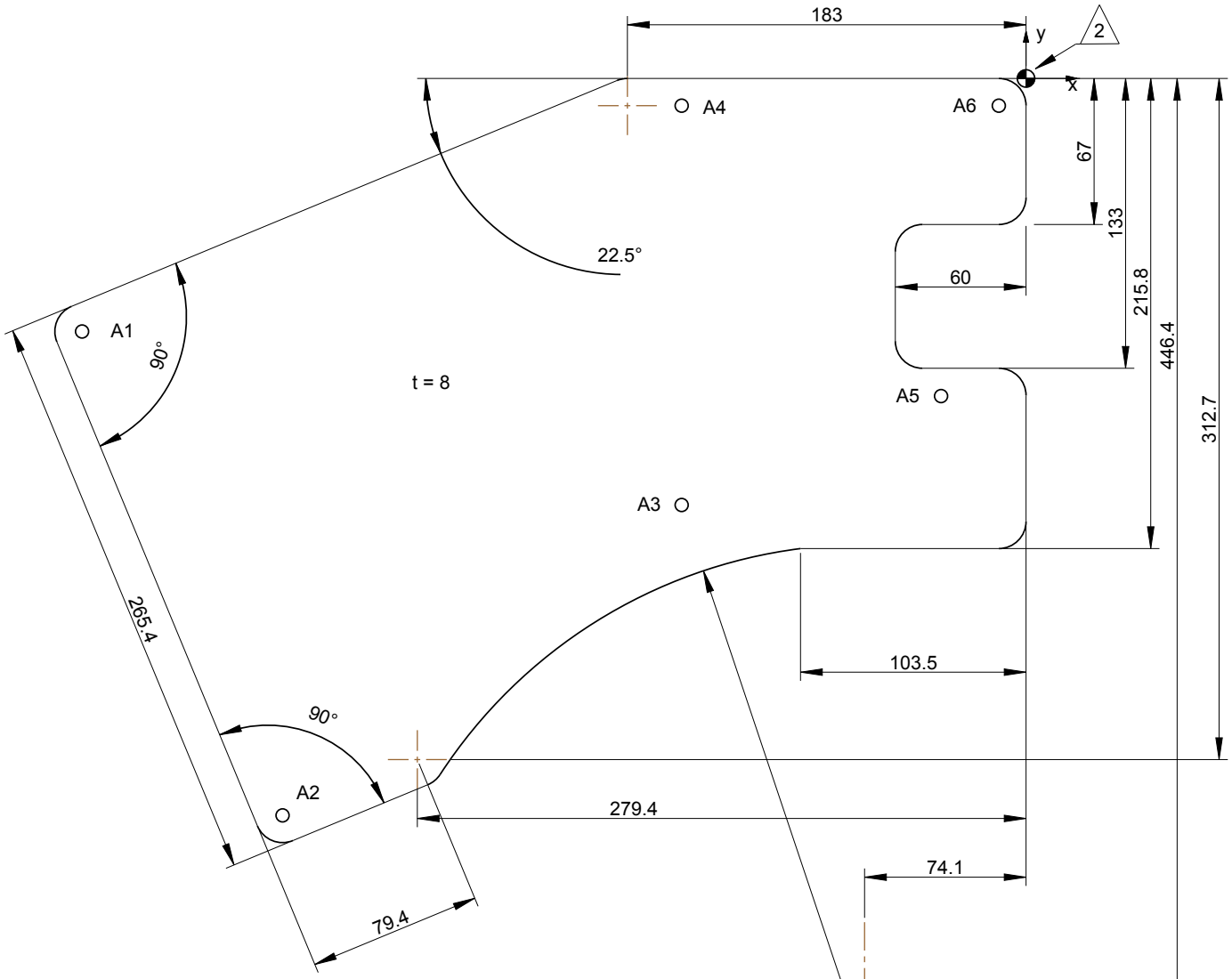

	Hole Chart		
Hole No.	X	Y	∅
A1	-433.2	-116.2	6.0
A2	-341.2	-338.3	6.0
A3	-158.0	-195.8	6.0
A4	-158.1	-12.5	6.0
A5	-39.0	-145.8	6.0
A6	-12.5	-12.5	6.0

ISO 2768-m

dim	tol
0.5<3	±0.1
3<6	±0.1
6<30	±0.2
30<120	±0.3
120<400	±0.5

NOTE:

1) ROUNDS R12.5 UNLESS STATED OTHERWISE

2 ORIGIN FOR HOLE LOCATIONS ONLY

DO NOT SCALE

All dimensions in mm unless otherwise stated .
All surfaces finishes as stated

3rd Angle

Drawn By: A J Edwards	Date: 20/4/10	MICYCLE. 980	
Checked By: M. Riese	Date: 07/05/10	Part Name: RIGHT COVER	
Authorised By: B. Cazzolato	Date: 07/05/10	Material: PERSPEX	
Version: 0	Scale: 1:2	Part No: 3.7.1	Qty: 1	Size A3	Sheet: 1 of 1

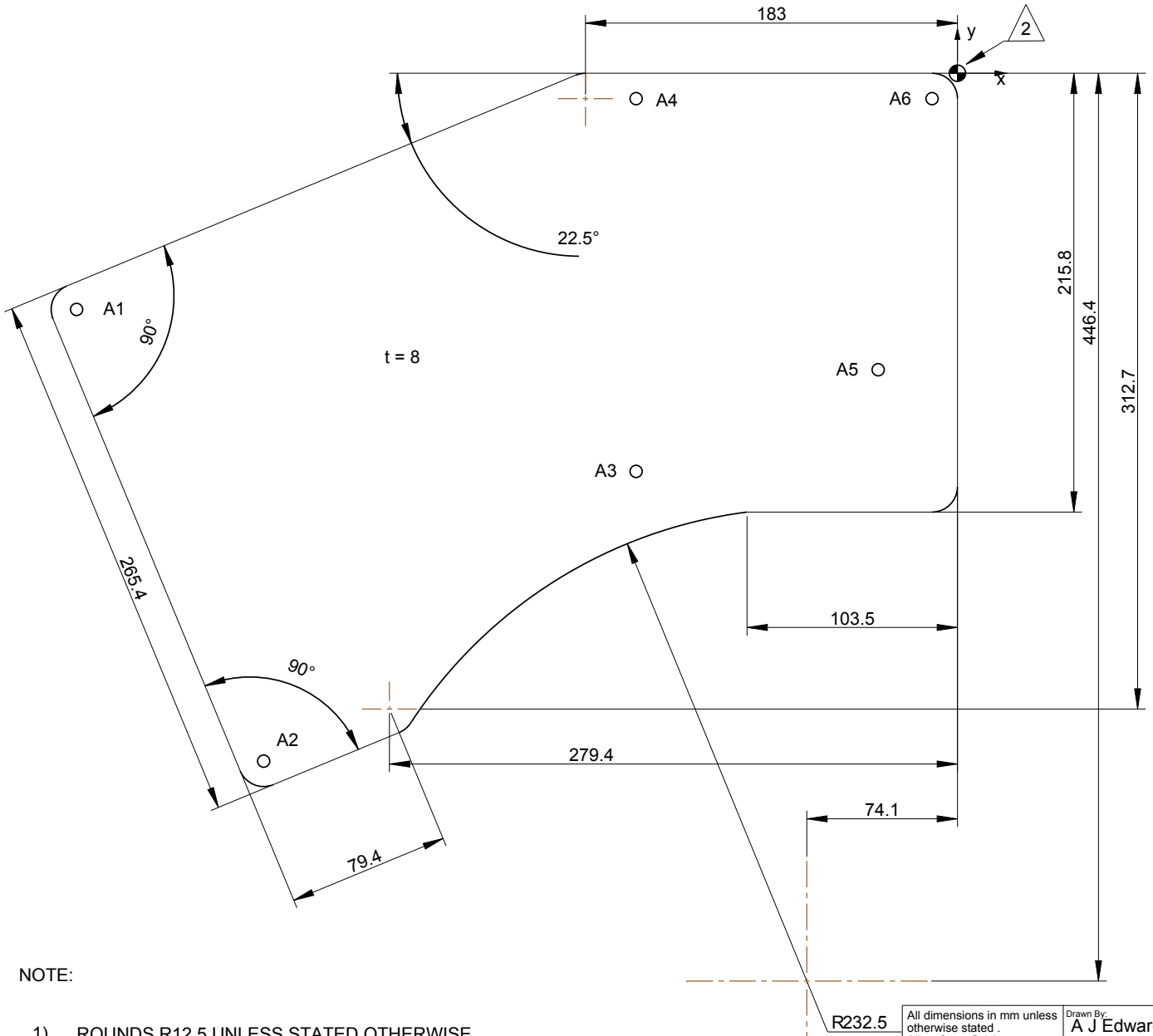

	Hole Chart		
Hole No.	X	Y	∅
A1	-433.2	-116.2	6.0
A2	-341.2	-338.3	6.0
A3	-158.0	-195.8	6.0
A4	-158.1	-12.5	6.0
A5	-39.0	-145.8	6.0
A6	-12.5	-12.5	6.0

ISO 2768-m

dim	tol
0.5<3	±0.1
3<6	±0.1
6<30	±0.2
30<120	±0.3
120<400	±0.5

NOTE:

1) ROUNDS R12.5 UNLESS STATED OTHERWISE

2 ORIGIN FOR HOLE LOCATIONS ONLY

All dimensions in mm unless otherwise stated .
All surfaces finishes as stated

3rd Angle

Drawn By: A J Edwards	Date: 20/4/10	MICYCLE. 980	
Checked By: M. Riese	Date: 07/05/10	Part Name: LEFT COVER	
Authorised By: B. Cazzolato	Date: 07/05/10	Material: PERSPEX	
Version: 0	Scale: 1:2	Part No: 3.8.1	Qty: 1	Size A3	Sheet: 1 of 1

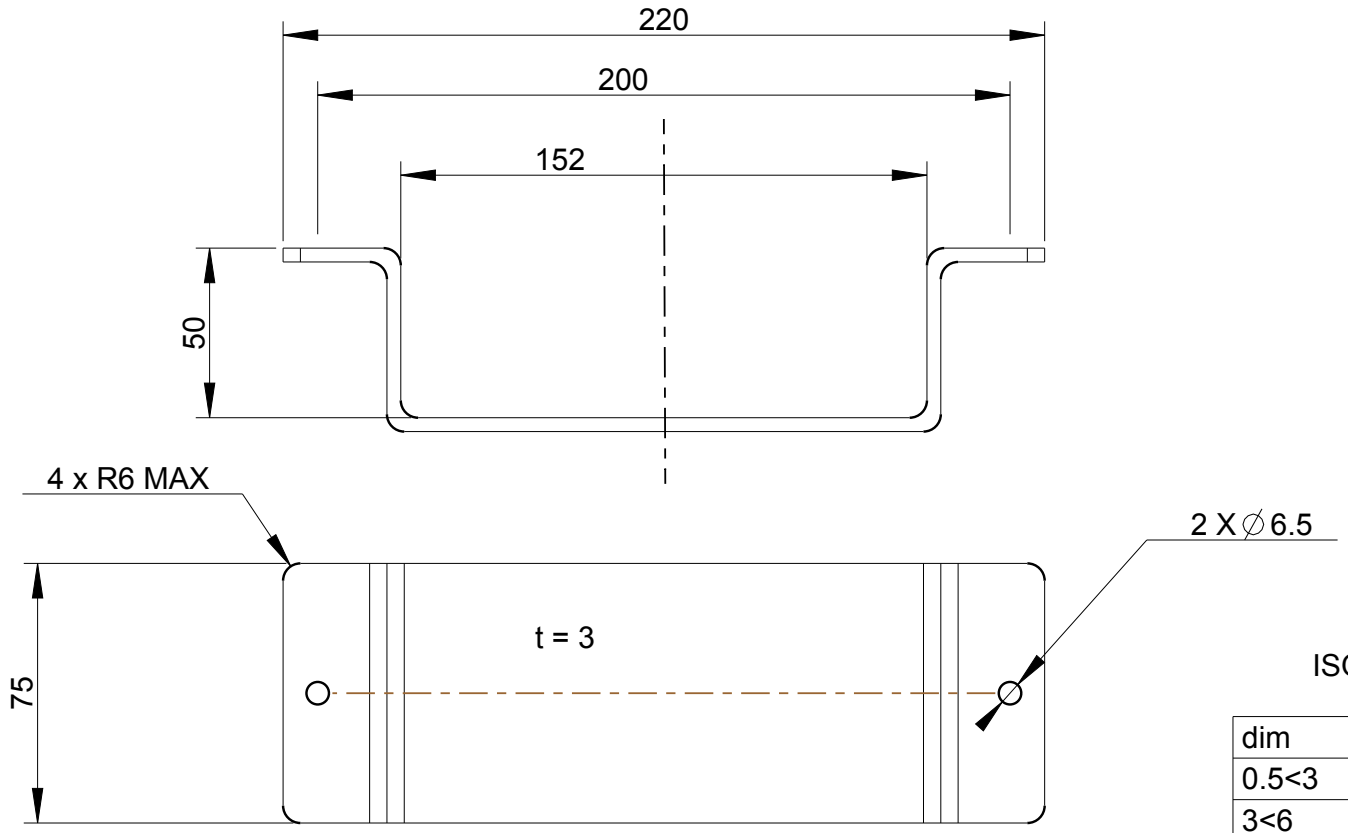

ISO 2768-m

dim	tol
0.5<3	±0.1
3<6	±0.1
6<30	±0.2
30<120	±0.3
120<400	±0.5

BREAK ALL EDGES

DO NOT SCALE

All dimensions in mm unless otherwise stated. surfaces finishes as stated

3rd Angle

Drawn By: D Caldecott	Date: 20/04/2010	MICYCLE. 980			
Checked By: M. Riese	Date: 07/05/10	Part Name: BATTERY CLAMP			
Authorised By: B. Cazzolato	Date: 07/05/10	Material: ALUMINIUM t=3			
Version: 0	Scale: 1:2	Part No: 3.9.1	Qty: 2	Size: A4	Sheet: 1 of 1

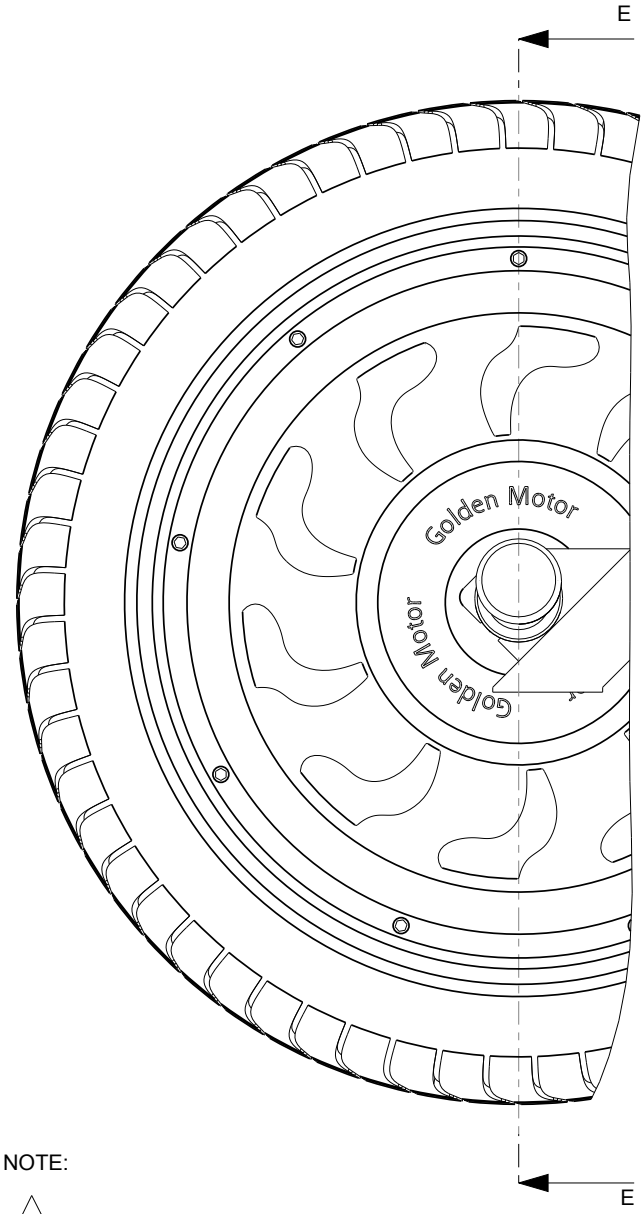

ITEM	DRG/PART NO	DESCRIPTION	QTY
1	---	MAGIC PIE HUB MOTOR	1
2	---	TYRE	1
3	---	CPR 4067-CAS FOOT PEG	2
4	---	M12 NUT	2
5	2.2.1	FOOT PEG SLEEVE	2
1 6	---	SPACER	2
7	2.1.4	FORK TAB LEFT	1
8	----	HUB MOTOR WASHER	2
9	2.1.5	FORK TAB RIGHT	1

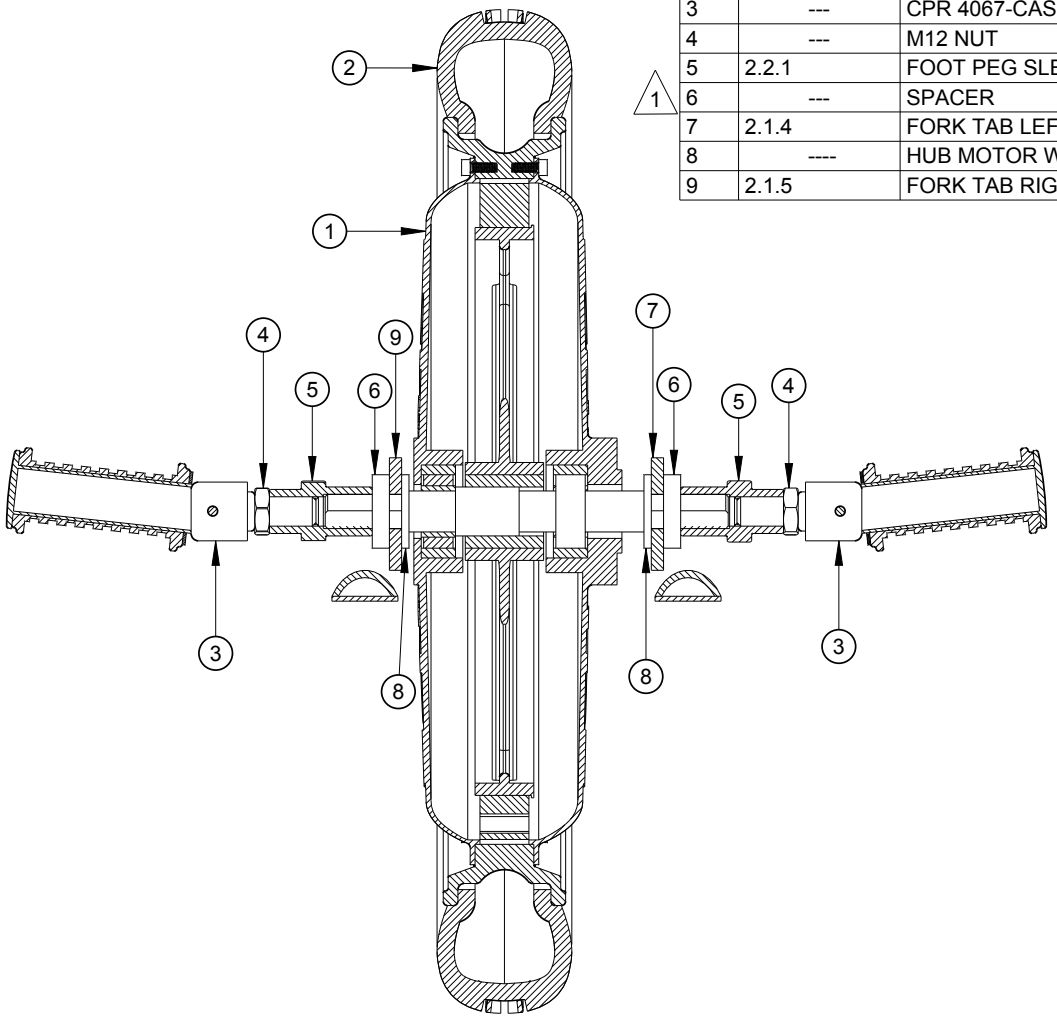

SECTION E-E

NOTE:

1 SPACER TO BE MADE FROM Al 5005
t = 7
OD = 30
ID = 15

DO NOT SCALE

All dimensions in mm unless otherwise stated . All surfaces finishes as stated	Drawn By: A J Edwards	Date: 3/5/10	MICYCLE. 980				
	Checked By: M. Riese	Date: 07/05/10	Part Name: WHEEL SUBASSEMBLY				
3rd Angle	Authorised By: B. Cazzolato	Date: 07/05/10	Material: REFER TO PART DRAWINGS				
	Version: 0	Scale: 1:2	Part No: 4.0.0	Qty: 1	Size A3	Sheet: 1 of 1	

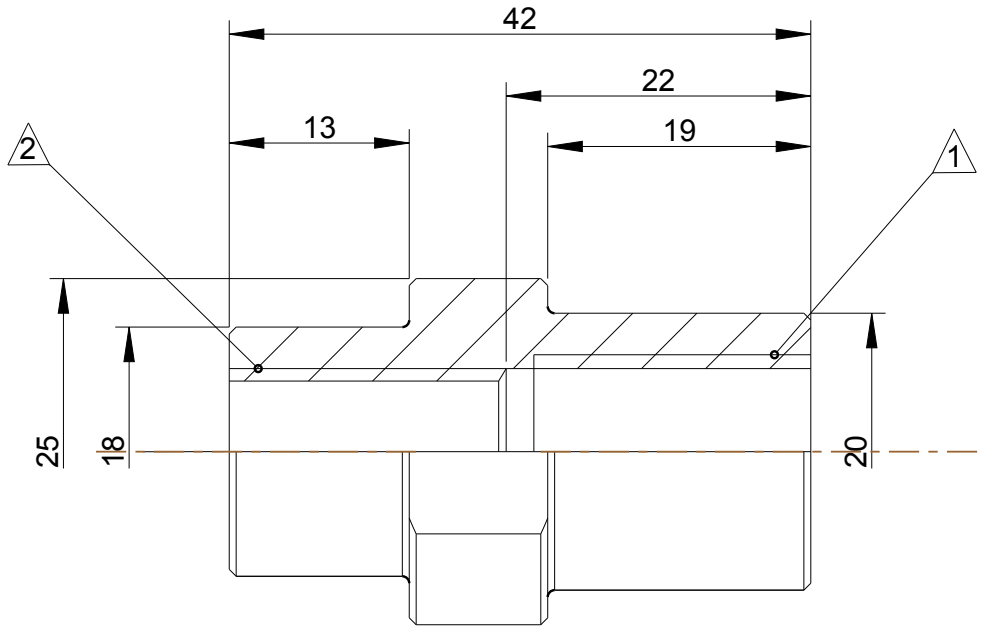

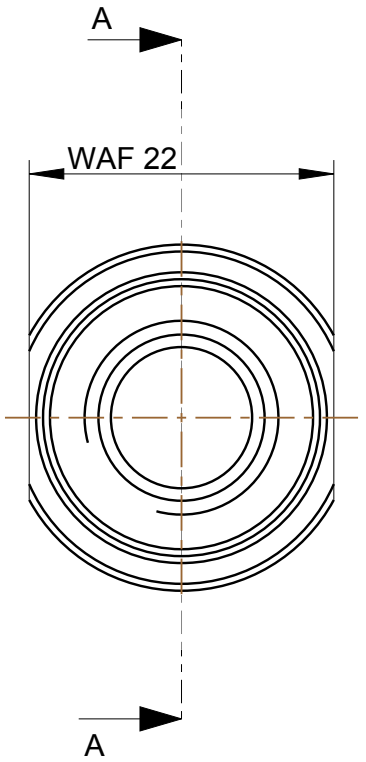

SECTION A-A

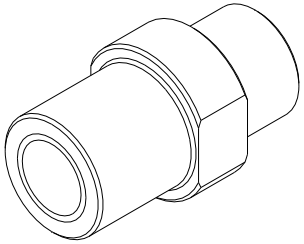

ISO 2768-m

dim	tol
0.5<3	±0.1
3<6	±0.1
6<30	±0.2
30<120	±0.3
120<400	±0.5

NOTE:

1. MATCH TO EXISTING THREAD ON HUB MOTOR
2. MATCH TO EXISTING THREAD ON FOOT PEG
3) TAP THREADS TO MAXIMUM LENGTH
4) 6.3 ALL OVER
5) ALL CHAMFERS 0.5 X 45°

BREAK ALL EDGES

DO NOT SCALE

All dimensions in mm unless otherwise stated. surfaces finishes as stated	Drawn By: M Jerbic	Date: 27/04/2010	MICYCLE. 980			
	Checked By: M. Riese	Date:	Part Name: FOOT PEG SLEEVES			
3rd Angle	Authorised By: B. Cazzolato	Date:	Material: MILD STEEL			
	Version: 0	Scale: 2:1	Part No: 4.1.0	Qty: 2	Size: A4	Sheet: 1 of 1